ELEMENTAL GROWTH PROCESS IN MOLECULAR BEAM EPITAXY

(分子線エピタキシー法における結晶成長素過程の研究)

A Thesis Presented to
the Graduate School of the University of Tokyo
in Partial Fulfillment of the Requirements for
the Degree of Doctor of Engineering

by
Takashi SUZUKI

Dissertation Supervisor

Professor Tatau NISHINAGA

Acknowledgements

The works described in this thesis have been carried out in essential part at the University of Tokyo, during the period from 1988 to 1993 when I was studying as a graduate student of the Department of Electronic Engineering of the University. Most of the work has been done while I was in the Doctor course from 1990 to 1993, although some parts (section 2.2 and 2.4) were done from 1988 to 1989 for the partial fulfillment of Master thesis.

I greatly appreciate my dissertation supervisor, Professor Tatau Nishinaga for his guidance and support. His enthusiasm for the research has provided the motivation to undertake and complete this work. I would like to thank Dr. Masaaki Tanaka, Lecturer, for his useful discussion and encouragements. I am also very grateful to Ms. Masako Washiyama for her constant support and help. I am also indebted to my colleagues in Nishinaga laboratory for providing such good advice and collaborations. I am particularly grateful to Messrs. Ikuhisa Ichimura, Ryuhei Sasagawa and Makoto Inoue for their experimental help.

I would like to thank Dr. Tomoya Shitara, Imperial College, London University for his constant support and for providing me an interesting and excellent environment to stay in London.

My thanks to Professor Bruce Joyce and Professor Dimitri Vvedensky, Imperial College, London University for providing me a great opportunity to work for short period.

I would like to thank Dr. Masakazu Ichikawa of Central Research Laboratory, HITACHI, Ltd. and Dr. Toshiro Isu of Central Research Laboratory, Mitsubishi Electric Corporation for their helpful advice about the experimental apparatus.

The fellowship of the Japan Society for the Promotion of Science for Japanese Junior Scientists was generously offered to me from 1991 April to 1993 March.

Finally I would like to thank my parents for their continual support.

Contents

Chapter 1

Introduction

1.1 Molecular Beam Epitaxy

Molecular beam epitaxy (MBE) is practically a refined form of vacuum evaporation. The molecular or atomic beams are produced by heating source materials in Knudsen cells and the molecules and the atoms impinge on a heated substrate almost without collisions. After arriving on the surface, the molecules or the atoms are incorporated into the crystal or re-evaporate after the adsorption time. The essential point of MBE is that the epitaxial growth takes place under ultra-high vacuum (UHV) conditions. Several important characteristics of MBE are summarized as follows:

(1)As UHV provides almost contamination free atmosphere, a substrate surface is kept clean for a considerably long period.

(2)Since it is possible to reduce a growth rate as slow as monolayer per several ten seconds due to (1), it is easy to control a growth thickness very accurately.

(3)The flux of the individual source can be switched easily on and off by simply opening and closing the shutter respectively. Therefore, an arbitrary hetero-structure or doping profile in the vertical direction can be obtained.

(4)One can get a lot of information concerning the growth mechanism from observations of surface during or after the growth. Among the in-situ measurements, reflection high energy diffraction (RHEED) has been widely used.

There are other types of MBE which employ gas sources, so-called metalorganic MBE (MOMBE) and gas source MBE (GSMBE). There are advantages to use gas sources such as growth thickness uniformity and the absence of oval defects.

However, more complicated chemical reactions are involved in the growth process, which make it difficult to understand the growth mechanism.

Many kinds of surface analytical facilities have been employed to study the MBE growth. Among them, in this thesis, conventional RHEED and scanning microprobe RHEED (μ-RHEED) system are employed for real time study of the MBE growth. The details of the μ-RHEED system is described in chapter 4.

1.2 Historical Background

Since a concept of superlattice was proposed, a great amount of effort has been made to grow ultra-thin films with the accuracy of monolayer. For the fabrication of man-made crystal like superlattice to study quantum effect, it is extremely important to control the crystal growth on an atomic scale. This is because imperfections of the crystal and a disorder in the heterointerface greatly deteriorate properties of the electronic or optoelectronic devices. To avoid such defects and poor interface, it is necessary to realize an excellent control over the composition, thickness and doping profile on an atomic scale in MBE as well as in metalorganic chemical vapor deposition (MOCVD). In this section, the emphasis is put on MBE and the historical development of understanding the growth mechanism will be described.

The investigation of the crystal growth mechanism of MBE was started by Arthur in 1968. After that, the further study was performed by Foxon and Joyce (1975, 1977). In both works, the chemistry of the growth process has been investigated using modulated beam mass spectrometry (MBMS). They proposed a model for the growth of GaAs from beams of Ga and As_2 or As_4.

From the early days of MBE development, RHEED has been used as a strong tool to observe in-situ the surface of a growing film because of its compatibility with the growth process. The pioneering work using RHEED was made by Cho (1970, 1971), who studied typical reconstructions of GaAs(001) and (111)B surfaces.

From 1981 when so-called RHEED oscillation was found (Harris *et al.* 1981, Wood, 1981), RHEED has been extensively used to observe in-situ the dynamics of the crystal growth. This is because the RHEED intensity oscillation has an ability to detect a layer-by-layer growth after two-dimensional (2D) nucleation and this provides information about the growth behaviors. After that, RHEED intensity oscillation is observed not only during the growth but also during the evaporation of GaAs. Among the studies so far made by using the RHEED intensity oscillation technique, one of the most important works for understanding the growth mechanism was done by Neave *et al.* in 1985. They observed disappearance of the RHEED intensity oscillation during MBE growth of GaAs on a vicinal surface as increasing the growth temperature. This

was explained as the change of the growth mode. Namely, at low temperature, 2D nuclei are formed between the steps. On the other hand, when the growth temperature is higher than a critical one, the atoms enter the step before they form a nucleus. These growth modes are called the 2D nucleation and the step flow respectively. So-called tilted superlattices were fabricated on misorientated GaAs substrates making use of the growth in step flow mode (Gaines *et al.* 1988). Neave *et al.* obtained a surface diffusion length of Ga by applying the Einstein relationship to the experimental result. However, Nishinaga and Cho (1988) pointed out the misunderstanding in their interpretation of the critical temperature and studied MBE growth according BCF theory. There is still some discussion concerning the explanation of the RHEED intensity oscillation during the growth on a vicinal surface and the surface diffusion length. However, RHEED measurements must play an invaluable role in understanding the MBE growth mechanism.

In the theoretical study, thermodynamics has been employed. The pioneering work was made by Heckingbottom in 1985, and later Seki and Koukitu (1986) extended the treatment to various kinds of materials by assuming that chemical equilibrium is established on the surface. This theory agrees with the experimental results of high temperature growth of GaAs and alloy semiconductors. But, there are still the questions left about to what degree and at which special places the equilibrium is established. Chapter 2 deals with this problem.

Another theoretical approach has been made by Clarke *et al.* (1989) and Irisawa *et al.* (1990) who have carried out Monte Carlo simulations by the computer and have compared the experimental results with the theory.

Other studies to find the elemental process in MBE are made by modified growth method. For example, growth interruptions and migration enhanced epitaxy (MEE) (Horikoshi *et al.* 1986) have been proposed for the purpose to smooth a surface, and widely used. In the method of growth interruptions, a great reduction of the step density is achieved by stopping Ga supply for several tens of seconds prior to the formation of the interface, which is shown by the recovery of RHEED intensity. In 1985, Sakaki *et al.* found that the growth interruptions lead to the drastic sharpening of the photoluminescence (PL) linewidth of quantum wells (QWs). They systematically

studied the interface structures and properties during MBE growth by applying this method. MEE growth method, in which group III and group V elements are supplied alternately, gives a good crystal quality at low growth temperature. The investigation by RHEED during MEE growth gives a lot of information on the surface structures, and shows that a smooth surface is maintained even at low growth temperature. As will be described in chapter 3, we propose a new modified growth named modulation MBE (M-MBE) which consists of an intermittent supply of group III atom and a continuous supply of As.

Recent development of analytical technologies has made it possible to study intensively the growth process in MBE. Since the UHV technique is used in MBE, many kinds of surface analytical facilities have been installed, such as an Auger electron spectroscopy (AES), a X-ray photoemission spectroscopy (XPS), *etc.* But from the viewpoint of crystal growth, a scanning tunneling microscope (STM) and μ-RHEED have a great advantage of being able to clarify the two dimensional structure of a surface. Pashley *et al.* studied the structure of the reconstruction and the step of the GaAs surface in 1988 by means of STM. We propose an atomic model for facet formation on the basis of their STM observation. This will be described in chapter 5. μ-RHEED technique was developed originally by Ichikawa *et al.* (1984) for the investigation of the growth mechanism in Si-MBE. After that, Yamada *et al.* (1988) and Isu *et al.* (1988a) succeeded to apply this technique to GaAs-MBE. Although STM can offer information on an atomic scale, μ-RHEED can be used in real time during growth. Yamada *et al.* (1989) observed formation and annihilation of Ga droplets during MBE. Hata *et al.* (1990) investigated the local distribution of the growth rate on the patterned substrate by using RHEED intensity oscillation and discussed the surface diffusion length. As will be described in detail in chapter 4, a scanning electron microscopy (SEM) or μ-RHEED is used for real time observations to understand the growth mechanism.

1.3 Purpose of the Present Study

From nineteen-thirties, a great number of theoretical works to understand crystal growth mechanism have been made. Especially, a great advancement was made by the excellent works of BCF theory (Burton *et al.* 1951) and computer simulations.

However, the progress in the experiments for that purpose has been much slow. This is because the phenomena in crystal growth are very complicated, and there is almost no tool to study it on an atomic scale.

MBE provides us a possibility to solve this difficulty and maybe the best tool among many kinds of growth methods. UHV environment and analytical facilities enable us to study the crystal growth mechanism on an atomic scale.

The purposes of the present thesis are to study elemental growth process in MBE on an atomic scale such as the incorporation into the step and kinks, and to present a new growth method on the basis of the study.

Firstly, in chapter 2, GaAs and related alloy semiconductors are grown under various conditions. Then surface diffusion and the degree of equilibrium at step edge are studied. In chapter 3, a new growth method called modulation MBE is proposed and the growth mechanism and advantages are investigated. In chapter 4, real time observations by SEM-MBE or μ-RHEED are made. Hence, the observation of various surface reconstructions, Ga and In droplet formation and disappearance, *etc.* are described. In chapter 5, an atomic model for facet formation is presented. Finally in chapter 6, conclusions are given.

Chapter 2

Growth Model of Molecular Beam Epitaxy

2.1 Introduction

MBE is one of the most powerful growth tools to realize a high performance devices with a high degree of crystal perfection because of its easiness both in controlling the film thickness and in obtaining an abrupt heterointerface. However, there has been a question about the growth mechanism of MBE why surface smoothness is accomplished with the insensitivity of the growth rate to the temperature and the substrate orientation. Many efforts to obtain surface diffusion length or surface diffusion coefficient have been made to account for this question (Neave *et al.* 1985, Ohta *et al.* 1988).

It is difficult to regard MBE as a simple deposition method in which every incident atom is incorporated immediately into the crystal without any reaction, because in such a simple way, the growth of single crystal like GaAs with stoichiometric composition and good quality can not be expected. Moreover, the surface segregation of impurity or one component of alloy semiconductor is well known to occur in MBE at relatively high growth temperature. These phenomena indicate that the atomic processes in the crystal growth are composed of surface migration of the growth elements and some kinds of reactions for which a quasi-equilibrium might be established at least at the growth point such as kinks in the steps.

There are some papers in which the thermodynamic technique is employed to study MBE process theoretically (Heckingbottom 1985, Seki and Koukitu 1986) and the result showed a good agreement with the experiment (Chika *et al.* 1986). But in these papers, the growth process is treated to occur only through solid-vapor phase as a whole, and there is no discussion about the atomic processes through which an

equilibrium is established.

The elemental growth mechanism of MBE has been extensively investigated theoretically and experimentally. Nishinaga and Cho (1988) have studied MBE growth of GaAs on GaAs vicinal surfaces according to the BCF theory (Burton *et al.* 1951) where the distribution of the surface diffusion atoms was obtained on the assumption that chemical equilibrium is established at the step edge. Clarke *et al.* (1989) and Irisawa *et al.* (1990) performed Monte Carlo simulations for MBE and found that nucleation occurs in the center region between steps with the assumption that the step acts as a more or less perfect sink. However, in the case of MBE, an evaporation flux calculated with the equilibrium vapor pressure of the growth element is usually much smaller than the incident flux, and it is possible that steps are not necessarily acting as sinks to establish the perfect chemical equilibrium.

Recently, Hata *et al.* (1990) reported that the diffusion length for atom incorporation is nearly 1μm, which indicates that the growth atom crosses many steps before it is incorporated into the crystal. This means that the capture rate of Ga by one step is much smaller than unity and the step edge concentration of the growth atom is far from equilibrium. However, in their experiment, the diffusion length of Ga was obtained by using the patterned substrate, and the growth condition might have been different from that of the usual planar substrate (Nisinaga and Suzuki 1991).

In the growth of III-V MBE where re-evaporation can be neglected, surface incorporation length of the group III element which is defined as a distance from the adsorption on the surface to the incorporation into the crystal is the most important to understand the growth mechanism, but it is a complicated function of many kinds of growth parameters, for example step density, step orientation, anisotropy of the surface diffusion, growth temperature, arsenic pressure and so on. So that, this situation makes it difficult to analyze the elemental growth process.

In this chapter, III-III-V alloy semiconductors and GaAs were grown on various vicinal surfaces at the temperature higher than the normal growth temperature for these materials where the re-evaporation of volatile III element is not negligible. In this situation, the incorporation of the diffusing atoms at the growth steps becomes a main process of the rate determining and the surface diffusion might play the minor role.

From the step density dependence of the alloy composition or the growth rate of GaAs, one can get a lot of information concerning the incorporation process at the step edges. Then we develop a theory to obtain the alloy composition and the growth rate, taking account of step kinetics as well as surface diffusion. By comparing the present theory with the experimental results, the degree of equilibrium at step edge is discussed in MBE of III-V compounds.

2.2 High Temperature Growth of III-III-V Alloy Semiconductors

A GaAs(001) orientated substrate within 0.5° and misorientated substrates with off angles of 2° and 5° tilted towards [110] and [1$\bar{1}$0] were typically used. After being degreased, they were chemically etched in a 7:1:1 (H_2SO_4:H_2O_2:H_2O) solution. Then they were mounted with indium on the same Mo block. After a removal of the native oxide of the substrate by heating up to 620°C under incident As_4 flux, GaAs buffer layer more than 300nm was grown at 580°C. Then the substrate temperature was set at the temperature higher than the normal growth temperature for III-III-V alloys. MBE growth was carried out by ULVAC-MBC300 for InGaAs and InAlAs, and by ULVAC-MBC508 for AlGaAs.

In the case of InGaAs and InAlAs, the growth conditions are chosen such as the flux ratio, F_{In}/F_{Ga} is 0.49/0.51 for InGaAs and F_{In}/F_{Al} is 0.52/0.48 for InAlAs. The growth rate and the thickness of layer are nominally about 0.7μm/h and 1.4μm respectively for both alloys. The growth thickness is much larger than the so-called critical thickness for the strain relaxation, hence one can neglect the effect of lattice strain in the following analysis. After the growth the concentration of In was determined by X-ray diffraction. For the growth of AlGaAs, the incident flux ratio F_{Al}/F_{Ga} is chosen as 0.133/0.867, the growth rate of 1.0μm/h and the thickness of layer of 1.0μm are nominally employed. After the growth the concentration of Al was estimated by PL measurements at 77K.

Figure.2-1(a), (b) and (c) show experimental results for InGaAs, AlGaAs and InAlAs respectively. It is difficult to reproduce substrate temperature accurately in many growth sequences. Therefore, the following method has been used to calibrate the growth temperature. Curve (1) in Fig.2-1(a) shows the dependence of the concentration of In on the growth temperature obtained from the periods of RHEED specular intensity oscillations in the growth of $In_xGa_{1-x}As$ (x=0.18) on a GaAs(001) substrate. With this curve, it is possible to get the curve (2) for x=0.49 with the thermodynamic theory (Seki and Koukitu 1986), and experimental results of InGaAs on GaAs(001) substrate were fitted to this curve (2). This curve (1) was also applied to the case of InAlAs to get a theoretical curve in Fig.2-1(c), to which the results of InAlAs on GaAs(001) were

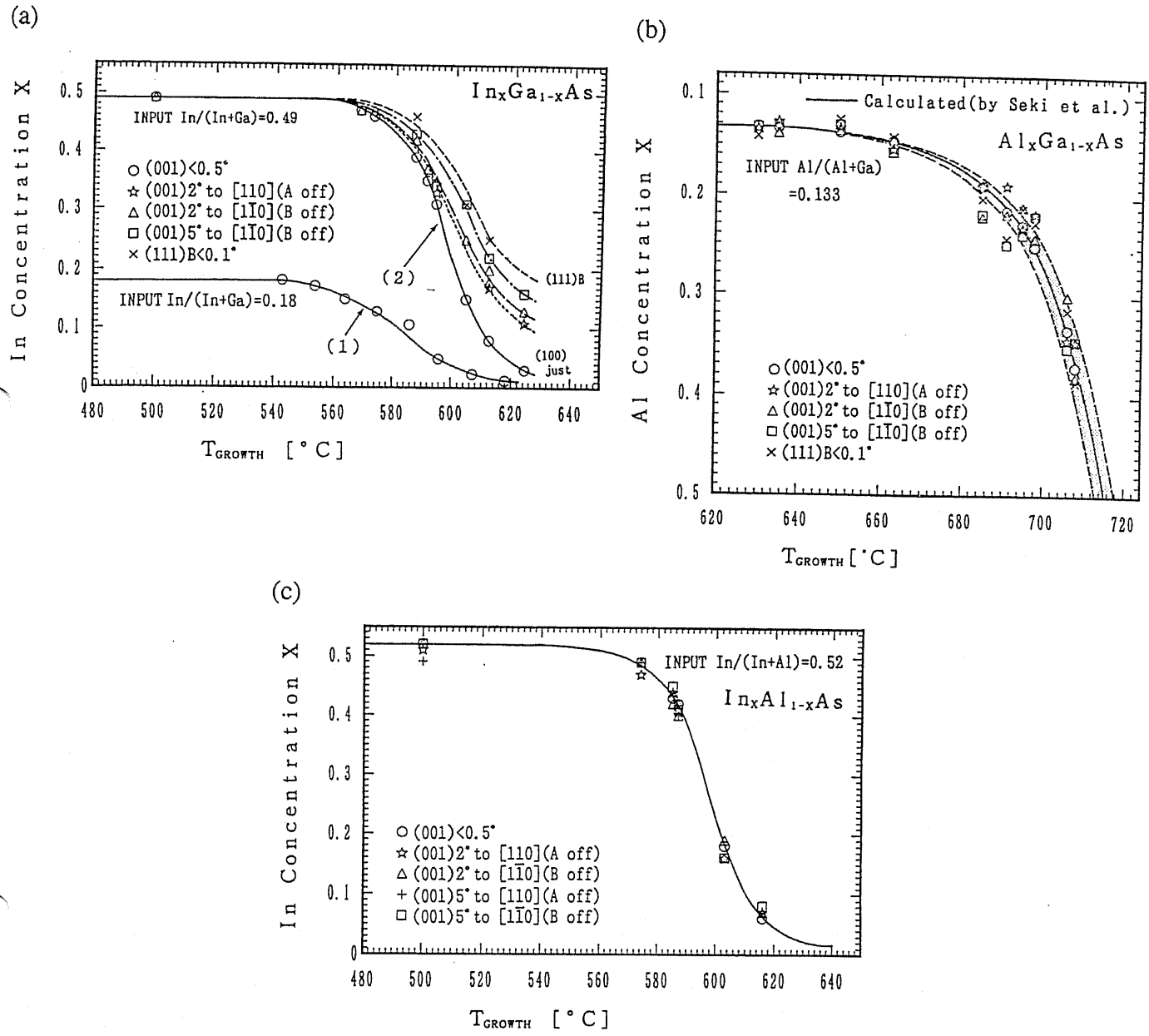

Fig.2-1. Substrate temperature and orientation dependence of (a)InGaAs, (b)AlGaAs and (c)InAlAs. Curve (1) in (a) shows experimental results on In concentration versus substrate temperature obtained by RHEED intensity oscillations and curve (2) shows the composition for x=0.49 after calibration. Shaded portion in (b) shows the range of the experimental error which comes mainly from the nonuniformity among the substrate temperatures on the same Mo Block (±2.5°C).

fitted. In this way, the true temperature for the set of substrates on one Mo block was determined. In the case of AlGaAs, the data of GaAs(001) is calculated by the thermodynamic theory with the parameter fitted to experimental conditions and the true temperature for the set of substrates was determined with the same technique employed for InGaAs. The concentration of In and Ga respectively in In contained systems and AlGaAs decreases rapidly with increasing the growth temperature because of the re-evaporation of In and Ga respectively. In the growth of InGaAs, however, In concentration has large orientation dependence which can not be explained by the thermodynamic theory and the following relationship is found in this experiment. Increasing the off angle at the same off axis, the concentration of In becomes higher, and at the same off angle (2°off) the concentration of In is higher for the substrate misorientated off to $[1\bar{1}0]$ than off to [110]. On the other hand, Ga concentration in AlGaAs and In concentration in InAlAs show no orientation dependence at all.

2.3 High Temperature Growth of GaAs

In this section, we investigate experimentally the Ga desorption rate on the vicinal surface as a function of step density to see to what extent the equilibrium is established in MBE of GaAs. In the experiments, the desorption rate is determined from the change of the growth thickness which is obtained by fabricating a GaAs single quantum well (SQW) structure and measuring the peak energy of PL.

Two GaAs SQWs with identical structures were grown sequentially, and consisted of the typical well width of 10nm sandwiched on both sides by a 5nm AlAs barrier layer. The first SQW was grown at a high substrate temperature where GaAs desorption was remarkable, whereas that of AlAs could be neglected, and the second was grown at a low temperature (580°C) where the desorption of both Ga and Al was negligible. No growth interruption was introduced, except in the case where the growth temperature was changed in the intermediate AlAs layer.

Experimental procedures and kinds of substrates were the same as described before. But a precisely (001) orientated substrate within 0.05° was used for GaAs(001). MBE growth was carried out by ULVAC-MBC300.

Figure.2-2 shows the typical relationship between growth rate and substrate temperature measured by the intensity oscillation of RHEED, where the incident electron beam was focused on the GaAs precise (001) substrate among the five substrates with different surface orientations. Above 670°C, the decrease of the growth rate became significant. However, this decrease was so rapid and sensitive to the substrate temperature that the data were scattered and appeared to contain relatively large errors. PL measurements were made at 77K, and the well width was determined by calculation employing a simple square potential model. All of the spectra showed two single peaks which correspond to the luminescence from the SQWs grown at high and low growth temperatures, respectively, as shown in Fig.2-3. The relative ratios of these two well widths calculated from PL peak energy are shown in Fig.2-4 as a function of off-angles of the substrates. Although no substrate rotation was performed, by employing these ratios it is possible to cancel the error introduced from the flux nonuniformity within the block.

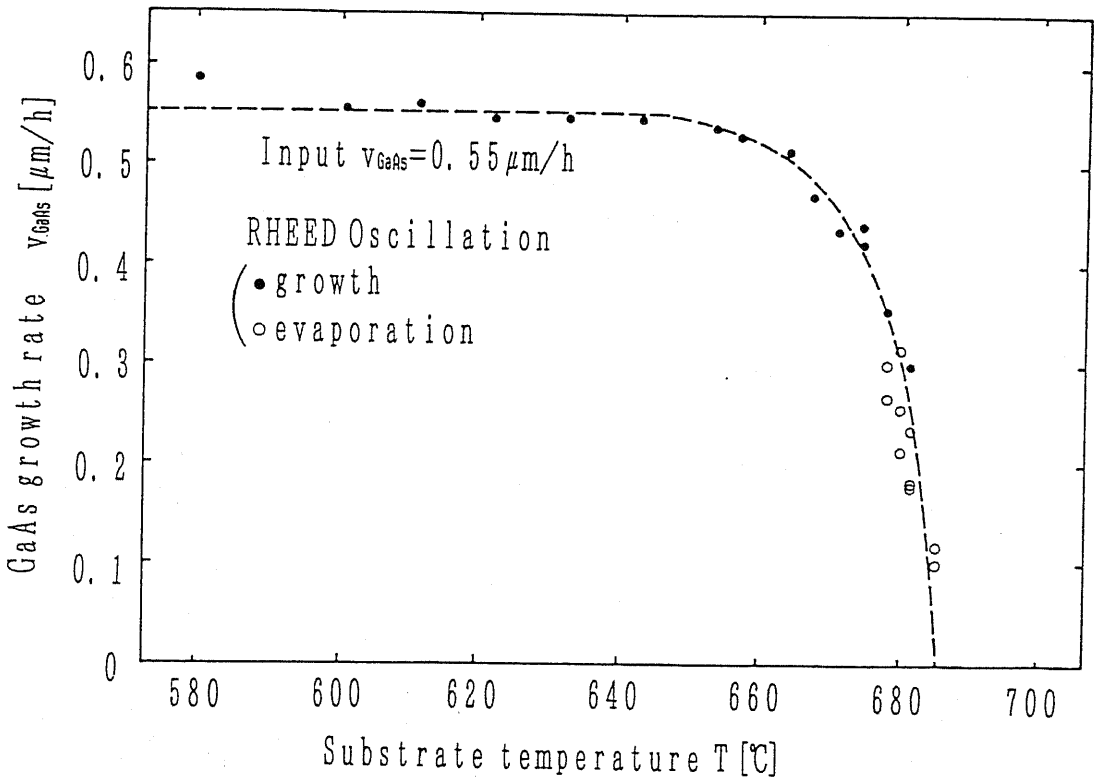

Fig.2-2. The typical GaAs growth rate on nominal (001) substrate vs the substrate temperature. The growth rate was obtained by the period of RHEED oscillations and is equal to the growth rate at low temperature minus the evaporation rate (Kojima *et al.* 1985, Van Hove *et al.* 1985).

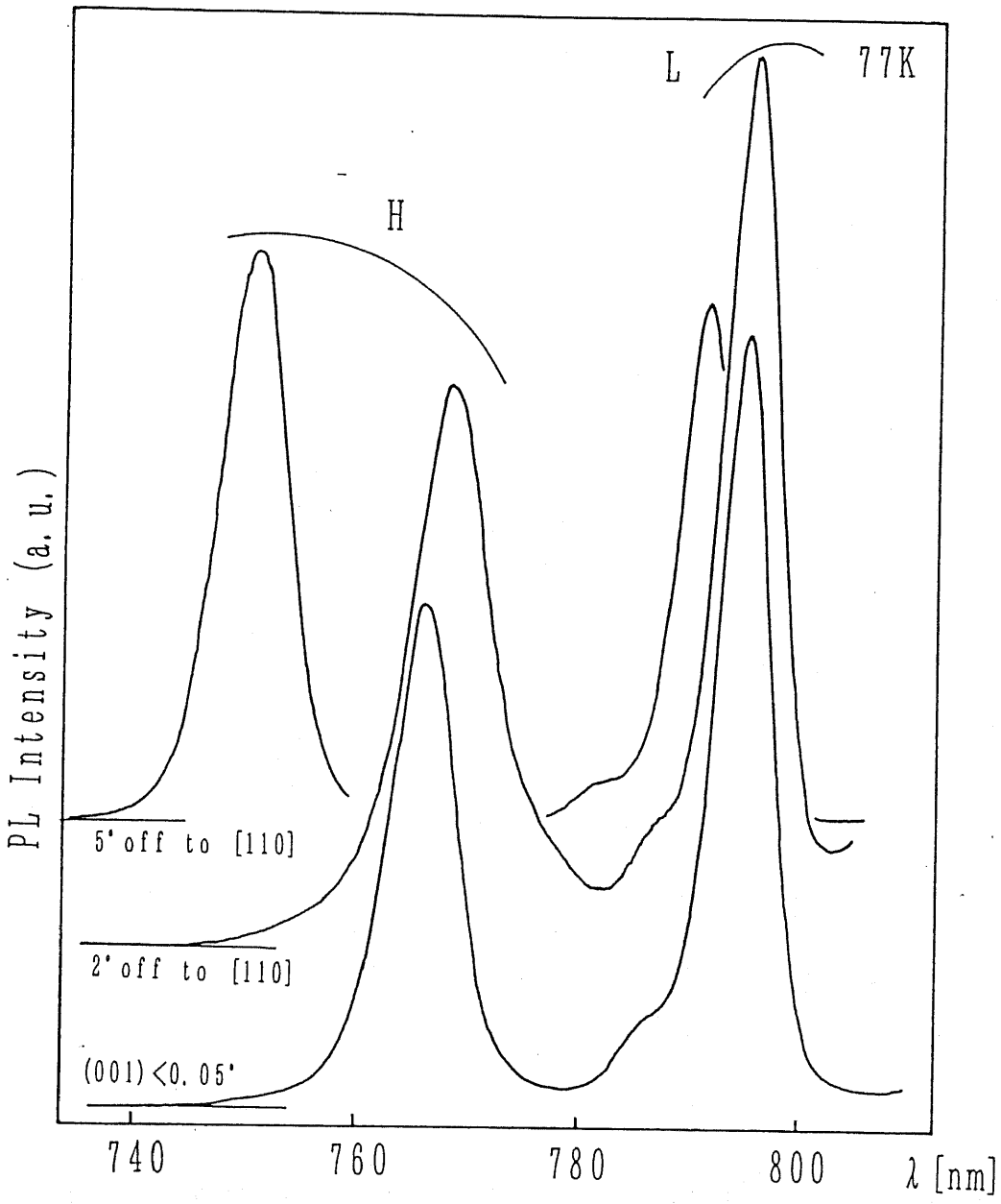

Fig.2-3. 77K photoluminescence spectra of SQWs. H and L correspond to the luminescence from SQWs grown at high (675°C) and low (580°C) temperature, respectively.

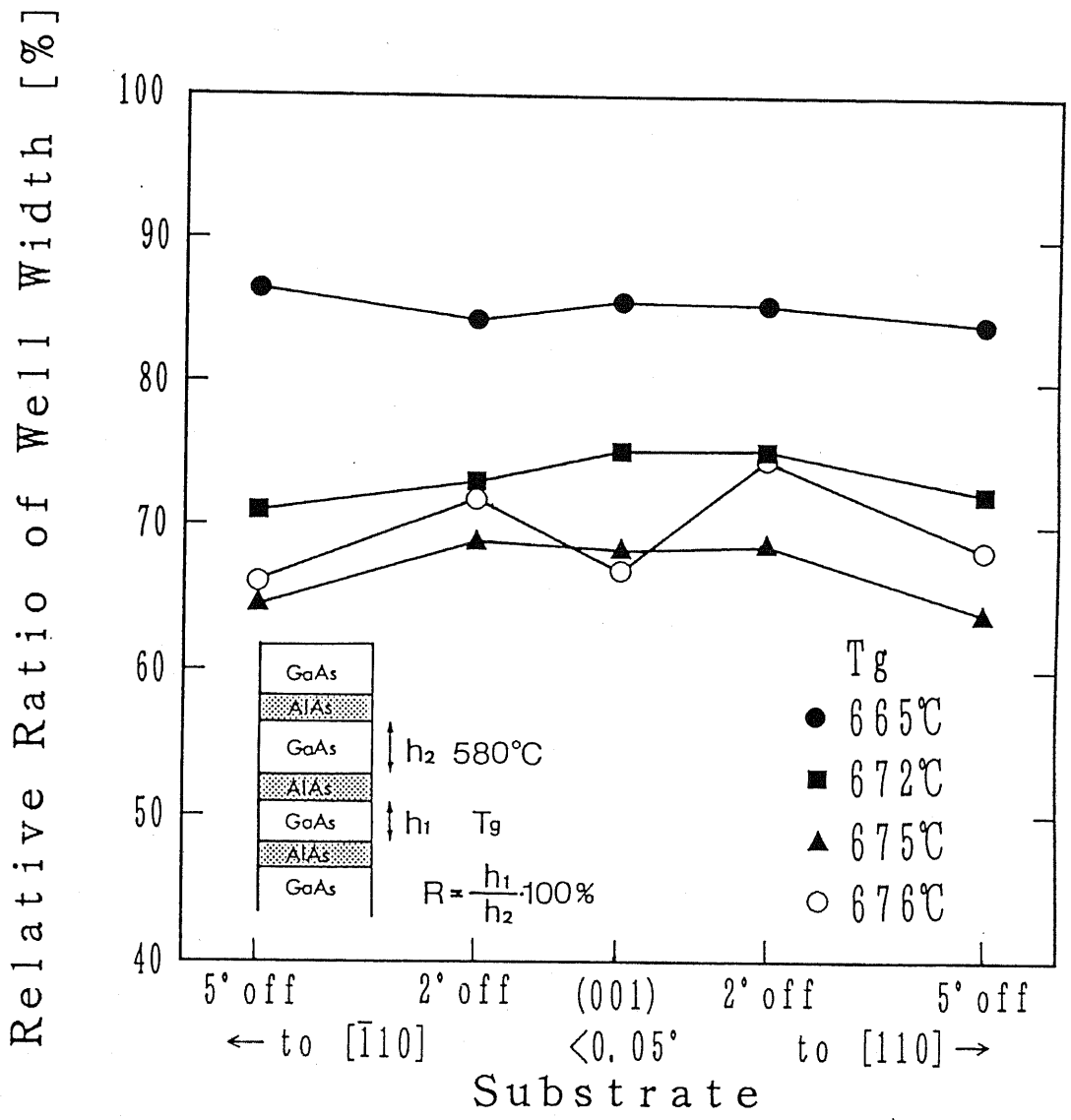

Fig.2-4. The ratio of high-temperature- to low-temperature-(580°C) grown well widths of SQWs as a function of off-angles from the (001) surface. The five substrates were mounted side by side and grown at the same time. The growth temperature indicated was calibrated by fitting the data of GaAs(001) to the curve of Fig.2-2 for lack of accurate reproducibility.

In this experiment, we used an almost precisely oriented GaAs (001) (<0.05°) substrate. When the substrate with even 0.5° misorientation from (001) was employed, it was found that there was no RHEED oscillation in the growth of GaAs on GaAs and AlAs at high growth temperatures. Moreover, it has been confirmed already that when AlAs was grown on such a substrate, RHEED oscillation is not evidenced again in this temperature region, although it is observed at low temperature (Tanaka *et al.* 1990). These clearly show that except for the precisely oriented substrate (<0.05°), the growth proceeds in a step-flow mode. Hence, it can be understood that experiments which afforded Fig.2-4 were carried out in a step-flow mode, and nevertheless, there was no clear dependence of GaAs desorption rate on step density within the sensitivity of the present experiment. The experimental error in Fig. 2-4 can be explained to stem mainly from the temperature nonuniformity in the block which is estimated within ±1.5°C by using Figs.2-2 and 2-4. On the other hand, time fluctuation of the substrate temperature which is estimated within ±1.5°C from Fig.2-2 is not so critical because it does not change the growth mode or affect the results.

2.4 Surface Diffusion Model Considering Step Kinetics

2.4.1 Basic Formulation

Figure.2-5 illustrates schematically the model of the present theory. An equi-distance step train on a vicinal surface is postulated. Therefore, the problem can be treated as one-dimensional. The surface diffusion equation is expressed as (Nishinaga and Cho 1988);

$$D_s \frac{d^2 n}{dy^2} + J^{in} - \frac{n}{\tau_s} = 0, \tag{2-1}$$

where n, D_s, J^{in} and τ_s, are respectively the concentration of adatoms, the diffusion coefficient, the flux incident to the growing surface and the resident time of adatoms. The third term in the left hand side denotes the re-evaporation flux. The solution of the above equation is given by (Shitara and Nishinaga 1989);

$$n(y) = J^{in}\tau_s + \left(n_{step} - J^{in}\tau_s\right)\frac{\cosh\left(\frac{y}{\lambda_s}\right)}{\cosh\left(\frac{\lambda_0}{2\lambda_s}\right)}, \tag{2-2}$$

with

$$\lambda_s = \sqrt{D_s \tau_s}, \tag{2-3}$$

where λ_s is the surface diffusion length and n_{step} is defined as;

$$n\left(y = \pm\frac{\lambda_0}{2}\right) = n_{step}. \tag{2-4}$$

With eq. (2-3), one gets the surface flux incident to the step edges $J^s(\lambda_0/2)$as;

$$J^s\left(\frac{\lambda_0}{2}\right) = -D_s \left.\frac{dn}{dy}\right|_{y=\lambda_0/2} = \left(J^{in} - \frac{n_{step}}{\tau_s}\right)\lambda_s \tanh\left(\frac{\lambda_0}{2\lambda_s}\right). \tag{2-5}$$

Here it is important to mention that the last expression derived by BCF theory (Bennema

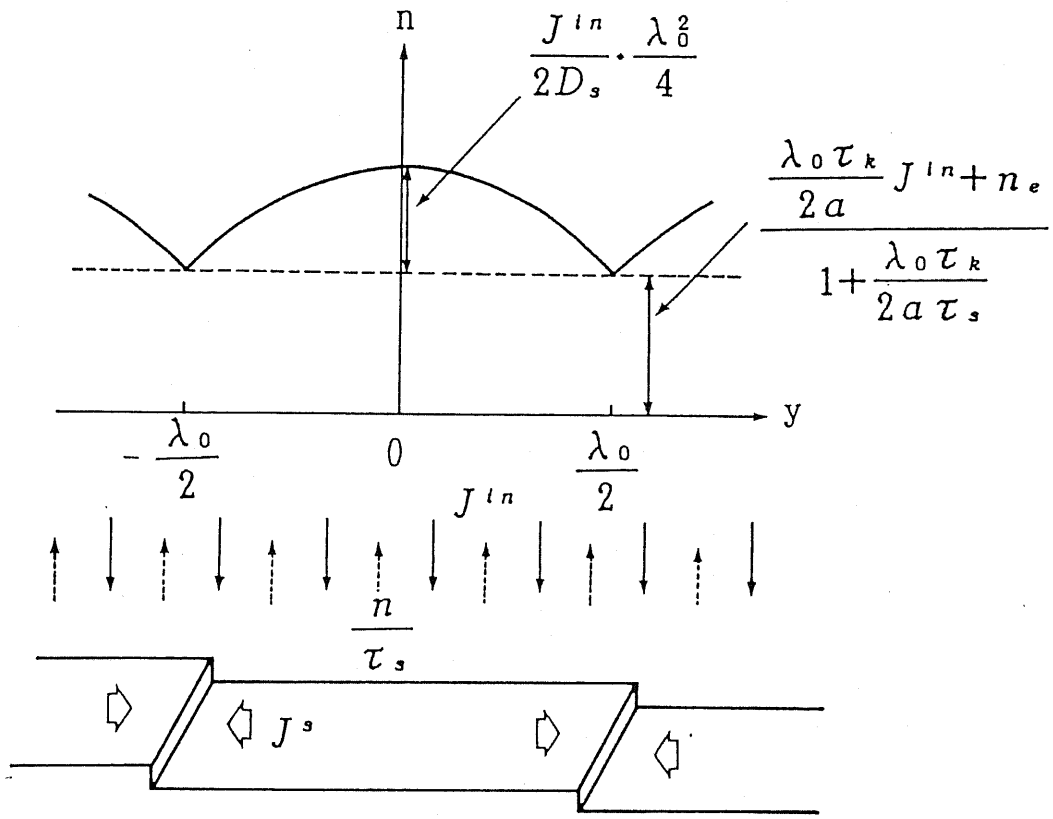

Fig.2-5. Schematic illustration of the present model with distribution of surface diffusion adatoms. An equi-distance step train is postulated.

and Gilmer 1973, Burton *et al.* 1951) contains the surface diffusion length which plays a major role. However, under usual MBE condition, and even if the re-evaporation is not neglected at rather high growth temperature, the residence time of the adatoms is longer than the time for diffusing atom to reach the step edge. Then, in most case, we can postulate the following condition,

$$\lambda_s >> \lambda_0. \tag{2-6}$$

From eq.(2-5) and the condition (2-6) we can obtain more simple form;

$$J^s\left(\frac{\lambda_0}{2}\right)=\left(J^{in}-\frac{n_{step}}{\tau_s}\right)\frac{\lambda_0}{2}. \tag{2-7}$$

In the next step, we define the concentration at the step edges, n_{step}. Hata *et al.* (1990) reported that the capture rate of Ga by one step was much smaller than unity by using the patterned substrate. It means that the step edge is far from the equilibrium and there is some potential barrier for adatoms to be incorporated into the crystal as shown in Fig.2-6. To include this process we introduce a parameter τ_k which governs the degree of deviation from the equilibrium at the steps, the inverse of which is the probability per unit time for adatoms within a jump distance to be incorporated into the step (Bennema and Gilmer 1973).

The flux into the step from one side on the surface is determined by the average number of adatoms within an elemental surface jump distance a (=4Å for GaAs). Since n_{step} is the number of adatoms per unit surface adjacent to the step, $n_{step}a$ is the number per unit step length and $n_{step}a/\tau_k$ is the number per unit step length per time going to the step from that side. On the other hand, the flux leaving the step is $n_e a/\tau_k$ where n_e is the equilibrium concentration of adatoms. Then the net flux incorporated into the steps is given by;

$$J^s\left(\frac{\lambda_0}{2}\right)=\frac{a}{\tau_k}n_{step}-\frac{a}{\tau_k}n_e\ , \tag{2-8}$$

where n_e is the equilibrium concentration of adatoms. From eqs.(2-7) and (2-8), n_{step} can be calculated and eq.(2-7) leads to;

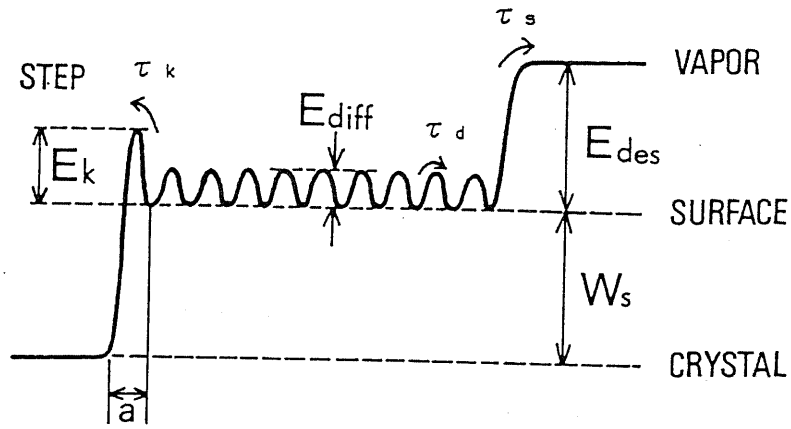

$$\tau_s^{-1} = \nu \exp\left(-\frac{E_{des}}{kT}\right)$$

$$\tau_k^{-1} = \nu \exp\left(-\frac{E_k}{kT}\right)$$

$$D_s = \frac{a^2}{\tau_d} = a^2 \nu \exp\left(-\frac{E_{diff}}{kT}\right)$$

$$\nu^{-1} \sim 10^{-13}\,\text{sec.}$$

Fig.2-6. Model of potential barriers for a growth unit to enter a crystal, assuming E_k is the same for the atoms entering from both of upper and lower sides of a step.

$$J^s\left(\frac{\lambda_0}{2}\right)=\left(J^{in}-\frac{n_e}{\tau_s}\right)\frac{1}{1+\lambda_0\tau_k/2a\tau_s}\cdot\frac{\lambda_0}{2}. \qquad (2\text{-}9)$$

In eq.(2-9), the first term expresses the macroscopical reaction between vapor and solid phase and agrees with the term which appears in the thermodynamic theory (Heckingbottom 1985, Seki and Koukitu 1986), and the second term denotes the role of the surface diffusion and the chemical reaction at the growth steps.

The concentration at the step edge is given from eqs.(2-7) and (2-8) as;

$$n_{step}=\frac{\tau_s}{1+\lambda_0\tau_k/2a\tau_s}\left(\frac{\lambda_0\tau_k}{2a\tau_s}J^{in}+\frac{n_e}{\tau_s}\right). \qquad (2\text{-}10)$$

2.4.2 Analyses of Experimental Results

To understand these two results of great contrast, we use eq.(2-9) to determine the alloy composition dependence on the growth temperature. In the case of InGaAs, In atom re-evaporates preferentially and the re-evaporation of Ga atom can be neglected. Then from eq.(2-9) one gets the concentration x in $In_xGa_{1-x}As$ as

$$x=\frac{J^s_{In}}{J^s_{In}+J^s_{Ga}}=\frac{\left(J^{in}_{In}-\frac{n_{eIn}}{\tau_{sIn}}\right)}{\left(J^{in}_{In}-\frac{n_{eIn}}{\tau_{sIn}}\right)\frac{1}{1+\omega_{In}}+J^{in}_{Ga}}, \qquad (2\text{-}11)$$

with

$$\omega_{In}=\frac{\lambda_0\tau_{kIn}}{2a\tau_{sIn}}, \qquad (2\text{-}12)$$

where subscripts mean the values for each atoms. From eq.(2-11) it is shown that as the step distance is increased at the same substrate temperature, the concentration of In is decreased and that as increasing the growth temperature which corresponds to decreasing the residence time τ_s, the step kinetics which is expressed by τ_k plays more important role in determining the alloy composition. Hence, from the alloy composition which contains the combined process of the re-evaporation and the incorporation, the

ratio $\tau_{kIn}{}^{B}/\tau_{sIn}$ can be calculated from the experimental data and is shown in Fig.2-7 where $\tau_{kIn}{}^{B}$ means the value for $[1\bar{1}0]$ off surface. The activation energy of $\tau_{kIn}{}^{B}/\tau_{sIn}$ was found as 5.3±0.8eV which contains desorption energy of In and step incorporation energy. Since τ_{kIn} depends on the structure of the step, $\tau_{kIn}{}^{A}$ for the surface off to [110] is not necessarily equal to $\tau_{kIn}{}^{B}$. Actually, $\tau_{kIn}{}^{A}$ is found to be larger than $\tau_{kIn}{}^{B}$ qualitatively.

With this $\tau_{kIn}{}^{B}/\tau_{sIn}$, n_{step}/n_e can be calculated by eq.(2-10) and is shown in Fig.2-8 as a function of $1/T$. Although the points are scattered somehow, clear tendencies are seen in the figure. Namely, n_{step} approaches to n_e as the growth temperature and the angle of misorientation are increased. The former is simple to be understood and the latter is clear since the higher density of the steps, in other words, the larger number of the reaction sites drives the reaction forward to the equilibrium.

Since the re-evaporation of Al can be neglected for AlGaAs and InAlAs, we can get an expression like eq.(2-11) for the composition of AlGaAs and InAlAs on the analogy of InGaAs. However, in the both cases, the experimental results show no dependence of alloy composition on the off angle as well as the crystal orientation. As for these alloy semiconductors which contains Al as one composition, it has been known that surface roughening is induced due to the strong bond between Al and As. In the present experiments, significant re-evaporation of Ga or In results in high concentration of Al in alloy composition. Hence, it is reasonable to suppose that there exist steps with higher density due to large number of nucleus than the original one. Actually in the growth of InAlAs, RHEED pattern showed dim spotty feature. This means growth of step flow mode was not established.

Assuming that the number of steps on the surface becomes infinitely large and hence λ_0 becomes nearly zero, we get

$$x = \frac{J_{Al}^{s}}{J_{Ga}^{s} + J_{Al}^{s}} = \frac{J_{Al}^{in}}{\left(J_{Ga}^{in} - \frac{n_{eGa}}{\tau_{sGa}} \right) + J_{Al}^{in}}, \qquad (2\text{-}13)$$

and

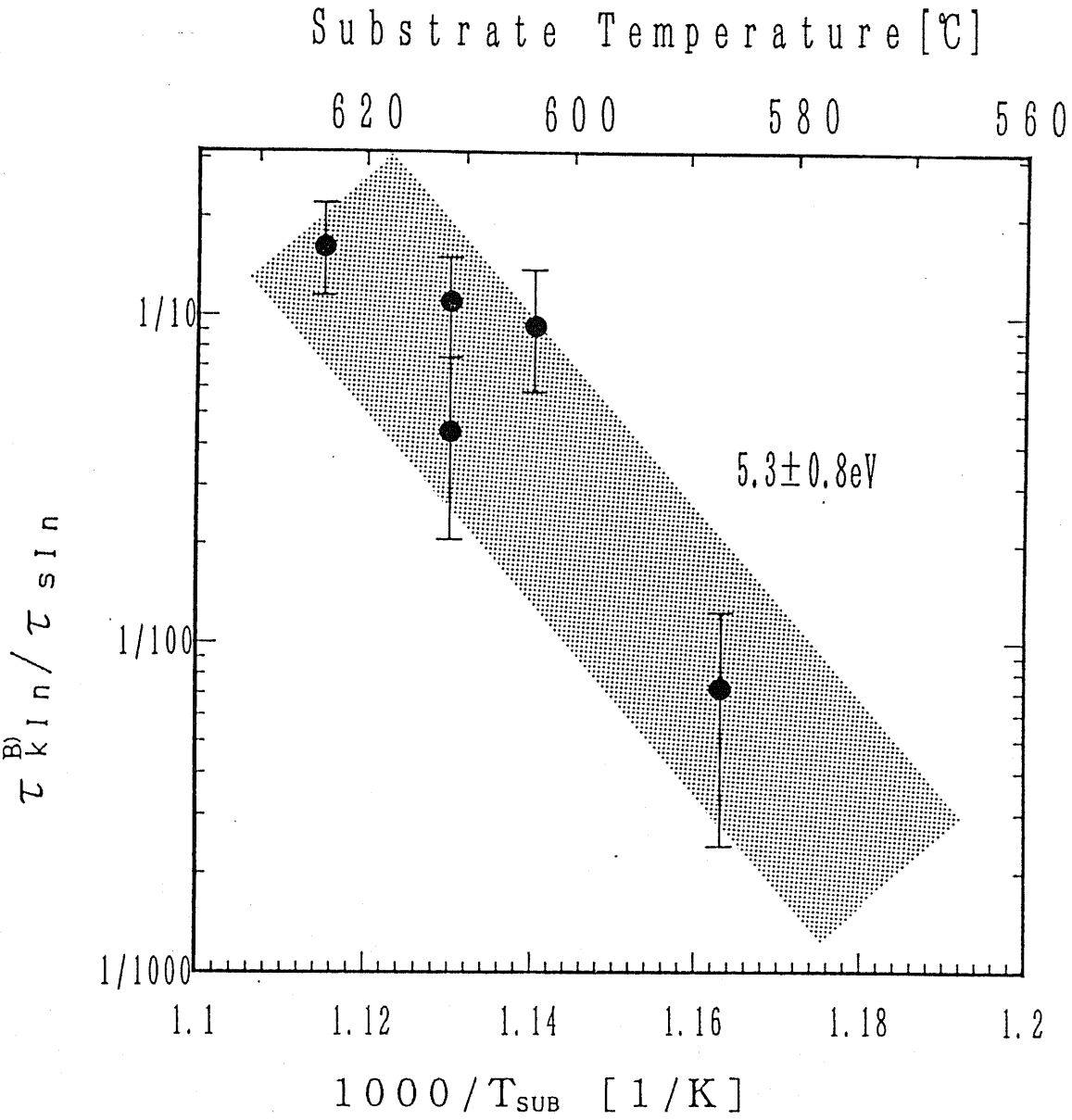

Fig.2-7. $\tau_{kIn}{}^{B}/\tau_{sIn}$ versus growth temperature in the InGaAs obtained from experimental results with the substrates of GaAs(001) 2°, 5° off to [1$\bar{1}$0]. The experimental error bar corresponds to the nonuniformity among the substrate temperatures and the activation energy was found to be 5.3±0.8eV.

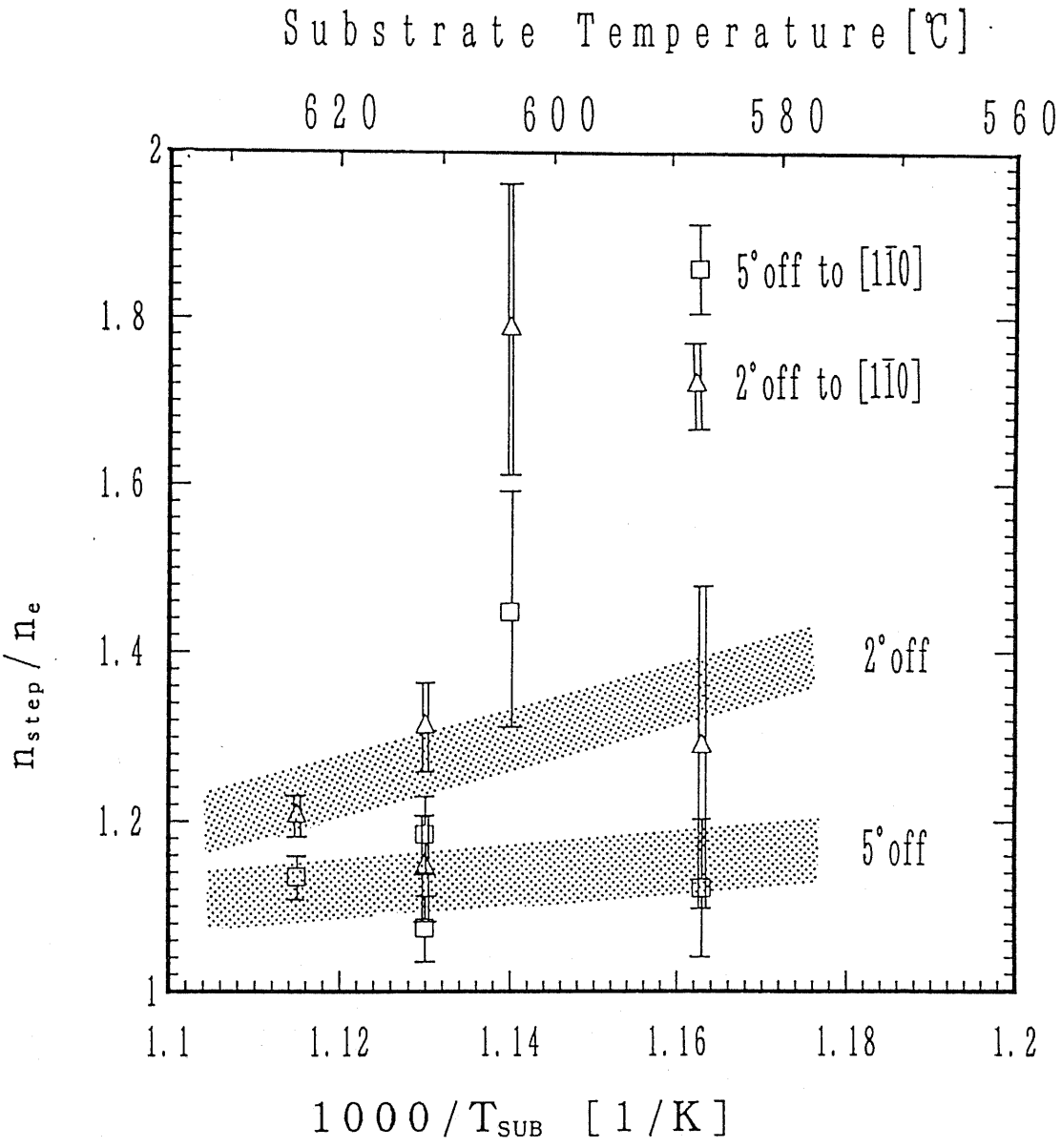

Fig.2-8. n_{step}/n_e versus. $1/T$ for In on B-surface. As the temperature and the angle of misorientation is increased, n_{step} approaches to n_e.

$$x = \frac{J_{In}^{s}}{J_{In}^{s} + J_{Al}^{s}} = \frac{J_{In}^{in} - \frac{n_{eIn}}{\tau_{sIn}}}{\left(J_{In}^{in} - \frac{n_{eIn}}{\tau_{sIn}} \right) + J_{Al}^{in}}, \qquad (2\text{-}14)$$

for $Al_xGa_{1-x}As$ and $In_xAl_{1-x}As$ respectively.

Eqs.(2-13) and (2-14) take the same expression as what the thermodynamic theory gives and it shows no dependence on the substrate orientation in agreement with the experimental results. However, this result does not necessarily mean that equilibrium is established only at the step edges like the case of GaAs discussed below. Increase of the step density makes the incorporation process closer to equilibrium between vapor and solid phase as a whole.

Next we discuss about the experiment of GaAs growth. Using eq.(2-1), we can obtain the expression for the vertical growth rate, v, as

$$v = J^{s}\left(\frac{\lambda_0}{2}\right)\frac{2h}{\lambda_0 n_0} = \left(J^{in} - \frac{n_e}{\tau_s} \right)\frac{h/n_0}{1 + \lambda_0 \tau_k / 2a\tau_s}, \qquad (2\text{-}15)$$

where n_0 and h are the number of atomic sites per unit area and the step height, respectively, and the factor 2 appears since the incident flux to the steps enters from two directions. As we have seen in the experimental results, the growth rate was independent of step distance λ_0. Since each v lies in the range within ±5% in Fig.2-4, we can obtain $\lambda_0\tau_k/2a\tau_s$ less than 5×10^{-2}. If we evaluate the maximum supersaturation at the step, it is given safely as

$$\frac{n_{step}}{n_e} - 1 < 0.2. \qquad (2\text{-}16)$$

However, 0.2 includes not only the factor due to the nonuniformity of the substrate temperature as mentioned before, but also that due to the uncertainty in the step distance for the precisely oriented substrate. Hence, the real supersaturation must be much smaller than 0.2. This means that the Ga concentration at the step in GaAs MBE is very close to the equilibrium concentration in this experimental range.

The present results show that in MBE, which is believed to be carried out under

nonequilibrium conditions, the growth step of GaAs in this temperature region behaves as an ideal step for adatoms at which they always take an equilibrium value. This fact agrees with the previous work which assumed the step-edge equilibrium and employed the BCF theory (Nishinaga and Cho 1988). Moreover, in the previous work, it was shown that the diffusion length was much longer than λ_0. The present results confirmed this independently. As compared with the case of InGaAs where nonequilibrium at the step is clear, it is suggested that the difference between InGaAs and GaAs might be due to the well-known In segregation effect in GaAs because In has a larger radius as compared with Ga (Guille *et al.* 1987).

It means that In atom is more difficult to be incorporated into the crystal (steps) than Ga atoms and it passes over or be reflected back at the step edges more frequently than Ga in the growth of GaAs. In other word, the difference exists in the degree of equilibrium established at the step edge, namely, Ga in GaAs is expected much more closer to an equilibrium than In in InGaAs.

2.5 Summary

MBE experiments at high growth temperature growth reveal that the solid composition of InGaAs depends very much on the degrees of the off angle and the off axis, however that of AlGaAs and InAlAs does not show any off angle dependency within an experimental error. This clearly indicates that the step kinetics plays an important role in the growth of MBE.

In order to investigate step density dependence of Ga desorption rate in GaAs, two GaAs SQWs have been grown sequentially on vicinal substrates by varying the growth temperature; the first at high growth temperature where the desorption of Ga was significant, and the second at low growth temperature where the desorption was negligible. From the ratio of the first to the second well widths calculated from the PL peak energy, it was found that the desorption rate of GaAs was independent of step density.

A theory is developed to understand the growth of III-V alloys taking account of the step kinetics in addition to the surface diffusion. By comparing the experiment with the theory, following results are concluded. InGaAs growth experiment shows that there is a segregation dependency of In which means a certain amount of supersaturation exists and the supersaturation ratio was found of the order of 1.5. In the alloy semiconductors of AlGaAs and InAlAs, simultaneous formation of 2D or 3D nucleation introduces many steps whose density is more than the original density of GaAs and makes the incorporation process close to the equilibrium. In the case of GaAs, it is shown that the equilibrium or near-equilibrium at the step edge with the supersaturation ratio of less than 1.2 is established. All of these experiments show that near-equilibrium is established at the step edges under relatively high temperature growth condition in MBE.

Chapter 3

Modulation Molecular Beam Epitaxy under Low As Pressure

3.1 Introduction

MBE has been used to fabricate many kinds of quantum structure because of its controllability and easiness to grow abrupt interfaces in the GaAs-AlAs system. However, increasing demands to make more exploratory and/or complicate devices that are greatly sensitive to the flatness of the interface, require to grow perfect interface. To meet these demands, so far several methods have been suggested as follows.

Growth interruptions have been suggested to improve the heterointerface (Sakaki *et al.* 1985) and have been employed widely to grow the quantum well structure, especially for AlAs on GaAs interface. In this method, the supply of the group III atom is stopped for a while at the interface under sufficient As flux. The mechanism of the smoothing effect is explained by the fact that under the absence of Ga flux the growth of large islands occurs by adatom detachment from the smaller islands and this greatly reduces the density of growth step. Such a picture is supported by in-situ RHEED where the specular beam intensity shows good recovery during the interruption, which indicates a reduction of the step density. Moreover, in the case of the GaAs on AlAs almost no improvement is found at the normal growth temperature (around 600°C). This also supports the above picture because the adatom detachment process is not possible owing to the Al-As strong bond. More recently, the direct observation by transmission electron microscopy (TEM) and STM was made, which showed the improvement of interface flatness by the growth interruption. However, in this method the diffusion on the As covered surface is important rate determining process, which is rather difficult to occur at low temperature as shown by RHEED oscillation measurement on the vicinal surface (Neave *et al.* 1985). Hence, this method is

applicable only for an appropriate growth temperature range depending on the materials (Tanaka and Sakaki 1988).

It has been reported by Sekiguchi *et al.* (1991) that with no growth interruption, but with a very careful adjustment of As_4/Ga flux ratio, SQWs grown by conventional MBE at 350°C exhibited a sharper PL linewidth than SQWs with one-atomic-layer fluctuation. They have interpreted that both of the upper and the bottom interfaces of QW grown at low temperature are equivalent to be pseudo-smooth where the lateral terrace size is much smaller than the exciton diameter and this gives PL emission with sharp peaks from both of the pseudo-smooth interfaces.

On the other hand, MEE has been used to fabricate quantum structures at low temperatures (Horikoshi *et al.* 1986, 1988, Horikoshi and Kawashima 1988a, 1988b). In this method, group III and group V elements are supplied alternately. This produces an alternate change of the surface from Ga-rich to As-rich and gives a persistent intensity change of the RHEED specular beam. A good crystal quality given by this technique at low growth temperature offers a great advantage to make a sharp doping profile and to grow heteroepitaxy system with a large difference of thermal expansion coefficient (for example GaAs on Si).

Another type of modified MBE called ALMBE has been proposed. In this case, only group V is supplied intermittently whereas incident flux of group III is kept constant like conventional MBE (Briones *et al.* 1987a, 1987b, 1989). This method also gives persistent changes of both the RHEED pattern and the specular beam intensity. A similar modification of the incident flux is employed by another groups to grow QWs (Longenbach *et al.* 1991) and GaAs on Si system at low temperature.

Among those growth methods such as MEE and ALMBE, much attention is paid to deposit the group III element *without any atmosphere of the group V element* in order to get a large diffusion length of the group III element. However, in the usual MBE apparatus which uses a solid As source, there remains As pressure even with the shutter closed, which must give a great influence to the interface and the crystal quality in this sense. On the other hand, the formation process of Ga droplets observed by SEM-MBE showed that *large diffusion length of Ga atom is realized on the (4×2) Ga-stabilized surface* (Inoue 1991, Osaka *et al.* 1990a, 1990b).

Although at the usual growth temperature around 600°C, shuttering off As beam makes the surface Ga-stabilized, it is necessary to note that an elimination of As flux is not always essential to obtain the Ga-stabilized surface. When the flux of As is reduced less than the equivalent flux of the group III during the growth, the group III stabilized surface can be kept even under As atmosphere. Therefore, this idea leads to a new possibility to get a long migration length of group III atoms even with simultaneous supply of group V element. The idea of the present work is based on this fact and we propose a new modified MBE technique, called "Modulation MBE" (M-MBE) where all the growth is carried out on a group III stabilized or group III rich surface by intermittent supply of group III element under a constant pressure of As. The growth mechanism involved in this technique is studied by using RHEED for a wide range of growth temperature. Then, we apply this technique to the system of heteroepitaxy and the flatness of the interface is investigated by optical measurements.

3.2 Experimental Procedure of Modulation MBE (M-MBE)

Figure 3-1(a) shows the schematic flux sequence of M-MBE comparing with that of MEE (Fig.3-1(b)). The characteristic points of this method are given as follows:

(a)Flux plus of group III element (Ga or Al) is supplied intermittently in the same manner as MEE. The amount of this pulse is chosen as 1 monolayer (ML) (6.3×10^{14}atom/cm^2 for GaAs or AlAs (001)), however, this value is not essentially important at least for GaAs growth as shown later. The time width of the pulse is $t_{Ga(Al)}$.

(b)Relatively low pressure of As_4 is applied continuously so that the flux ratio $F_{As4}/F_{Ga(Al)}$ takes a value less than 0.5 when the shutter of group III is opened (Foxon and Joyce 1977).

(c)The interval time, Δ_t between each flux pulse of group III element is chosen longer than Δ_{min} which is the minimum interval time needed to produce a periodic change of RHEED pattern. This value depends on both the substrate temperature and As_4 flux as shown later.

The growth under low As_4 pressure is one of the most characteristic points in this method, which provides the periodically rich condition of group III element on the growing surface although the shutter of As is always kept open. Beam modulation of group III elements has a great advantage technically compared with MEE or ALMBE where the flux of As must be modulated. This is because in the conventional MBE which uses solid source, the beam of As_4 incident on the substrate is very difficult to control due to an instability of solid As source in the crucible. This instability takes place in both of the short term in a day of the experiment and the long term from the full to the near empty of the As source. Moreover, there is a high background pressure of As even the shutter is closed. In order to obtain the big ratio of ON/OFF beam equivalent pressure and to reduce the As pressure during the opening time of group III elements, specially designed effusion cell (Briones *et al.* 1987b) or a method to put a waiting time before the opening of group III source (Horikoshi and Kawashima 1989a) are employed in ALMBE and MEE. However, we need not to worry about these points

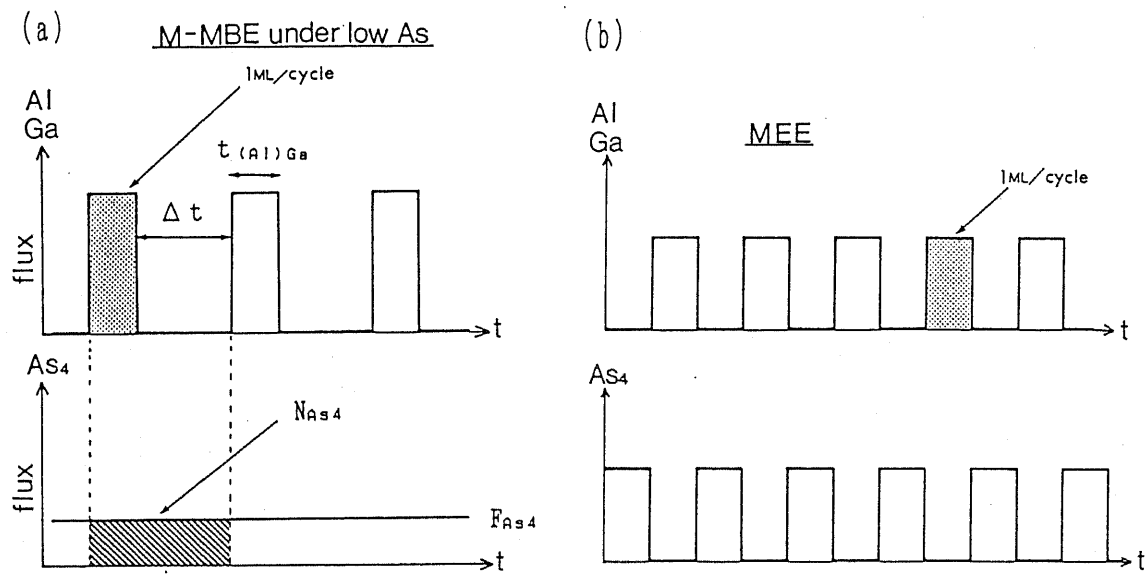

Fig.3-1. Schematic flux sequence of (a)M-MBE and (b)MEE.

in M-MBE and hence, M-MBE has a good compatibility with the conventional MBE system.

In this paper, we employ a typical flux value which is about one-tenth as small as the As flux in usual MBE growth. This keeps background very low, for example in our system, the ion gauge located at the top of ion pump indicates on the order of 10^{-10} Torr constantly during the growth.

The flux of group III element is calibrated by the oscillation period of RHEED intensity in the normal MBE growth mode and that of As_4 is obtained from the RHEED oscillation which is observed during As_4 incorporation process in the excess Ga (Neave *et al.* 1984) at 400°C, where the period is almost independent upon the substrate temperature and show the maximum growth rate. This kind of oscillation has been reported (Lewis *et al.* 1986, Garcia *et al.* 1989) and more precise description will be described in the section 4.5.

Here, we introduce the parameter, p as follows;

$$p = \frac{t_{Ga(Al)} + \Delta_t}{t_{As_4}} \qquad (3\text{-}1)$$

where t_{As4} is the RHEED oscillation period of the As_4 incorporation which is inversely proportional to its growth rate while $t_{Ga(Al)}+\Delta_t$ is the period of the pulse modulation which is inversely proportional to the growth rate in M-MBE mode. As we select 1ML for the amount of III-element pulse flux per cycle, the total growth rate in this method, v (ML/s), is expressed as;

$$v = \frac{1}{t_{Ga(Al)} + \Delta_t}. \qquad (3\text{-}2)$$

The parameter, p indicates the ratio of the total amount of V to III elements, and it is analogous to the V/III flux ratio, in the normal MBE. Therefore, p=1 is a critical condition for the growth under an excess Ga condition (p<1) and an excess As_4 condition (p>1). It should be noticed that p is the total V/III flux ratio integrated in the long term, so that in this growth method, flux modulation provides a Ga-rich and a As-rich conditions alternately in the short term periodically.

When we assume that GaAs is produced by a reaction of one As_4 molecule and

two Ga atoms as suggested by Foxon and Joyce (1977), the flux of As_4, F_{As4} is expressed as;

$$F_{As_4} = \frac{n_0}{2 \times t_{As_4}}$$

$$= \frac{N_{As_4}}{t_{Ga} + \Delta_t} \qquad (3\text{-}3)$$

where n_0 and N_{As4} denote respectively the density of the surface site on GaAs(001) and the amount of As_4 molecules incident to the unit surface area during one cycle. We use this definition for As_4 flux afterwards.

Growth was carried out on GaAs(001) substrates (<0.5°) in the conventional MBE system with a solid source. RHEED measurements were done under the condition of 20kV beam voltage with [110] azimuth. After the removal of native oxide by heating the substrate up to 620°C under As_4 flux, a GaAs buffer layer with the thickness more than 300nm was grown at 580°C under normal MBE condition and then the temperature of As_4 cell was decreased to about 50°C under and after that, RHEED intensity measurements were performed. The temperature of the substrate was monitored by the thermocouple at the back side of Mo block and by the optical pyrometer.

3.3 Experimental Results——Homoepitaxial Growth

3.3.1 Growth of GaAs

Firstly, we investigated RHEED intensity change and surface reconstructions. Figure 3-2 shows the typical RHEED data during the growth of GaAs on GaAs at 580°C with t_{Ga}=1.7 s, Δ_t=8.5 s and F_{As4}=1.0×10^{14}molecules/cm^{2}s. In this case p is 3.4 and a persistent and periodic change of both the RHEED intensity and the surface reconstruction has been be observed. Just after the opening of Ga shutter, the intensity of the specular beam soon becomes dark and a sharp change of the RHEED pattern to Ga-stable (4×2) structure is observed. This reconstruction is kept for a while after the end of Ga pulse and a sudden recovery to the original reconstruction, (1×1) or (3×1) is observed, which is believed to have lower As coverage than As-stable (2×4) surface (Inoue 1991). Here, we have chosen the As flux so low that the RHEED pattern does not show As-stable (2×4) surface at the growth temperature of 580°C. Therefore, in this growth method the surface is kept under Ga rich condition throughout the growth. This is different very much from MEE condition where the surface always comes back to As-stable one under As flux.

From the fact that the original surface has very low As coverage and that the opening of the Ga shutter changes the surface suddenly to Ga-rich pattern, we can assume that Ga pulse produces the Ga droplets on the surface and these Ga droplets are annihilated under As pressure after the termination of Ga supply and these processes are repeated. This model is confirmed by directly observing the Ga droplets creation/annihilation processes accompanied by a domain formation of the surface reconstruction by MBE equipped with a SEM as shown in chapter 4. Moreover, it will be described that the number of Ga droplets is not changed but only the size increases during the Ga supply. The amount of Ga in each Ga pulse is not necessary to be 1ML strictly in this method for this reason.

Another characteristic point of this method is that with an adequate interval time, Δ_t, the specular beam intensity becomes much brighter than the initial one in contrast to MEE and conventional MBE, in which the intensity of the specular beam gets always darker during the growth. In a first few cycles, the maximum beam intensity just before

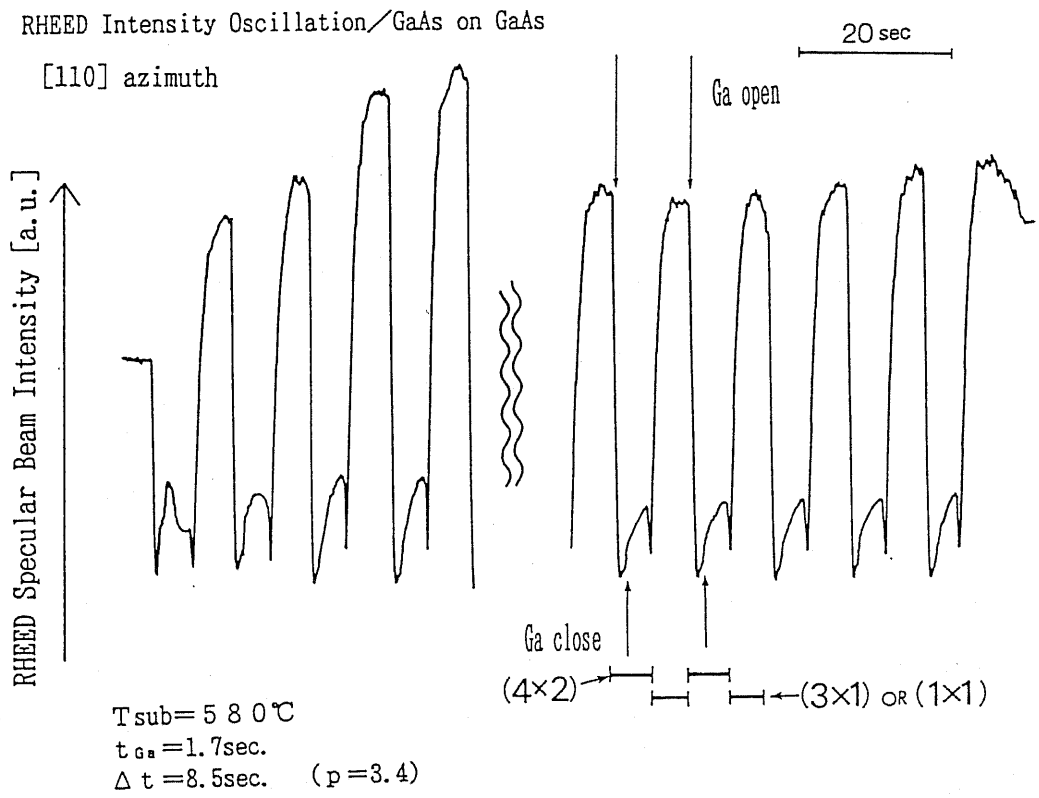

Fig.3-2. Typical RHEED intensity of specular beam during the growth of GaAs on GaAs at 580°C. The azimuth of electron beam is along [110]. Surface reconstructions are also indicated.

the opening of the Ga shutter, increases and reaches the steady state. This is always observed at 580°C, which indicates that the surface showing the maximum beam intensity is different from the steady state surface before Ga shutter opening. When the shutter is kept closed, the intensity decreases gradually and reaches the initial one. If we postulate that the intensity depends only on the step density, it is said that the surface with less step density than the original surface can be obtained using this growth method. However, it has been pointed out that the intensity contains the information of not only the step density but also the surface structure and diffraction process, *etc.* (Zhange *et al.* 1987). Hence, the situation might not be so simple.

The idea of growth interruption is believed to be one of the methods to obtain the sharp heterointerface, where growth is stopped at the heterointerface by shuttering off the group III element under group V beam flux. In this respect, M-MBE can be said to be *a growth interruption method at the every monolayer*. However, there are a few different points from the normal growth interruptions. Since the As pressure is lower than usual MBE condition, the recovery of the specular beam intensity is much faster than the growth interruption technique, which indicates the quick recovery of the flatness (Fig.3-3). Another different point is that there is a change of the surface reconstruction.

When the interval time is less than Δ_{min}, the RHEED intensity never recovers as shown in Fig.3-4(a) for p=1.2. This is because the next Ga pulse is incident to the surface before the Ga droplets are consumed by As, and Ga droplets are formed. Figure 3-4(b) is the example of the critical condition (p=2.2) where Δ_t is equal to Δ_{min}. Although the Ga droplets are consumed just in one cycle, the intensity recovery is not enough so that it shows very unstable behavior. In this condition, the period of (4×2) Ga-stable surface reaches 70-80% of the entire growth time.

A similar persistent change of RHEED intensity is observed even at low temperature such as 300°C (Fig.3-5). At this temperature, the intensity becomes to show a different profile from those obtained at 580°C. The RHEED intensity now increases during the Ga pulse and after closing the shutter, it decreases to the initial value. The surface shows (1×1) RHEED pattern with a sharp specular beam through the growth. This feature is always observed even if Δ_t is changed from 1.5 s (p=1.16).

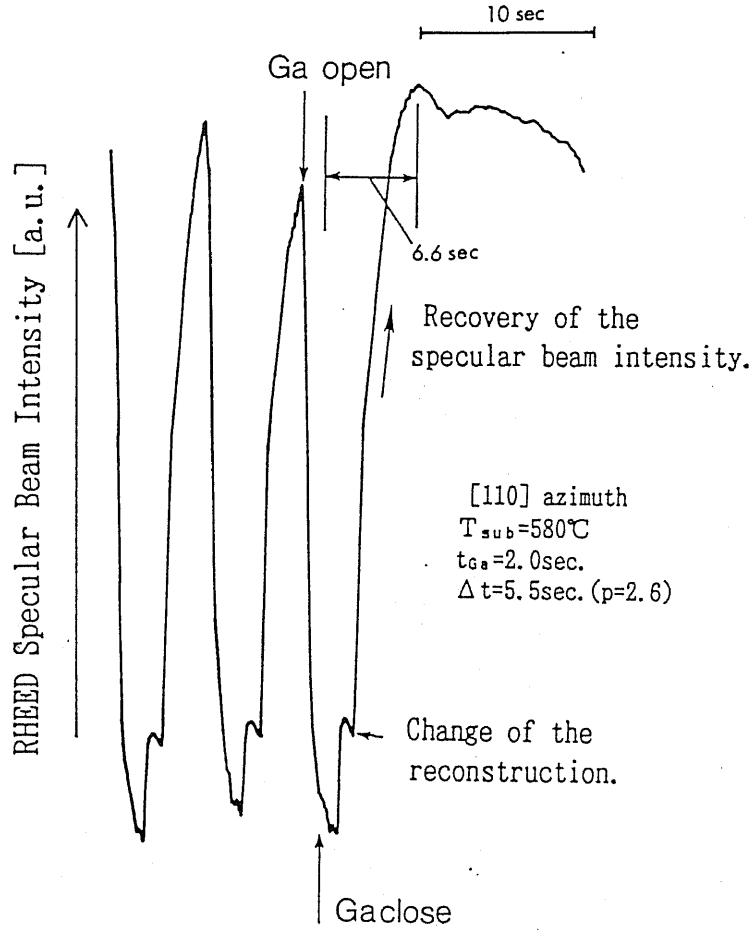

Fig.3-3. Specular beam intensity profile after stopping the Ga pulse. There are a change of the reconstruction and quick recovery of the intensity.

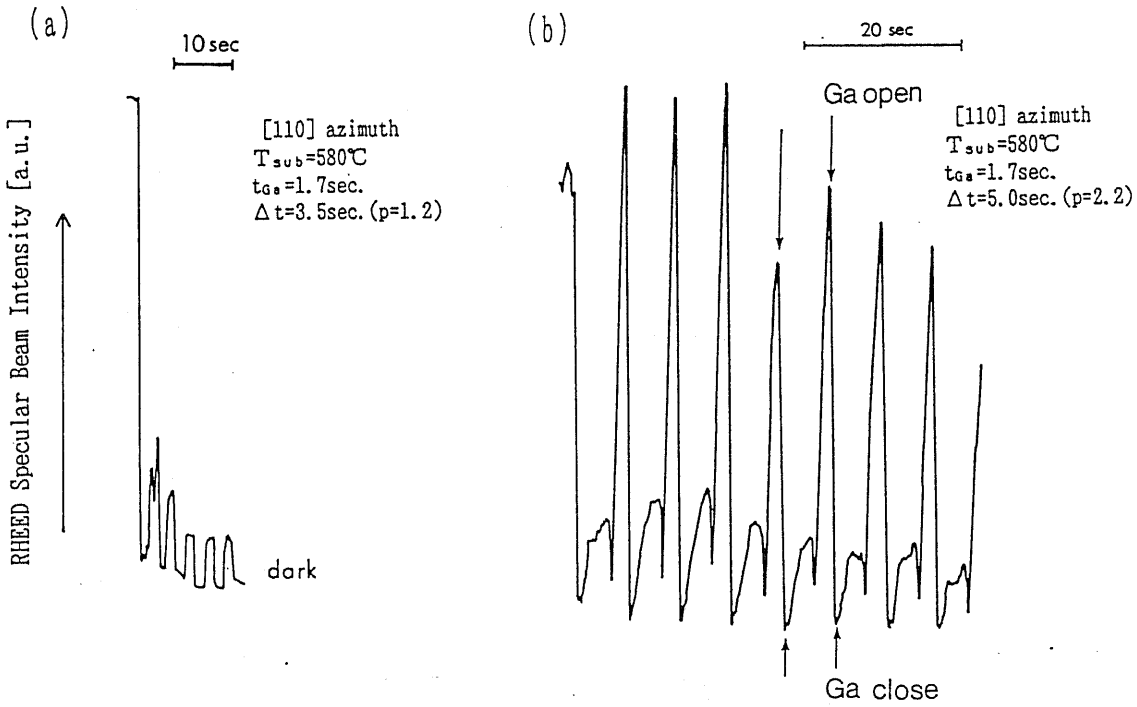

Fig.3-4. Typical RHEED intensity with various interval times. (a)Interval time is less than the minimum value; $\Delta_{min}>\Delta_t$. Excess Ga is accumulating. (b)Interval time equals the minimum value; $\Delta_{min}=\Delta_t$. Recovery of the intensity is not enough and shows unstable behavior.

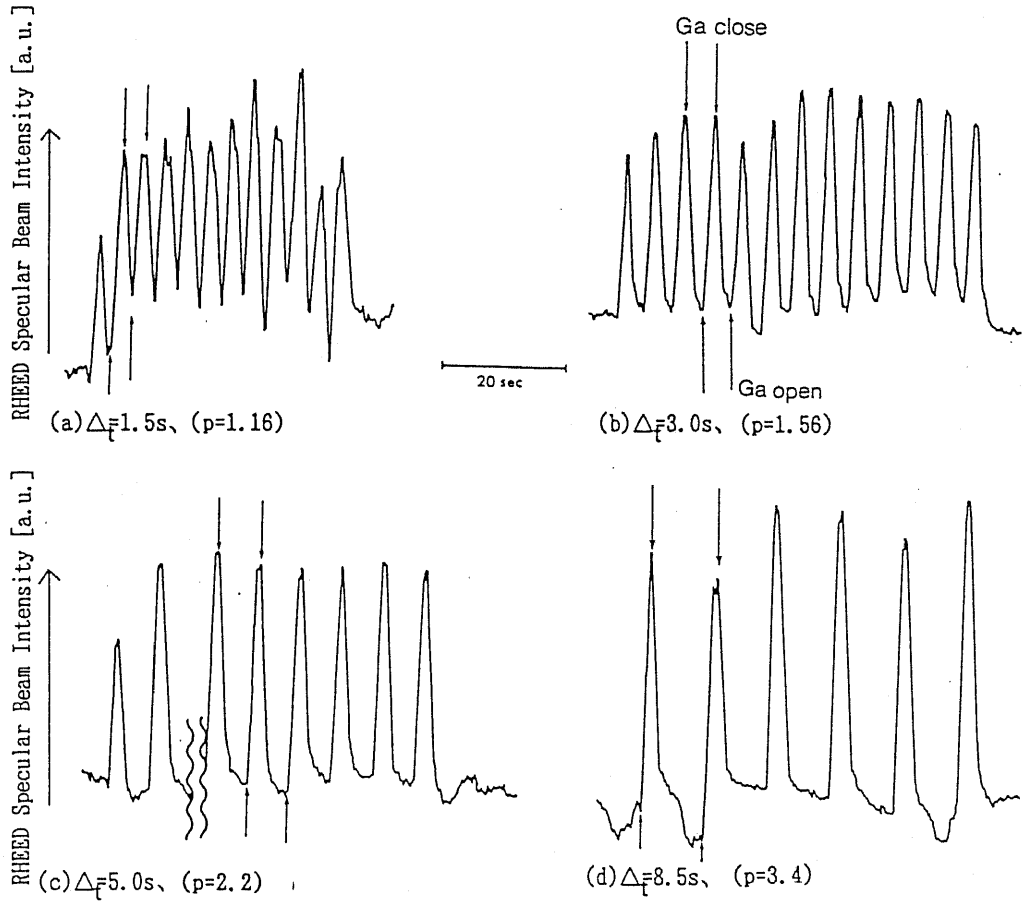

Fig.3-5. Typical intensity change of RHEED during the growth of GaAs on GaAs at 300°C. Surface RHEED pattern always keeps unreconstructed (1×1). The interval time of the Ga pulse was (a)1.5 s, (b)3.0 s, (c)5.0 s and (d)8.5 s with other parameter unchanged. The values of p are also indicated.

to 8.5 s (p=3.4). Horikoshi and Kawashima (1989b) have reported that in low temperature MEE, very accurate control of As_4 flux is needed to obtain both the clear change of the surface reconstruction and the good intensity profile in order to prevent the excess As adsorption. In our method, however, we observed only well-defined (1×1) pattern, not c(4×4) As excess pattern, during the growth and no serious decrease of the RHEED intensity even under the condition of p>1. We can explain this by assuming that As pressure used here is too low for this growth temperature to make excess As adsorption.

When the interval is shorter than the critical condition of p=1, the RHEED pattern becomes spotty indicating that Ga droplets are formed on the surface. But at lower temperature than about 500°C, it becomes difficult to determine the critical interval Δ_{min} accurately because no clear change of the RHEED pattern is observed. Figure 3-6 demonstrates the substrate temperature dependence of this critical interval Δ_{min} under two different As flux of 9.4×10^{13} and 6.3×10^{13} molecules/cm^{2}s with F_{Ga}=1 ML/1.7 s. In the same figure is shown the growth velocity by As incorporation calculated from the RHEED intensity oscillation which appears upon opening As shutter after the pre-deposition of excess Ga (4-5ML). In this figure, we can see three characteristic temperature regions as follows.

(a)T_{sub}>640°C: Because of very low As pressure, surface always shows Ga-stable (4×2) pattern even without Ga flux. In this case, the present method can not be used.

(b)500°C<T_{sub}<630°C: RHEED pattern shows a clear change during Ga pulses. When the growth temperature is increased, a longer interval time between the Ga pulses is needed to keep a persistent RHEED intensity change and the maximum growth velocity is decreased. These results show that the sticking coefficient of As_4 on the Ga stable surface is not unity but is getting smaller as increasing the substrate temperature.

(c)T_{sub}<500°C: Only (1×1) unreconstructed surface is observed throughout the growth.

Hence in the region (c), the accurate value of Δ_{min} can not be measured as explained above. However, the maximum growth velocity is roughly proportional to that of As

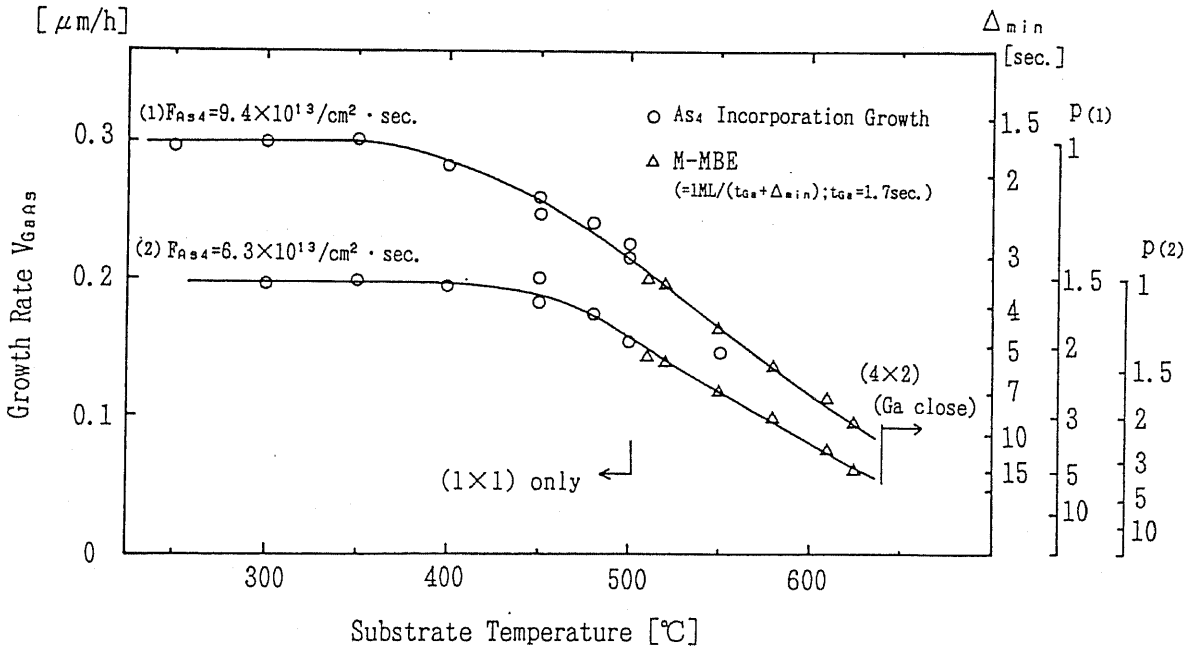

Fig.3-6. The maximum growth rate as a function of substrate temperature in the case of two different As_4 flux. Triangles show the value calculated from the minimum interval time between Ga pulses in the M-MBE mode. In the right axis, p values for each As_4 flux are indicated. Circles show the As_4 incorporation growth rate.

incorporation. At the temperature less than 400°C, the As incorporation growth velocity takes nearly a constant value, however, it shows very weak temperature dependence which has been reported before (Lewis *et al.* 1986, Garcia *et al.* 1989). Hence, in this temperature region, the maximum growth velocity is limited only by the As flux incident to the surface in contrast with the normal MBE growth where Ga flux uniquely determines the growth velocity.

3.3.2 Growth of AlAs

We have applied this growth method to the homoepitaxial growth of AlAs. Figure 3-7 shows the RHEED intensity oscillation at 580°C with a different interval time between the Al pulses for F_{As4}=6.3×10^{13}molecules/cm^{2}s and F_{Al}=1 ML/1.9 s A persistent change of both the RHEED intensity and the RHEED pattern have been observed and As-stable (2×4) pattern has not been seen like the case of GaAs. But there are some points of difference from GaAs homoepitaxial growth at this high temperature. The change of the surface reconstruction is more complicated than that of GaAs. For instance, after the opening of the Al shutter, the initial (1×1) pattern is changed to the Al-stable (4×2) one through (3×1) and this pattern is kept for a while under As flux. After that, the change of the pattern occurs in the reversible manner. Although the atomic structure of AlAs reconstruction has not been known, we can suggest that this (3×1) reconstruction may have the intermediate coverage of As between (1×1) and (4×2) like the case of GaAs.

When the interval time Δ_t is decreased to 6.0 s which corresponds to p=1.7, we can observe a persistent intensity oscillation where the intensity before the next Al pulse starts does not show full recovery to the initial value. However, it comes back to the initial value after the end of all Al pulse cycles. In the case of Δ_t=5.0 s (p=1.5), the intensity gets weaker and weaker and the RHEED shows a spotty pattern indicating an accumulation of Al metal which is not consumed by residual As flux in each interval. Since such a deteriorated surface shows no more recovery to a smooth surface even after the growth of a buffer layer, the critical condition of Δ_t=Δ_{min} is difficult to

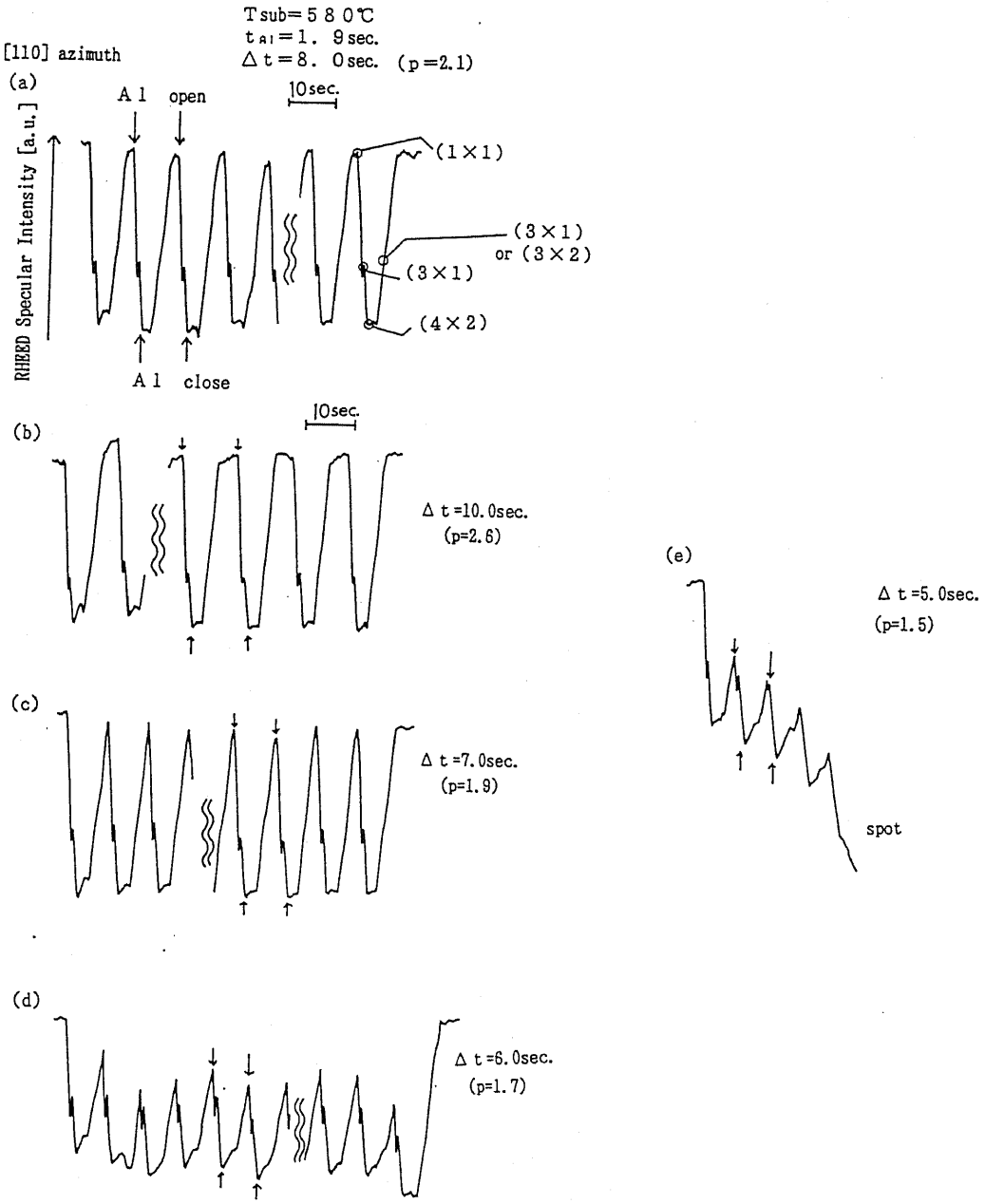

Fig.3-7. Typical intensity change of RHEED during the growth of AlAs on AlAs at 580°C, when the interval time was (a)8.0 s, (b)10.0 s, (c)7.0 s, (d)6.0 s and (e)5.0 s Change of the surface reconstruction is also shown in (a). In (e), the intensity gets weaker and RHEED shows a spotty pattern.

determine. However, it is interesting to note that the persistent intensity oscillation is obtained under the condition of p=1.7 while p=2.2 was the critical condition in GaAs growth. The sticking coefficient of As upon the Al-stabilized surface is supposed to be larger than that in the case of GaAs due to the strong bonding force between Al and As.

At the low temperature such as 300°C, persistent RHEED intensity oscillations can be obtained as shown in Fig.3-8. The whole behavior of the RHEED pattern and its spot intensity before and after the shutter operation is similar to those in the case of GaAs at 300°C.

We have not confirmed at this moment the formation and the disappearance of Al metal clusters on AlAs surface. Ohta *et al.* (1991) have reported about the RHEED intensity oscillation of the As incorporation into very thin Al films. In this report, it is pointed out that the RHEED intensity after the opening the As shutter upon the pre-deposited Al film generally shows very slow recovery or no recovery at 300°C. This means the excess Al metal seriously deteriorates the surface smoothness. However, in our case, complete and steep recovery is always observed at growth temperature from 580°C to 300°C. This is probably due to the fact that As atmosphere during Al pulse effectively reduce the formation of Al metal clusters on AlAs. This situation might be the same as the case of GaAs.

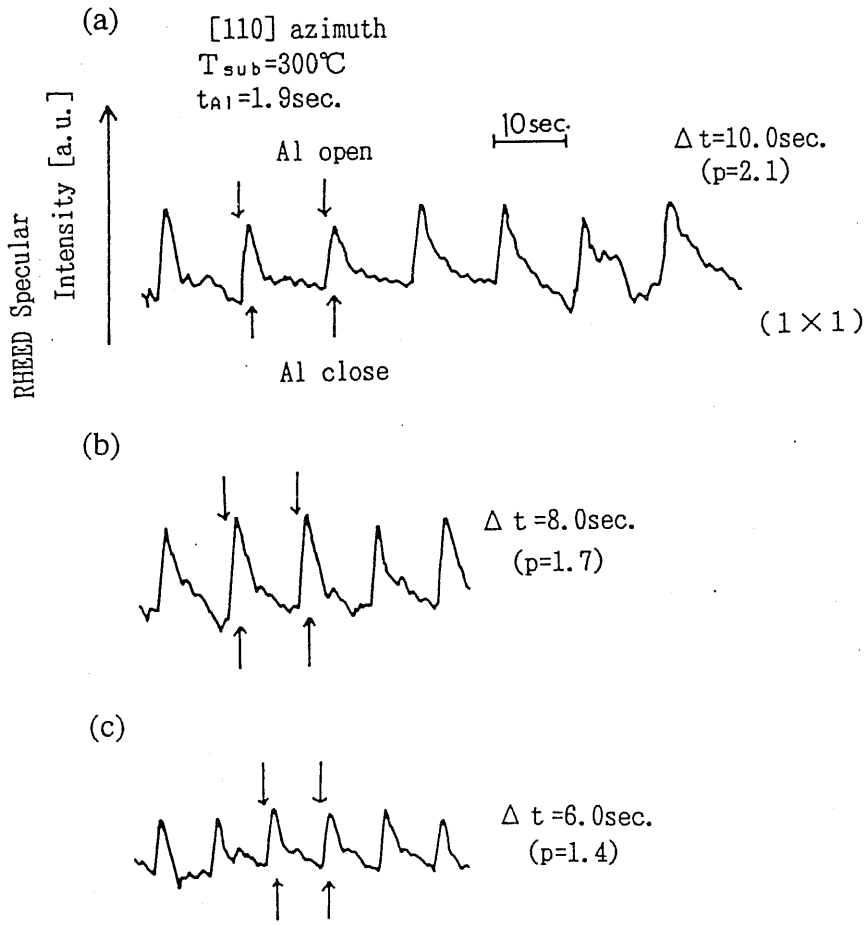

Fig.3-8. Typical intensity change of RHEED during the growth of AlAs on AlAs at 300°C, when the interval time was (a)10.0 s, (b)8.0 s and (c)6.0 s. Surface reconstruction during the growth always keeps well-defined (1×1) pattern.

3.4 Experimental Results——GaAs-AlAs Heteroepitaxial Growth

When this growth method was applied to the heteroepitaxial system of GaAs-AlAs, the growth behaviors were found very much different from the homoepitaxy. Figure 3-9 shows an example of the RHEED intensity at 580°C for F_{As4}=6.7×10^{13}molecules/cm^{2}s, F_{Ga}=F_{Al}=1 ML/1.9 s and Δ_t=10.0 s In this condition, p is 2.6 for both of Ga and Al, and the flux of As is enough for the AlAs growth but not enough or moderate for GaAs to obtain good recovery of a RHEED intensity. A quite irregular profile around the heterointerface is observed and only (1×1) unreconstructed surface is found. This irregularity continues until the growth enter the steady state phase of homoepitaxy. This period of irregular oscillations continues for about 10 pulses for AlAs on GaAs, and about 4 pulses for GaAs on AlAs. This indicates that the growth of another material produces a large change of the surface structure, for example the formation of a nucleus, and the creation of a large number of steps associated with the surface segregation and so on.

On the other hand, as the growth temperature is decreased, a period which shows this irregularity at the heterointerface becomes shorter as shown in Fig.3-10. Especially, at the temperature lower than 400°C, an abrupt change within one or two group III pulses is observed.

The irregularity of the intensity oscillation means there is a structural and chemical disorder at the heterointerface and this deteriorates the flatness in quantum structures. In this respect, our growth method can give better interfaces at lower growth temperature in contrast with the conventional MBE where a higher growth temperature is preferable for this purpose.

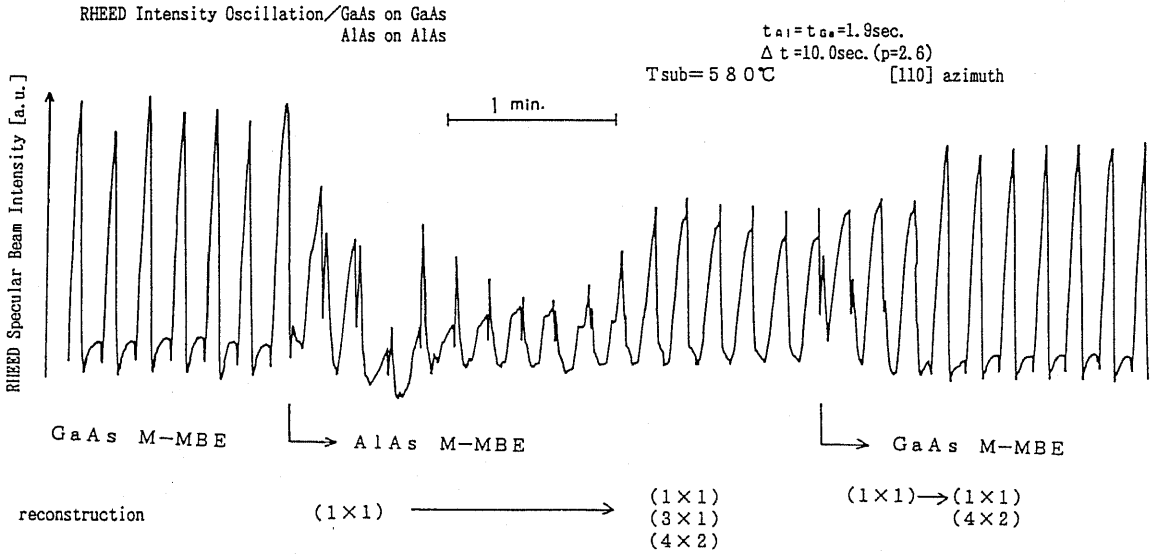

Fig.3-9. Typical RHEED intensity during GaAs-AlAs heteroepitaxial growth by M-MBE at 580°C. Irregular profile and unreconstructed pattern were observed around the interface.

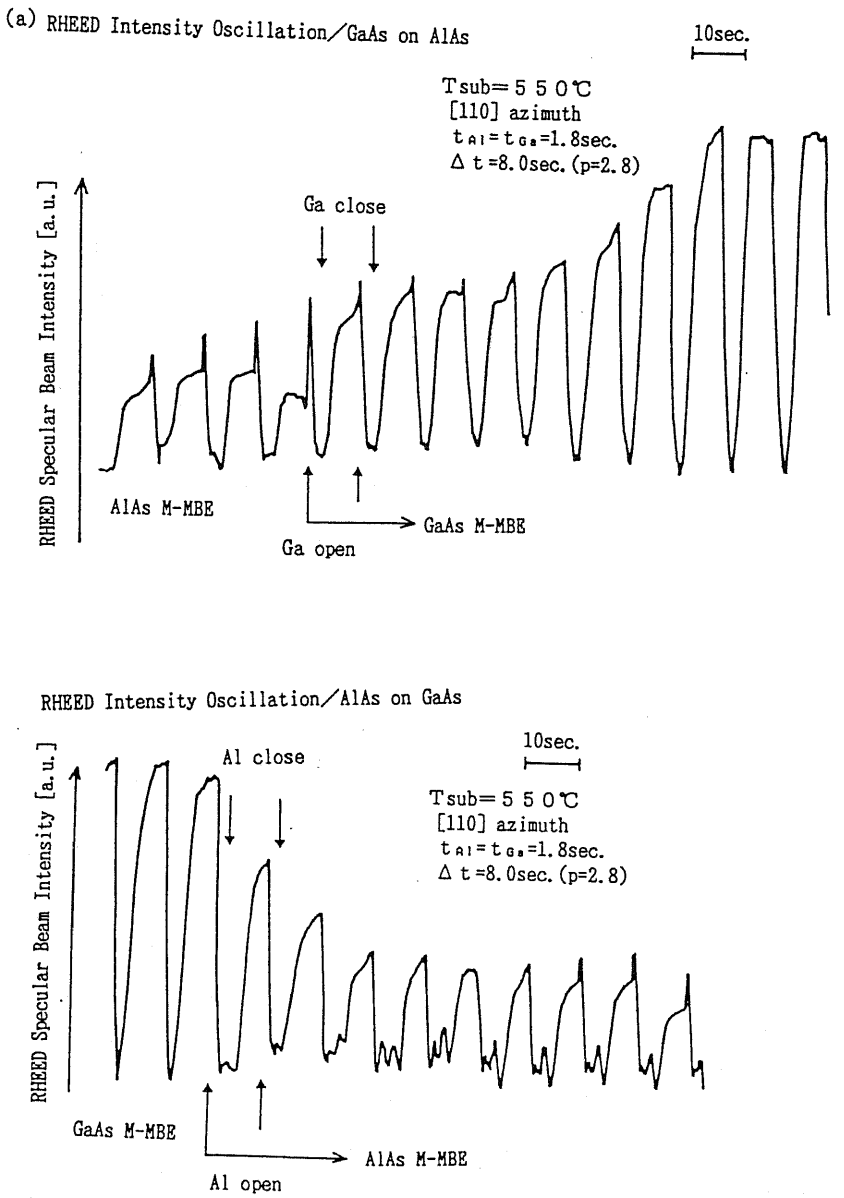

Fig.3-10(a). Typical RHEED intensity during GaAs-AlAs heteroepitaxial growth by M-MBE at 550°C.

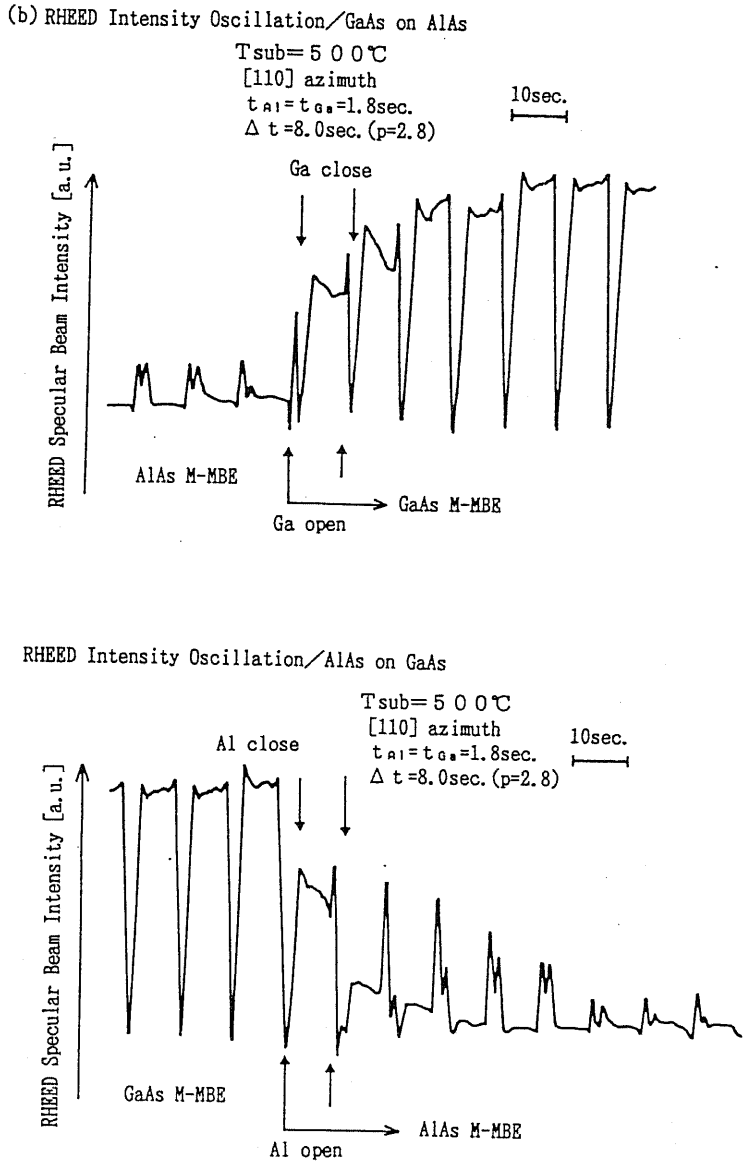

Fig.3-10(b). Typical RHEED intensity during GaAs-AlAs heteroepitaxial growth by M-MBE at 500°C.

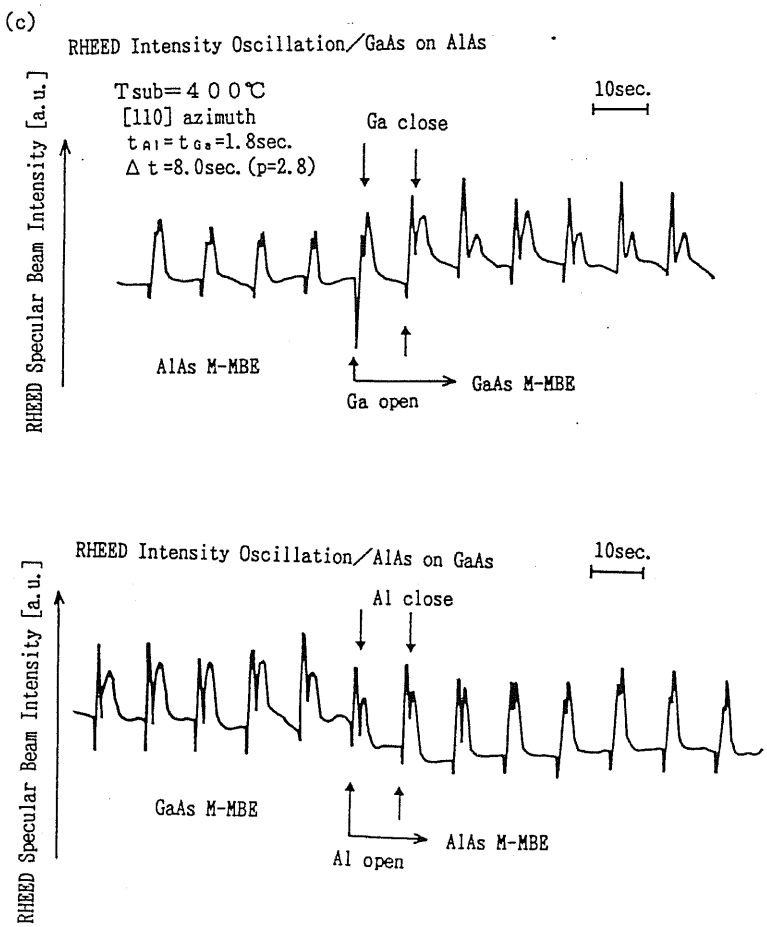

Fig.3-10(c). Typical RHEED intensity during GaAs-AlAs heteroepitaxial growth by M-MBE at 400°C. Irregular profile was not observed around the interface at the temperature less than 400°C.

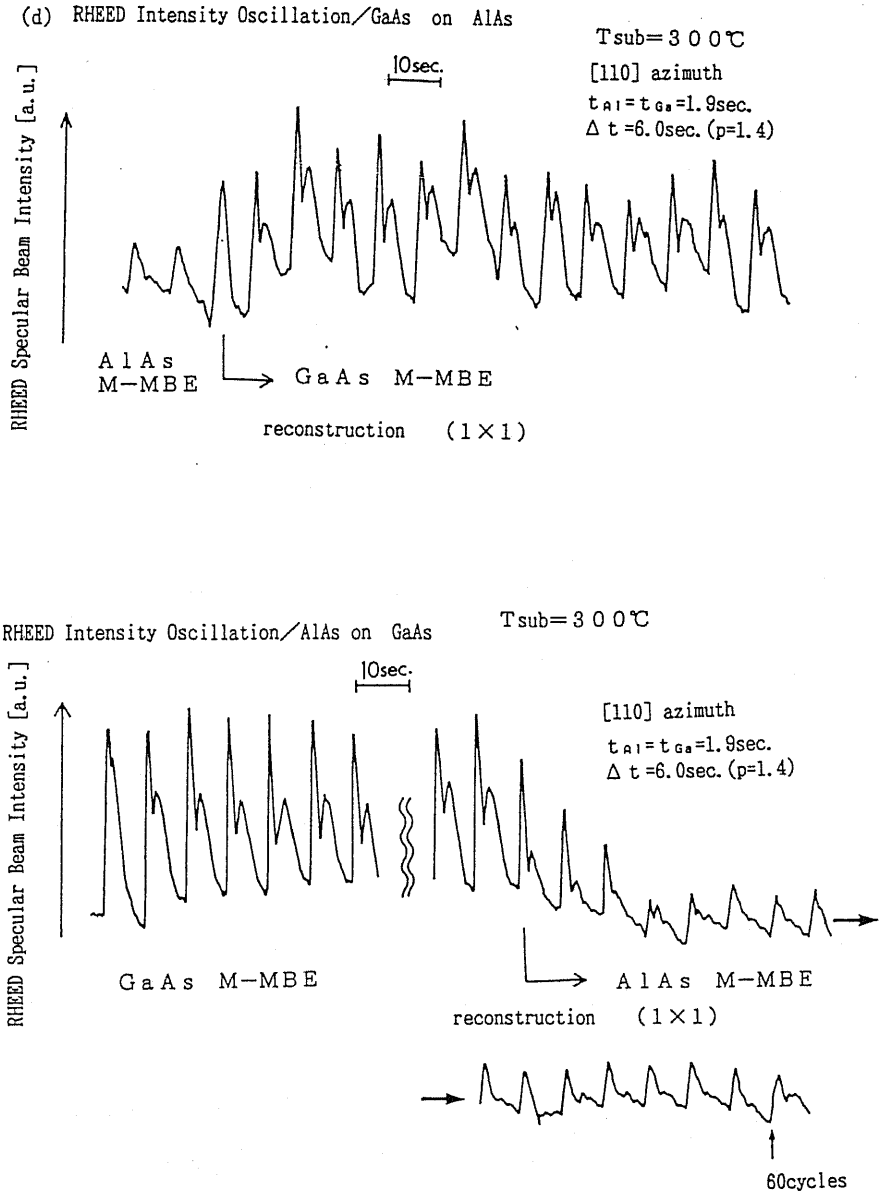

Fig.3-10(d). Typical RHEED intensity during GaAs-AlAs heteroepitaxial growth by M-MBE at 300°C.

3.5 Growth and PL Measurement of Single Quantum Well Structure

To confirm the above conclusion, we have grown SQW structures by this method at a various growth temperature. The SQWs has a structure of the well width of 13-24ML (3.8-6.7nm) GaAs sandwiched on both sides by 18ML (5.1nm) AlAs with a cap layer of 36ML (10nm) GaAs. To keep the same surface prior to the growth of SQW, a GaAs buffer layer with the thickness more than 300nm was grown at 580°C by conventional MBE condition with sufficient As_4 flux. After that, the substrate was cooled down to a growth temperature. In this procedure, As_4 flux was stopped at the substrate temperature lower than 500°C to prevent the surface reconstruction change to c(4×4) (Fig.3-11). Then the growth was started by sending Ga pulse and low As flux from another As_4 source.

PL measurements were made at 77K by using 488nm Ar^+ ion laser with the excitation power density of ~0.5W/cm^2. Figure 3-12 shows the typical PL spectra from the SQWs with the well width of 5.1nm. Each SQW was grown at the temperature of (a) 580°C and (b) 300°C. For reference, Fig.3-12(c) shows the PL spectra of SQW of the same structure which was grown at 580°C in conventional MBE mode with 90 s growth interruption at the both heterointerfaces. Although the spectra of SQW grown at 580°C shows very broad peak at the lower energy position than the calculated one, that of SQW grown at 300°C shows single sharp peak. It should be noted that the spectra of all SQWs grown at 300°C show strong intensity comparable to that of SQW grown in conventional MBE mode, and the peak energy agrees with the calculated value. This indicates that a high quality film can be obtained by M-MBE method at low growth temperature.

Next, we evaluated the FWHMs of SQWs with various well widths as a function of the emission wavelength. In Fig.3-13, solid circles show the FWHMs of SQWs prepared by the present growth method at 300°C. For reference, open circles and triangles show respectively the reported (Tanaka and Sakaki 1987) and our data of QWs prepared by conventional MBE method with a growth interruption. The broken line denotes the calculated broadening by assuming one monolayer fluctuation of the well width. As seen from the figure, the SQWs grown at 300°C in M-MBE mode have

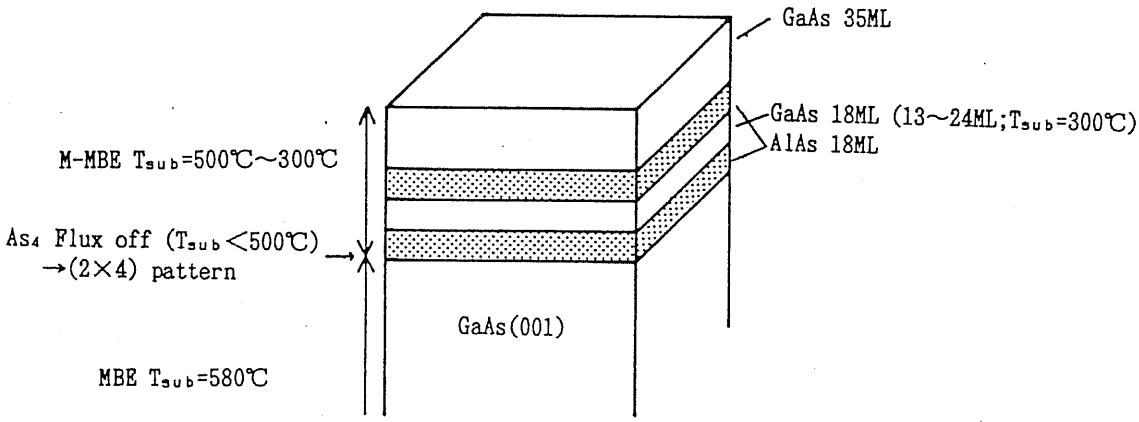

Fig.3-11. The structures of SQWs and the growth condition in this study.

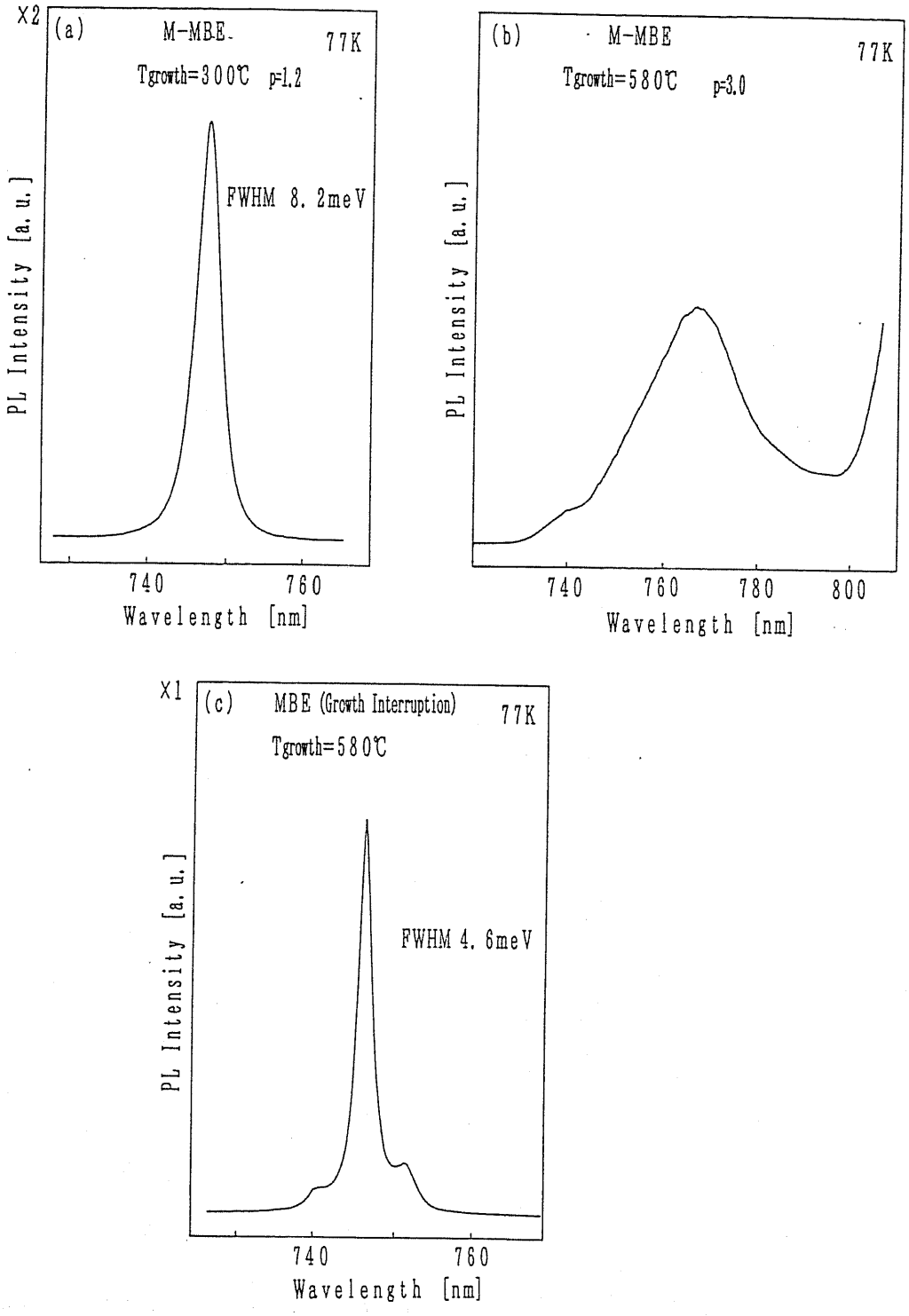

Fig.3-12. 77K photoluminescence spectra of GaAs-AlAs SQWs with well width of 5.1nm grown by M-MBE at (a)580°C and (b)300°C. For reference, (c) shows the spectrum of SQW grown by conventional MBE at 580°C with 90 s growth interruption at the both interfaces.

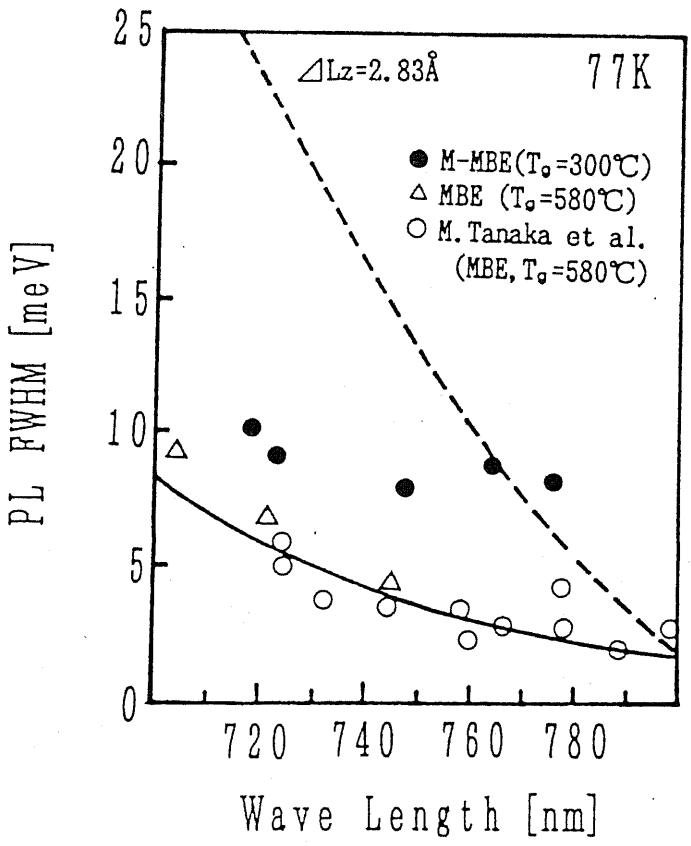

Fig.3-13. The full width at half maximum of PL spectra from GaAs-AlAs SQWs as a function of peak wavelength. The broken line denotes the calculated broadening due to one monolayer fluctuation of the well width. The solid circles are the experimental data of M-MBE grown SQWs, whereas open circles show the reported and our data of the SQWs grown by conventional MBE with growth interruptions (90 s).

effective roughness of less than one monolayer. This agrees with the RHEED intensity behavior.

It is worth noting that this method gives the narrow FWHM at 300°C for any interval of Ga pulse in the range of p=1.2-1.4. This means that we need not to take care precisely about the effective quantity of incident As flux so far as the interval time is longer than the minimum one, Δ_{min}. Hence, since it is rather difficult to control the As flux precisely in the conventional MBE system especially when the solid As source is used, the present growth method has the great advantage to MEE, in which one must choose strictly As quantity within one pulse. However, in this growth method, we employ extraordinary low As flux which never produces the excess As condition on the growing surface even at 300°C because the desorption flux of As is more than the incident As flux. This is supported by the absence of c(4×4) surface reconstruction which appears for excess As condition.

On the other hand, we could not obtain sharp PL spectra from the QWs grown at 580°C. In order to understand this phenomenon, we fabricated SQWs with the same structure by combining this growth method (M-MBE) with the conventional MBE as follows. Figure 3-14 indicates the individual parts to which M-MBE or MBE is applied. The growth temperature was kept always at 580°C and in the case of type I and II, a growth interruption of 2 min was applied at the top interface. On the switching from M-MBE to MBE modes, the shutter of the second As source was opened when the interval time was finished. Then, after the intensity of RHEED got stable in about 5 s, the flux of the group III element was sent continuously.

The PL spectra is given in Fig.3-15. The luminescence from SQWs of type I and II shows the sharp peak with the FWHM of 8.0, 8.7meV respectively, which is no better than that obtained by conventional MBE as shown in Fig.3-12(c). The FWHM is much less than the calculated value of monolayer roughness whereas the SQW of type III clearly shows the larger FWHM. From these data, by assuming that the conventional MBE mode gives an "ideal" interface judging from the PL spectrum as shown in Fig.3-12(c), one can discuss the possible origins for the induced disorder at the heterointerface.

Firstly, it can be pointed out that the intermixing of Ga and Al may occur easily at

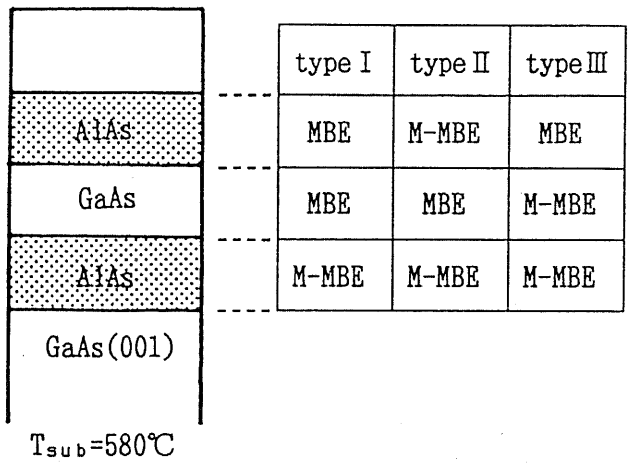

Fig.3-14. Schematic illustration of three type GaAs-AlAs SQWs with well width of 5.1nm. In the type I and II, growth interruption with 90 s was applied at the upper interface. Schematic illustration of the supplied flux at the growth mode change from M-MBE to MBE, is also shown.

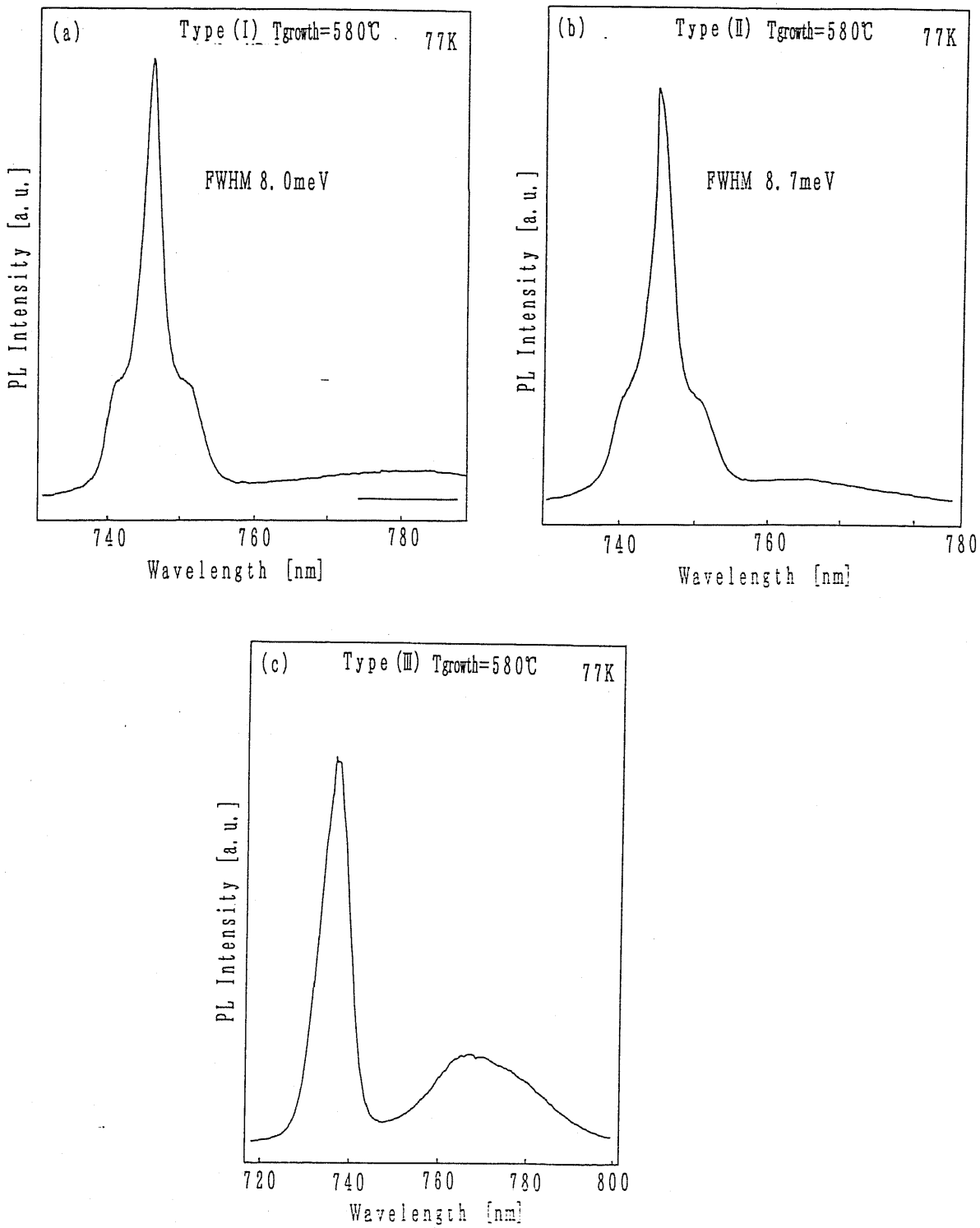

Fig.3-15. 77K photoluminescence spectra of GaAs-AlAs SQWs of 5.1nm well width grown by M-MBE and MBE at 580°C. Each type of growth mode is described in Fig.3-14.

the interface since very low As flux in this growth method makes the growing surface metal rich where the exchange reaction between the substrate and the deposited layer may easily takes place. If this is the case, we can conclude that the behavior of the RHEED intensity does not necessarily indicate this intermixing. This is because the irregularity of the RHEED intensity is pronounced at the AlAs on GaAs interface, on the other hand, this interface has no strong influence on the FWHM as seen by comparing PL spectra from type II and type III SQWs.

The second point is that there is a difference in the optimum As flux for AlAs and GaAs at high temperature. For instance, when the growth was carried out in M-MBE mode with $t_{Ga}=t_{Al}=1.8$ s and the interval time of 9.0 s, the total As flux within one interval is enough for AlAs but not enough for GaAs to obtain good recovery of RHEED intensity. This might be the reason for the poor quality in GaAs grown on AlAs by M-MBE and hence for the wide FWHM in the PL spectra from type III SQW.

Recently, Foxon *et al.* (1990) showed by measuring PL, PLE and X-ray diffraction that MEE at a temperature higher than 530°C gives much poorer quality than the MBE samples. In our case of M-MBE, the situation is close to their case and low coverage of As atoms or a formation of Ga droplets may occur when the Ga shutter is turned open and this deteriorates the crystal quality and the interface sharpness although the situation is dramatically improved.

3.6 Summary

We have proposed a new growth method called modulation MBE (M-MBE). This consists of an intermittent supply of group III atom and a continuous supply of As with very low pressure which is much lower than that of the group III flux. Periodic and persistent RHEED intensity oscillations have been observed in the temperature range from 630°C to 300°C. At higher temperature, the persistent changes of the RHEED pattern were also observed, from which we know that the growth was carried out under metal rich condition. We can understand that the present method as consisting of growth interruption and As incorporation growth at every monolayer under low As flux.

The present method was applied to fabricate GaAs-AlAs heterostructure. However, an irregular RHEED oscillation at the interface have been observed. It was found that the irregularity depends on the growth temperature and the growth sequence. The PL spectra from GaAs-AlAs SQWs grown at 580°C show peaks with wide FWHM which corresponds very well to the irregular oscillation of the RHEED intensity. When the low temperature (300°C) was employed to grow SQWs, an excellent smoothness within one monolayer effective roughness has been obtained easily and reproducibly without any special attention to keep the amount of As flux.

We can conclude that this method can give excellent crystal quality at the low growth temperature. It is also concluded that the condition of As-free atmosphere such as in the case of MEE can not be the key factor for obtaining good crystal quality but an establishment of the group III stable surface is essential for realizing the long diffusion length of the group III atoms which is crucially important to get good epitaxial films.

Chapter 4

Real Time Observation of Growing Surface during Molecular Beam Epitaxy

4.1 Introduction

For studying the crystal growth mechanism in MBE of III-V compound semiconductor, RHEED has been a strong tool and widely used so far. Because it is compatible with growth process, it enables us to obtain wide range of information about the growing surface (Harris *et al.* 1981, Wood 1981, Neave *et al.* 1983). On the other hand, there are many demands to get the spatial knowledge on the growing surface to fabricate more complicated structures. However, only spatially averaged information is possible to obtain by RHEED technique. In addition, it has been reported by Neave *et al.* (1984) that there is a difficulty in analyzing a RHEED pattern and diffracted intensity.

STM combined directly with MBE growth chamber through an ultra high vacuum path has given us one possibility to get the spatial information. A large amount of knowledge concerning the surface reconstruction and the step structure has been accumulated (Pashley *et al.* 1988, 1991, Biegelsen *et al.* 1990). However, what we can get by STM is the surface images only after the growth.

μ-RHEED (Ichikawa *et al.* 1984) or SEM-MBE hybrid system enables us to observe a surface image in real time. The observations of GaAs surface at growth temperature were reported firstly by Yamada *et al.* (1988) and Isu *et al.* (1988a). Yamada *et al.* (1989), Osaka *et al.* (1990a, 1990b, 1990c) and Inoue (1991) have observed the formation and disappearance of Ga and AlGa droplets under deficient As_4 flux. Recently Kanisawa *et al.* (1991) of the same group have studied the degree of As coverage of the GaAs(001) surface by measurements of the secondary electron intensity. Hata *et al.* (1990) have investigated the local distribution of the growth rate

on the patterned substrate by using RHEED intensity oscillation. Isu *et al.* (1991) also have observed the features of formation and disappearance of Ga droplets by μ-RHEED during the growth with an alternating supply of Ga and As.

In this chapter, real time observations of growing surface by SEM-MBE or μ-RHEED are described. First, in section 4.2, the experimental apparatus used in this study is explained. Then, in section 4.3, a growing surface of GaAs(001) under excess Ga condition is described. It was found that there is a spatial distribution of the surface reconstructions. This is the first evidence to show the coexistence of domains of different reconstructions on the surface of III-V compounds. In section 4.4, the density of Ga droplets is measured under a wide range of both incident flux and growth temperature. By using nucleation theory for these results, formation mechanism of Ga droplets is discussed. In section 4.5, As_4 incorporation growth rate is measured by RHEED intensity oscillation. Then the relationship between As_4 incorporation growth and annihilation process of Ga droplets is studied. Finally, in section 4.6, In droplet formation and its disappearance on GaAs(001) are described.

4.2 Experimental Apparatus

Figure 4-1 schematically illustrates the MBE system used in this study. An electron gun for SEM is installed in the specially designed MBE (ULVAC) which is equipped with solid source Knudsen cells. The basic design of this system is similar to that reported by other groups (Yamada *et al.* 1988, Isu *et al.*1988b). A SEM image of growing surface is obtained by the secondary electron detector placed in front of a substrate. Diffraction patterns from the substrate are observed on a fluorescent screen. A particular diffraction spot is selected by using an optical lens and the intensity is measured by a photomultiplier. A μ-RHEED image is produced from this intensity by scanning the electron beam.

To get high resolution, the electron gun of the field emission type (HITACHI: S-800) is used. The section of the electron gun is separated from the growth chamber by a gun valve and pumped out differentially by three ion pumps. In order to shield the heat radiation from the substrate heater and to prevent high background pressure of As_4 to enter the gun section, Mo shield plate is placed below the objective lens. This allows us to use the microscope under As_4 partial pressure of up to 10^{-5} Torr with keeping the working distance of 5-20mm. The spatial resolution for the direction perpendicular to the beam azimuth is about 50nm in SEM mode. Images of growing surface are taken by photographs at the rate of 1 frame per 80 s or recorded by a commercial video recorder at the rate of 60 frames per 1 s. The whole system is put upon the anti-vibration stage to keep off the disturbance caused by mechanical vibration. The base pressure in the growth chamber is kept less than 5×10^{-10}Torr. An image processor is employed to integrate 2-4 frames for the purpose to reduce the noise.

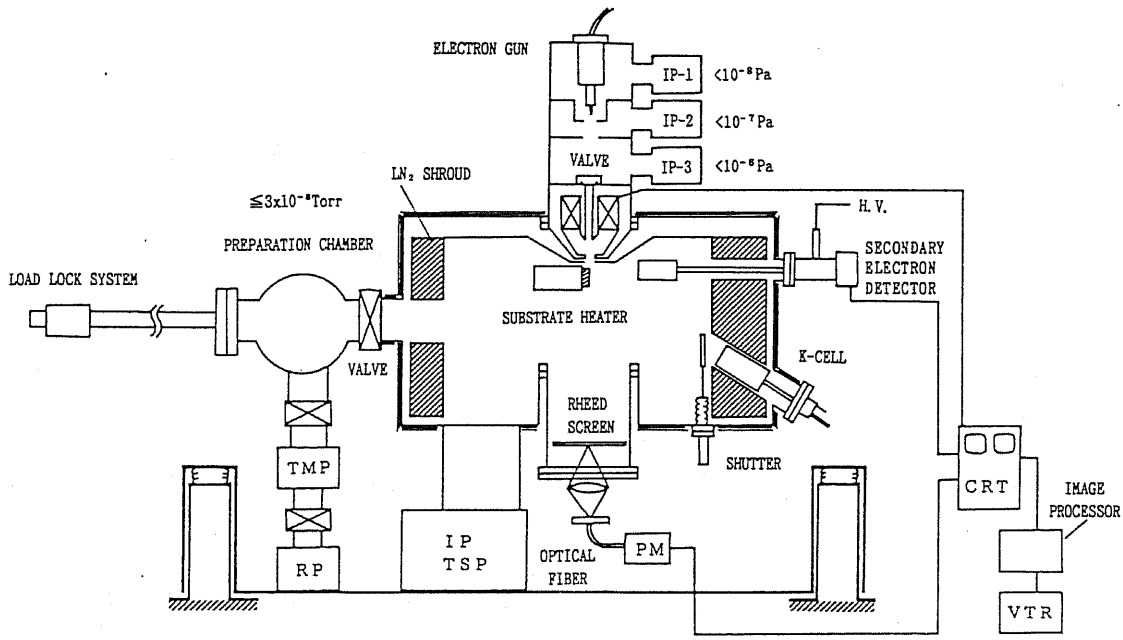

Fig.4-1. Schematic illustration of MBE system equipped with a scanning microprobe RHEED. In this figure, IP, TSP, TMP and RP respectively denote an ion pump, a titan sublimation pump, a turbo molecular pump, a rotary pump.

4.3 MBE Growth under Excess Ga Flux Condition

4.3.1 Experimental Procedure

Figure 4-2 schematically shows the flux diagram of this experiment. As shown in the figure, the whole experimental process is divided into three regions as follows.

(a)Region I; the substrate is kept under As_4 flux without no supply of Ga.

(b)Region II; the shutter of Ga is opened with a continuous supply of As_4. When the equivalent flux of Ga is more than that of As_4, the formation of Ga droplets is observed.

(c)Region III; the shutter of Ga is closed. It is observed that the droplets which formed in the region II disappear.

In the chapter 3, we have proposed M-MBE method in which a persistent RHEED intensity oscillation is observed by sending modulated beam of group III flux under a continuous supply of As_4 flux. It has been shown that the M-MBE has a great advantage to obtain the film with good quality when the low growth temperature is employed. Since the flux sequence of Fig.4-2 is exactly one cycle of M-MBE, one can get much information concerning the growth mechanism of M-MBE.

In the experiments of this section, GaAs(001) substrates with an accuracy of $\pm 0.5^\circ$ were used and the growth temperature was kept always at 580°C. After removal of the native oxide by heating the substrate up to 620°C under As_4 flux, a GaAs buffer layer with the thickness more than 300nm was grown at 580°C. Since the formation of Ga droplets makes the surface rough as reported before, a GaAs buffer layer was grown under As-stabilized condition every time after one cycle of experiment from I to III in Fig.4-2.

The flux of Ga is calibrated by the periods of a RHEED intensity oscillation, whereas that of As_4 was determined by the growth rate of As_4 incorporation on the pre-deposited Ga at 400°C where this rate becomes almost independent on the substrate temperature as will be explained in section 4.5. The azimuth of the electron beam was chosen along $[1\bar{1}0]$ direction, and the acceleration voltage and the incident current were respectively 25KeV and 1-3nA. As the glancing angle of the incident beam was about

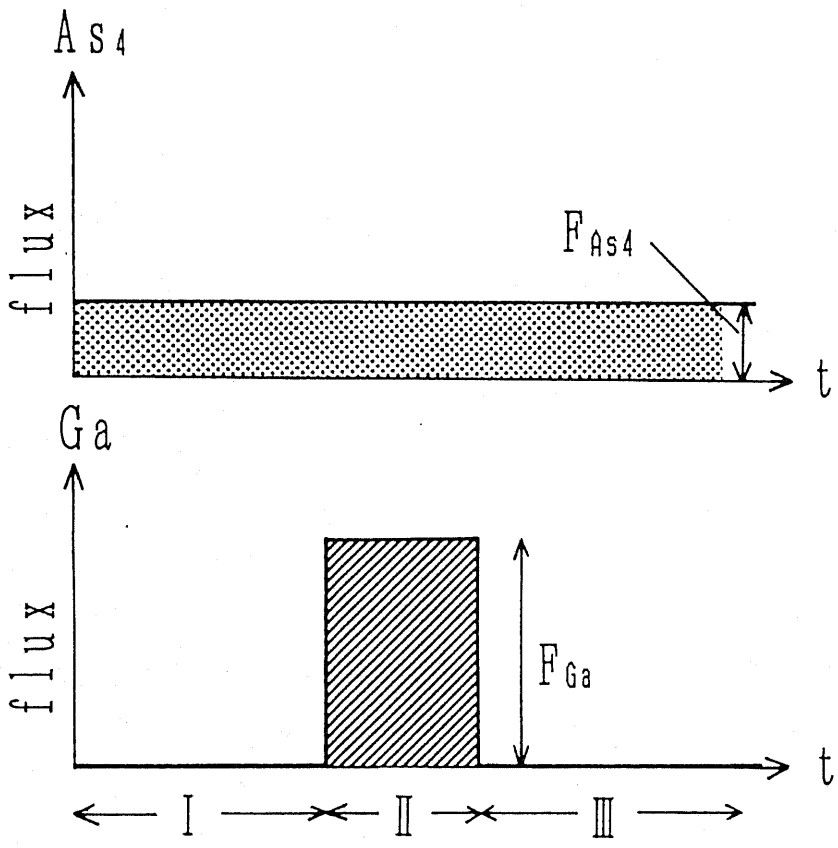

Fig.4-2. Flux diagram of As_4 and Ga in the experiment.

3.3° in this study, the images were foreshortened in the vertical direction as indicated by the each scale. In this section, the SEM images from the video tape recorded in TV scan mode are presented.

4.3.2 Transition of Surface Reconstruction

(a)Formation of Ga droplets in region II

Figure 4-3(a)-(c) shows the SEM images of the growing surface with the incident flux of F_{Ga}=1.1×10^{14}atoms/cm^{2}s and F_{As4}=1.0×10^{14}molecules/cm^{2}s. After opening the Ga shutter, the bright domain appears (Fig.4-3(a)) and it expands quickly (Fig.4-3(b)). Although this domain expansion is seen to proceed in lateral direction because of the shortening effect in vertical direction, we are not sure about the anisotropy of the expansion speed now.

After this event, it is seen that the black points emerge inside the bright domain (Fig.4-3(c)). The width of this bright domain reaches about 200μm and another bright domain at the upper position is getting larger as seen in (b) and (c). It is observed that the number of Ga droplets does not increase although the size of each droplets increases. Figure 4-3(d) illustrates this process schematically. At last, these bright domains cover the entire surface and then the black points become to cover the whole surface. A similar picture for the domain expansion and the droplet formation has been observed also by μ-RHEED mode. We could not determine accurately the minimum amount of Ga atoms which produces Ga droplets, because the shutter operation disturbed the observation. However, when the growth condition of M-MBE described in the chapter 3 was employed, Ga droplets appeared after 0.5-0.75ML Ga supply. Therefore, it is confirmed that there occur the creation and the annihilation of Ga droplets in the M-MBE growth at 580°C.

It is worth noting that the macroscopic domain is never observed when the shutter of As_4 is closed and black points appear as soon as the Ga shutter is opened (Inoue 1991). Therefore, these black points shown in Fig.4-3 should be the image of Ga droplets, which are produced by the presence of excess Ga atoms which are not

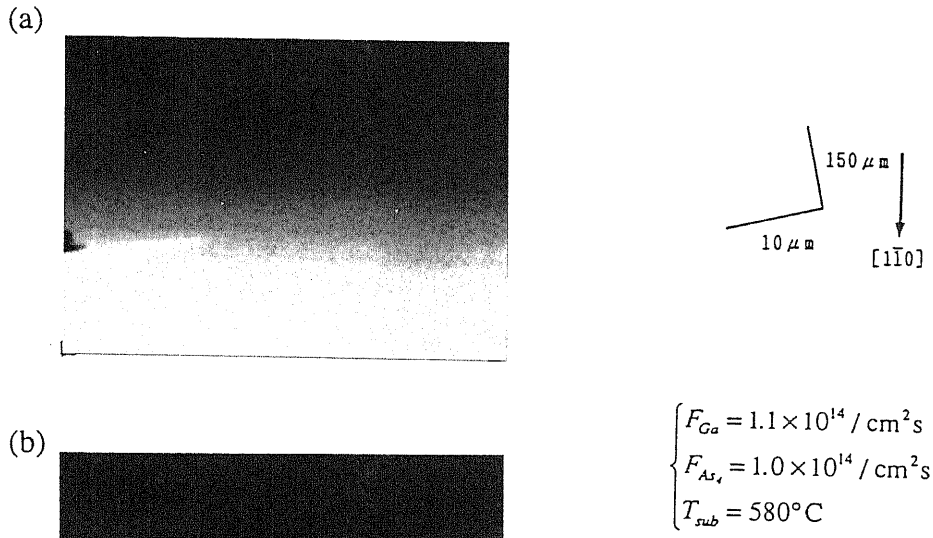

Fig.4-3. Successive SEM images of Ga droplet formation in region II at 580°C. The images are foreshortened in the vertical direction indicated by the scale. In a while after opening the Ga shutter, bright domain quickly expands to the right in (a). (b) shows the image about 1 s after the picture of (a). (c) is the picture after 17 s from (b). Ga droplets are seen inside the bright domain. There is another bright domain at upper position. Dark particle in the left side is a marker for focusing. (d) shows the schematic illustration of domain expansion process.

consumed by As_4. We will describe about the droplet density and a formation mechanism of these Ga-droplets in section 4.4.

By fixing the electron beam stationary on each domain, one can know the kind of surface reconstructions of the domains by RHEED patterns. Figure 4-4(a)-(c) shows the RHEED patterns in region I and at the each position in region II. Before opening the Ga shutter, the so-called (2×4)α reconstruction is observed, where the intensity of the central, or 2/4ths streak is weak relative to that of 1/4th and 3/4th streaks in $[1\bar{1}0]$ direction (Fig.4-4(a)). When the shutter of Ga is opened, the RHEED pattern for the dark area in the SEM images of Fig.4-3 changes abruptly to (1×1) bulk streaks (Fig.4-4(b)). On the other hand, the bright domain gives (4×2) Ga-stabilized reconstruction as shown in Fig.4-4(c). There have been a lot of observations of the surface reconstruction which appears between As-stabilized (2×4) and Ga-stabilized (4×2) surface. For example (3×1), (1×1), (4×6), (4×1), (1×6), *etc.* have been reported. Among them, (3×1) reconstructed surface is found most typically. But in the present experiment, 3 fold symmetry in $[1\bar{1}0]$ direction can not be seen in the dark area. Hence, it is understood that this dark region has a less As coverage than that of (2×4)α reconstruction which is estimated to be 50% with two missing dimer of As by Farrel and Palmstrøm (1990).

The most remarkable thing in Fig.4-3 is the large domain size and the high speed of its expansion. It takes 1 s from Fig.4-3(a) to (b). Therefore the expansion speed in [110] direction is estimated to be about 17μm/s. The exact measurement of the domain size is difficult. This is because domains appear generally at random position, namely, the domain expansion starts from the edge of the wafer, and sometimes from the center. Moreover, many domains coalesce to each other. Since the domain has a size of hundreds μm order as shown in Fig.4-3, the electron microscope is not a desirable tool to measure the domain.

It is noted that the domain expansion is sensitive to the incident flux of Ga. When the Ga flux is increased to 4.1×10^{14}atoms/cm^{2}s, such a domain is not observed and the Ga droplets appear as soon as the Ga shutter is opened. This situation is similar to that under no As flux. On the other hand, the formation of both domains and Ga droplets is not observed when the Ga flux is kept less than 6.5×10^{13}atoms/cm^{2}s. This indicates

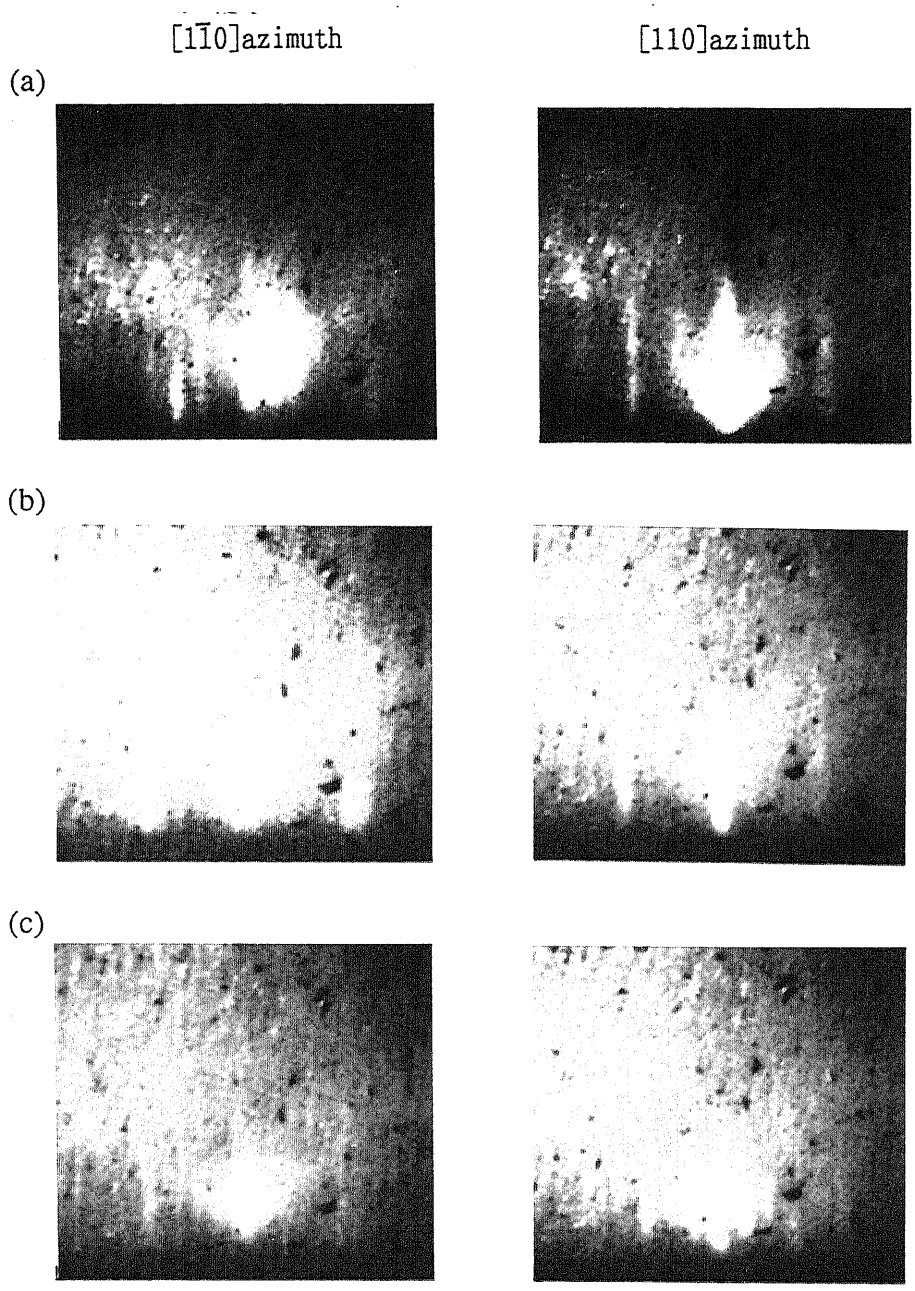

Fig.4-4. Typical RHEED patterns observed along each direction by fixing the electron beam positioned on particular place.

(a)(2×4) As-stabilized patterns in region I under As_4 flux and no incident Ga flux.

(b)RHEED patterns obtained from dark domain of SEM image in region II; (1×1) bulk streak appears.

(c)RHEED patterns obtained from the inside of bright domain of SEM image in region II; (4×2) Ga-stabilized pattern can be seen.

that the excess Ga flux which is not consumed by As_4 is attributed to the formation of domains and Ga droplets. We believe that no observation of the domain in the condition of high Ga flux relative to As_4 flux is caused by both of high domain density and high expansion speed.

The bright domains in Fig.4-3 correspond to the place where the intensity of a secondary electron is larger than the other area. Although we did not measure an exact intensity of the secondary electron, this feature agrees with the report given by Inoue (1991) and Kanisawa *et al.* (1991).

(b)Disappearance of Ga droplets in region III

There are two modes in droplet disappearance. The different mode appears depending on the droplet density, n_s. The critical value is about $n_s=10^{10}/m^2$ at 580°C.

(b-1)High droplet density mode ($n_s>10^{10}/m^2$)

Figure 4-5 shows typical SEM images when the continuous As_4 flux of 1.0×10^{14}molecules/cm^2s is supplied. After closing the shutter of Ga, Ga droplets become getting smaller (Fig.4-5(a)). At the time when these droplets have disappeared, many dark domains start to expand quickly and cover the entire surface. This is just the reverse process of the droplet formation. The expansion speed is much higher than that of bright domain. Thus, the size of domains is difficult to measure. It is observed that a dark domain covers the entire area of the SEM image in about 2 s in the case of Fig.4-5.

(a)

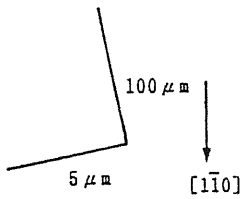

$$\begin{cases} F_{As_4} = 1.0 \times 10^{14} / \mathrm{cm^2 s} \\ T_{sub} = 580^{\circ}\mathrm{C} \end{cases}$$

(b)

(c)

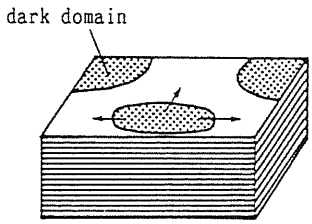

Fig.4-5. SEM images of droplet disappearance in high density mode. By closing the Ga flux, the droplets are getting smaller in (a) and around the time when the droplets disappear, dark domains expand quickly and cover the entire surface in (b). (c) shows schematic illustration of dark domain expansion.

(b-2)Low droplet density mode (n_s<10^{10}/m^2)

When the droplet density is less than about 10^{10}/m^2, the disappearance behavior changes greatly as shown in Fig.4-6 where the As_4 flux of 1.6×10^{14}/cm^{2}s is applied. When the shutter of Ga is closed, dark areas appear immediately outside the regions around the Ga droplets. Ga droplets gradually get smaller with the shrinkage of the bright domains surrounding them. At last, both of Ga droplets and the bright domains disappear. In contrast with the high droplet density mode, the bright domains shrink much slowly. It takes about 23 s to disappear for the total amount of 7ML Ga. The observation in this mode has been reported briefly by Inoue (1991).

It is suggested that the size of the bright domain can be determined by the equilibrium relationship between incident As_4 flux and the laterally diffusing Ga adatoms emitted from Ga droplets. Therefore, both of Ga droplets and the bright domain disappear when the Ga source is exhausted. This local growth of GaAs at the position of bright domains may introduce the surface roughening.

The surface reconstruction is expected to show (2×4) again during the supply of As_4. The RHEED pattern of the dark area shows (1×1) bulk streak as soon as the Ga shutter is closed and then it changes gradually to (2×4) reconstruction which is the same as the original one in region I. This transition from (1×1) to (2×4) is not clear. So that it is suggested that there is no formation of a macroscopic domain in the transition from (1×1) to (2×4).

4.3.3 Analysis of Domain Formation

The experimental results of SEM images and RHEED patterns clearly show the coexisting of the two surface reconstructions simultaneously and there is a spatial transition of reconstructions during growth even under the uniform incident flux. At present, we have no knowledge of a similar phenomenon in the III-V compound semiconductors. But there have been some reports about the reconstruction transition in

(a)

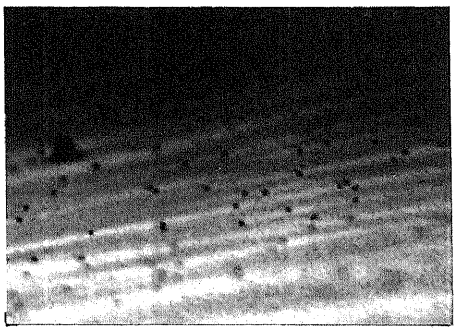

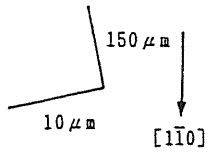

(b)

$$\begin{cases} F_{As_4} = 1.6 \times 10^{14} / \mathrm{cm^2 s} \\ T_{sub} = 580^{\circ}\mathrm{C} \end{cases}$$

(c)

(d)

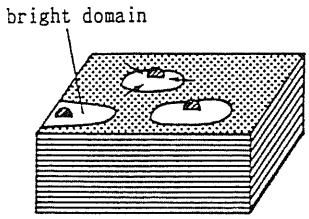

Fig.4-6. Successive SEM images of droplet disappearance in low density mode. Dark particle in the left side is a marker for focusing.

(a)As soon as Ga supply is stopped, dark areas appear outside the regions around Ga droplets.

(b)Both bright areas and droplets gradually shrink. The time interval between (a) and (b) is about 8 s.

(c)About 23 s after (a), the dark areas cover the entire surface.

(d)Schematic illustration of droplet disappearance process in low droplet density mode.

the case of Si(111). Osakabe *et al.* (1980, 1981) have observed the phase transition which occurs spatially between (1×1) and (7×7) domains on Si(111) by using a reflection electron microscopy (REM). This kind of transitions has been studied by another group (Aseev *et al.* 1991).

However, there are a few points of difference between Si(111) and GaAs(001) studied in the present experiment. Firstly, steps play an important role in the transition of Si(111). Namely, on cooling, domains of the (7×7) structure nucleate preferentially on the upper terraces along the step, and the reversed process takes place on heating. Thus, the domain size is limited by a distance between the steps. On the other hand, in the present case of GaAs(001), the domain size reaches a few hundreds μm, which means there are a great number of atomic steps in a single domain originated from 2-dimensional nucleation and/or produced due to a substrate misorientation. Therefore it can be concluded that the existence of steps plays almost no role in the domain expansion of GaAs(001). Secondary, the phase transition of Si(111) occurs due to the change of the surface structure, and this process accompanies growth or evaporation. However, domain expansion (shrinkage) on GaAs(001) is observed only during the growth, and the behavior depends on the growth condition very much as mentioned before.

To understand the mechanism of domain expansion (shrinkage), one should pay attention on the difference between the bright and dark domains in Fig.4-3. In the bright domains which show (4×2) Ga-stabilized surface, the excess Ga that is not consumed by As_4 agglomerate to form droplets. This indicates that Ga atoms migrate on (4×2) surface as long as the same order of the mean distance between droplets. However, there are no droplets in the dark areas. So that it is suggested that if the surface diffusivity on (1×1) reconstruction is relatively smaller than that upon (4×2) Ga-stabilized surface, the excess Ga atoms are forced to form Ga atomic clusters the sizes of which are much smaller than the resolution of SEM. The domain expansion upon opening the Ga shutter is performed by absorption of Ga clusters at the edge of bright domains. Figure 4-7 schematically illustrates the domain formation process.

On the other hand, the observation in region III is more striking. Figure 4-8 illustrates the droplet disappearance process suggested by the SEM observations. There

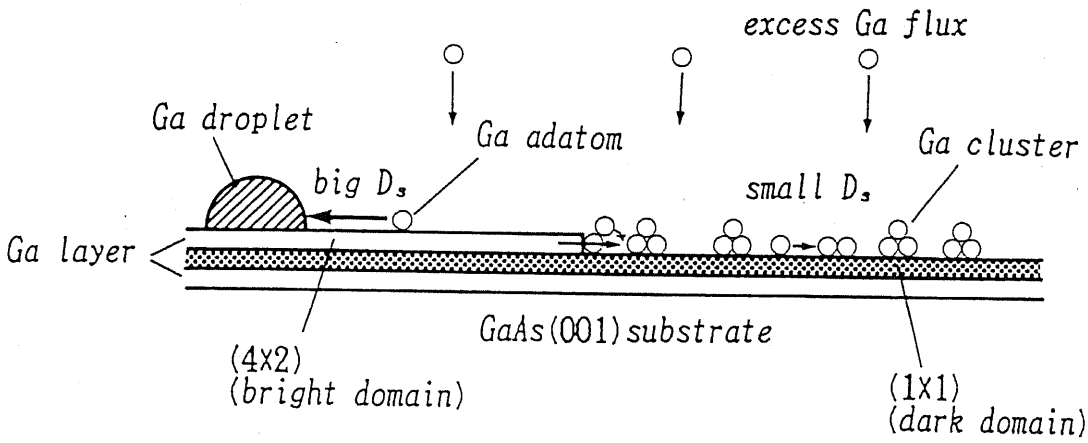

Fig.4-7. Schematic explanation of the bright domain expansion. Upon the bright domain in SEM image of Fig.4-3 that is (4×2) Ga-stabilized surface, the excess Ga atoms which are not consumed by As_4, diffuse on the surface and accumulate in the form of droplet. On a dark domain, no droplets emerge but excess Ga atoms form atomic clusters. The domain expansion is advanced by a dissolution of the Ga clusters into a continuous film at the edge of domain.

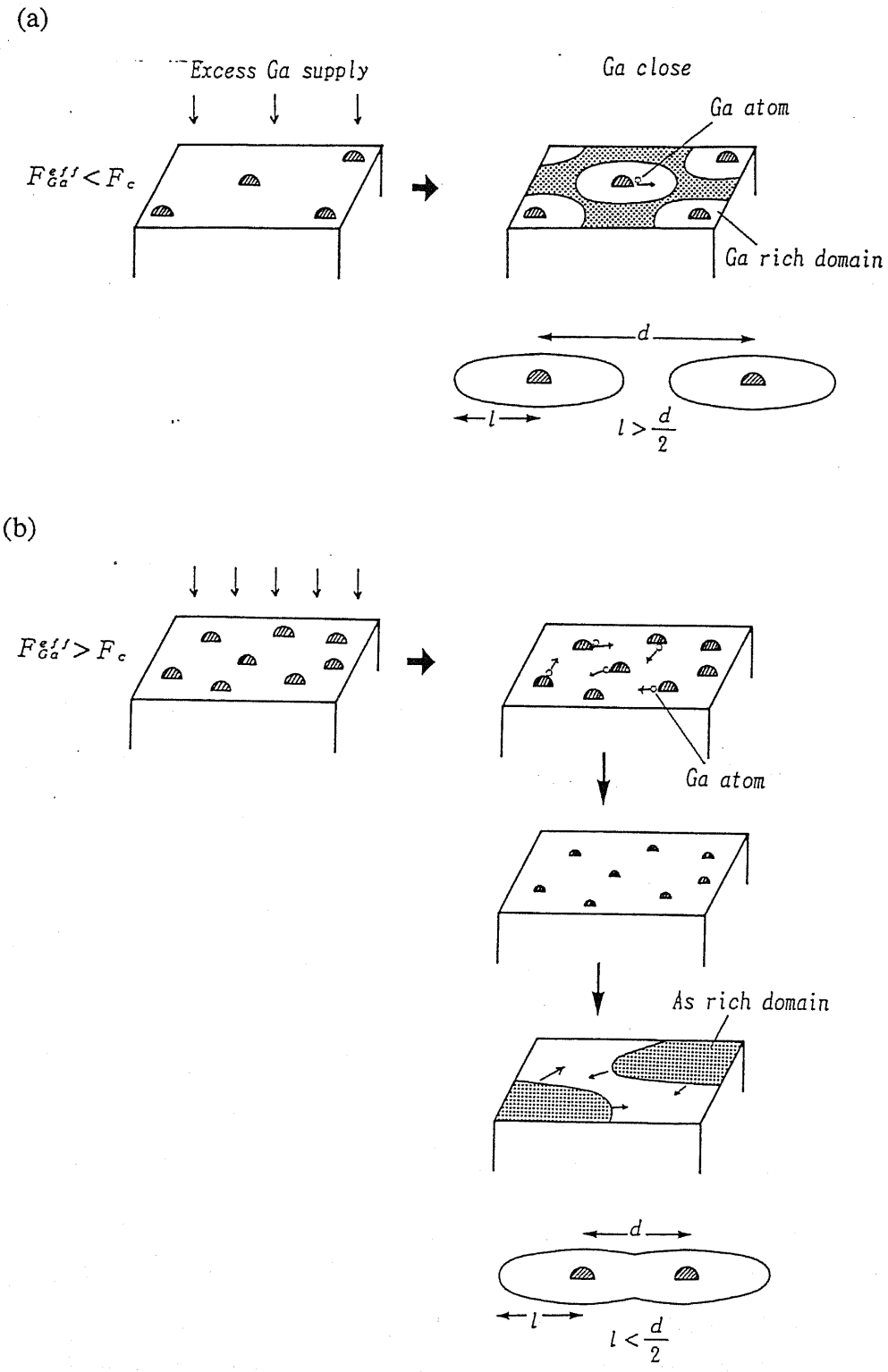

Fig.4-8. Schematic illustrations of the droplet disappearance in two modes; (a)low droplet density mode, (b)high droplet density mode. d is the mean distance between Ga droplets and l denotes the size of the region surrounding each Ga droplet.

is some area around each Ga droplet within which the lateral surface flux of Ga emitted from Ga droplets surpasses the incident As_4 flux and keeps the Ga-stabilized surface. We assume that the area around Ga droplets has a circular shape with the radius of l. When the half of the mean distance between Ga droplets, $d/2$ is longer than l, the most of the surface takes As-rich reconstruction, leaving the area of each Ga droplet (4×2) surface. When Ga droplets are exhausted, the size of the area decreases and finally fades out. This is what is observed in small n_s mode.

In large n_s mode, $d/2$ becomes smaller than l, which means an overlapping of each area occurs. This makes the entire surface Ga-stabilized. In this mode, incident As_4 flux consumes Ga uniformly and all droplets are getting smaller simultaneously as shown in Fig.4-8(b). When both of droplets and surrounding areas disappear, the whole surface is covered by As-rich domains. We believe that the decomposition of Ga continuous layer of (4×2) reconstruction into atomic clusters takes place preferentially at the edge of bright domains and this results in the expansion of dark domain. The existence of these two modes has been independently confirmed by RHEED oscillations during As_4 incorporation growth. This will be described in section 4.5. The experimental value of l is roughly estimated to be about $d/2=n_s^{-1/2}/2\sim5\mu m$ at the growth temperature of 580°C.

It has been reported that the mean distance between Ga droplets depends on the incident Ga flux, and this is explained by the surface diffusion of Ga atoms upon Ga-stabilized surface and nucleation process (Osaka *et al.* 1990b). However, both of the surface diffusion and an effect of emissivity of Ga atoms from droplets have a strong influence to determine the length of l.

From early seventies, there have been many reports describing the intermediate surface reconstruction between (2×4) As-stabilized and (4×2) Ga-stabilized ones during growth of GaAs. The pioneering work made by Cho (1971) showed a hysteresis feature between these reconstructions. The most commonly reported characteristics about this intermediate reconstruction are its unstableness and the difficulty in reproducing and keeping it for the purpose of other measurements such as STM (Biegelsen *et al.* 1990). The present observations of the spatial transition explain the unstable behavior of this intermediate reconstruction. Yamada *et al.* (1989) have

observed the growing surface of GaAs under the similar growth condition. However, there is no description about a macroscopic transition of surface reconstructions. We guess that the large difference from our experiment exist in the scan speed of the electron beam. In their experiment, it took 10 s to complete one scanning reflection electron microscopy (SREM) image. But we have found that high scan speed is essential for a successful observation of the domain transition. Especially for the observation of droplet disappearance in the high n_s mode, the scan speed of one frame per 0.5 s is necessary. But this speed is not fast enough, because the whole transition process occurs sometimes within several frames with this speed. In the case of Ga droplet formation, a careful choice of flux gives a small number of bright domains. This makes an observation easier even at the slower scan rate of the electron beam. However, the experimental repetition of a slow expansion of the domain gives rise to surface roughness which is recognized as a partly cloud looks of the wafer surface after the growth.

4.3.4 Summary

Real time observations of the growing GaAs(001) surface under excess Ga flux have been performed by using SEM and μ-RHEED MBE. It has been found that surface reconstruction transition between (1×1) and (4×2) occurs not uniformly but by the expansion of domains the size of which is as large as a few hundreds μm order. Ga droplets are formed inside the domains which show the (4×2) Ga-stabilized reconstruction. There are two modes for the disappearance of these droplets depending on the droplet density. The formation mechanism of the domain is discussed by the model in which excess Ga atoms are assumed to accumulate to create atomic clusters in the domain of the (1×1) reconstruction. Finally, the droplet disappearance process is outlined.

4.4 Formation Mechanism of Ga Droplets

It is well known that in MBE growth of GaAs, the formation of Ga droplets causes surface roughening and deteriorates the crystal quality (Yamada *et al.* 1989). Especially in MEE method where Ga and As are supplied alternately (Horikoshi *et al.* 1989), it has been suggested that both of formation and disappearance of Ga droplets occur during the growth. This process has been observed in real time by means of a SEM-MBE (Osaka *et al.* 1990a, Inoue 1991) and μ-RHEED (Isu *et al.* 1991). Recently, the observation experiment is extended to the formation of GaAl alloy droplets on GaAs(001) (Osaka *et al.* 1990c) and that of Ga(or Al) droplets on GaAs(111)B (Morishita *et al.* 1992). Among these works, the most systematic study has been performed by Osaka *et al.* (1990c). They have found the relationship between the droplet density and the incident Ga flux, and tried to understand it by a simple surface diffusion model.

In the previous section, we have described that the growth under excess Ga and low As_4 flux is very much different from that without As_4 flux. The formation and disappearance of Ga droplets are closely related to the reconstruction of the domains. When the Ga shutter is opened, bright domains as large as a few hundreds micrometer expand quickly and Ga droplets appear inside these bright domains in the SEM image. These domains show (4×2) Ga-stabilized reconstruction and become to cover the entire surface.

In this section, the Ga droplet density is investigated by SEM-MBE under a wide range of growth conditions. Then we will discuss the formation mechanism by using nucleation theory.

4.4.1 Experimental Procedure

The present results are all obtained in SEM mode. The acceleration voltage was 25KeV and the typical glancing angle was around 3° with the azimuth along [$1\bar{1}0$]. The SEM images were recorded by taking photographs or by the commercial video tape

recorder. The density of Ga droplets was measured from the photographs or the integrated images of the recorded frames produced by the image processor.

GaAs(001) substrates with the accuracy less than 0.5° were used. In order to reduce the error in growth rate introduced by non-uniformity of incident flux, we used substrates with relatively small size such as $6\times6\times0.5mm^3$. The preparation process of substrates was the same as explained in section 4.3.1. A series of measurements was performed by opening the Ga shutter under continuous but low As_4 flux. In the case of an experiment without As_4 flux, the shutter of As_4 was closed about 1 minute before the Ga supply to reduce the As_4 atmosphere around the substrate. When the growth temperature less than 500°C was employed, the As_4 shutter was closed to prevent the change of surface reconstruction to c(4×4). Since a formation of Ga droplets gives rise to surface roughening (Osaka *et al.* 1990a), a GaAs buffer layer was grown under sufficient As_4 flux at 580°C every time after the observation of Ga droplet formation. This is important to keep the surface identical throughout the experiment before the measurement.

4.4.2 Ga and As_4 Flux Dependence of Ga Droplet Density

In SEM image, Ga droplets appear as soon as the Ga supply starts and the droplet image is seen as dark point as shown in Fig.4-9. At this time, the RHEED pattern shows Ga-stabilized (4×2) reconstruction. It is observed that the number of these droplets is not changed but the size increases during the Ga supply. This agrees with the previous reports by Osaka *et al.* (1990a) and Inoue (1991). As we concentrate the study on the droplet density in the present experiment, not much attention is paid to the total amount of deposited Ga.

Figure 4-10 shows the Ga droplet density as a function of both Ga and As_4 flux at the growth temperature of 580°C. The density of $10^{10}/m^2$ means that the distance between each Ga droplets is as long as 10μm. In the condition without As_4 flux, the droplet density decreases as decreasing the incident Ga flux. On the other hand, when there is continuous As_4 flux, the density decreases rapidly as increasing the As_4 flux.

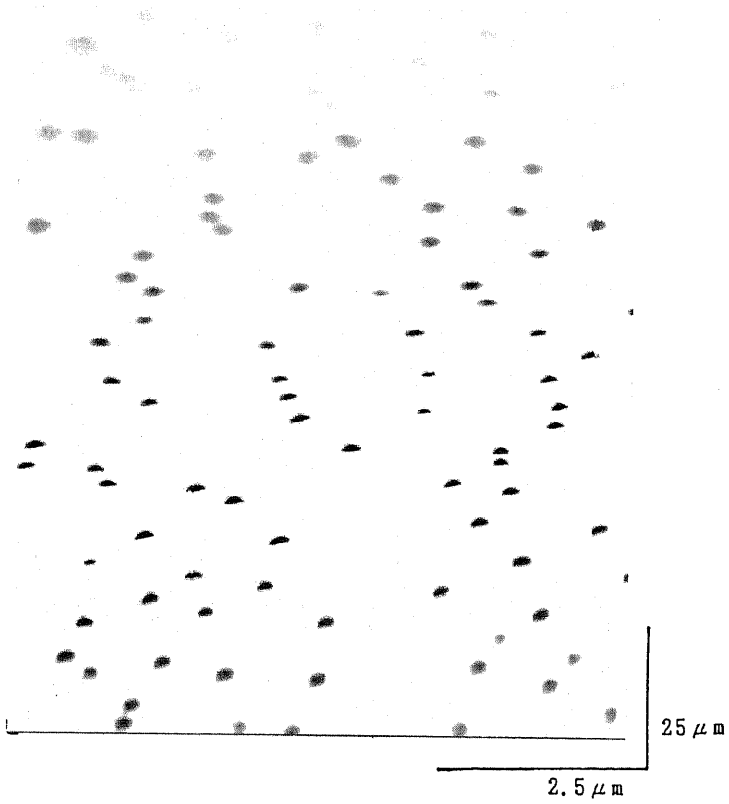

Fig.4-9. Typical SEM image of Ga droplets on GaAs(001) at 580°C. The image is foreshortened in vertical direction.

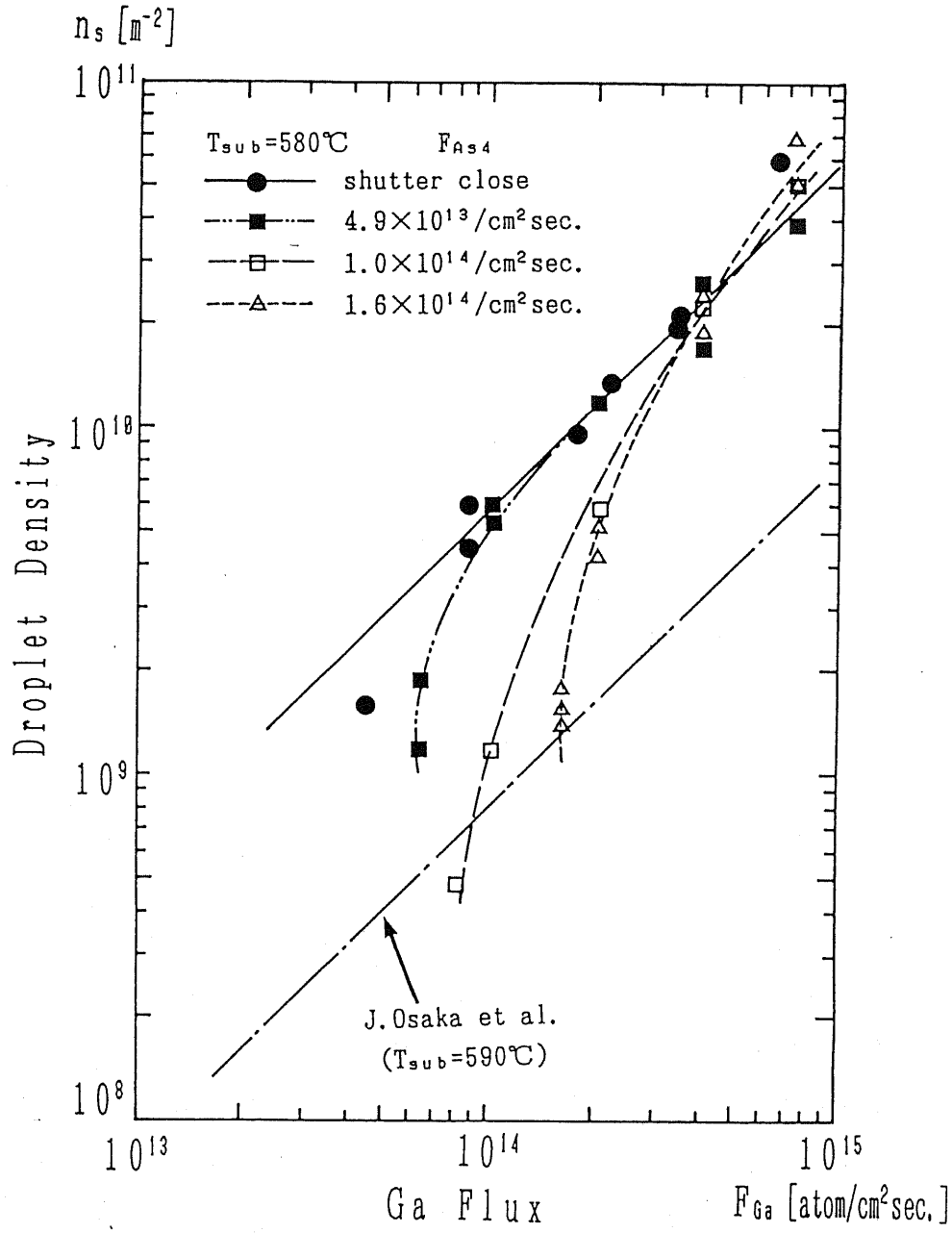

Fig.4-10. Droplet density as a function of Ga and As_4 incident flux at 580°C. The reported values at 590°C by Osaka *et al.* (1990c) is also plotted.

In the previous chapter, we have proposed a new growth method called Modulation MBE where the group-III element is supplied intermittently under low As_4 pressure. The decrease of Ga droplets caused by As_4 flux shows the superiority of this growth method to MEE. This is because in MEE, Ga is supplied under the absence of As_4 flux, which produces more number of Ga droplets and results in the surface roughening.

It can be understood that the simultaneous supply of As_4 effectively reduces the excess Ga flux which produces the droplets. To see this, we define an effective Ga flux, F^{eff}_{Ga} as follows.

$$F^{eff}_{Ga} = F_{Ga} - F_{GaAs}. \qquad (4\text{-}1)$$

Here, F_{GaAs} is the maximum Ga flux under which the droplets does not appear in a SEM image. This is exactly the Ga flux consumed by the simultaneously supplied As_4. The replotted data by using this parameter is presented in Fig.4-11. The droplet density is proportional to the effective Ga flux irrespective of the incident As_4 flux. Therefore, it is concluded that the As_4 does not effect the formation of Ga droplets but reduces effectively Ga flux.

4.4.3 Substrate Temperature Dependence of the Droplet Density

Next, we have investigated the substrate temperature dependence of the droplet density. The result is shown in Fig.4-12. In this experiment, the flux of Ga was chosen as 3.51×10^{14} or 8.93×10^{13}atom/cm^{2}s and As_4 flux was stopped. In this figure, there are two temperature regions named region A (625°C-525°C) and region B (475°C-400°C), where logarithm of the droplet density is inversely proportional to the temperature. At 650°C, which is just above the region A, the droplet density decreases rapidly to as small as 4.1×10^8/m^2. This is because significant reevaporation occurs at this temperature. In the region A, where the conventional MBE growth is performed, the density increases as decreasing the substrate temperature with the activation energy of 1.20±0.05eV.

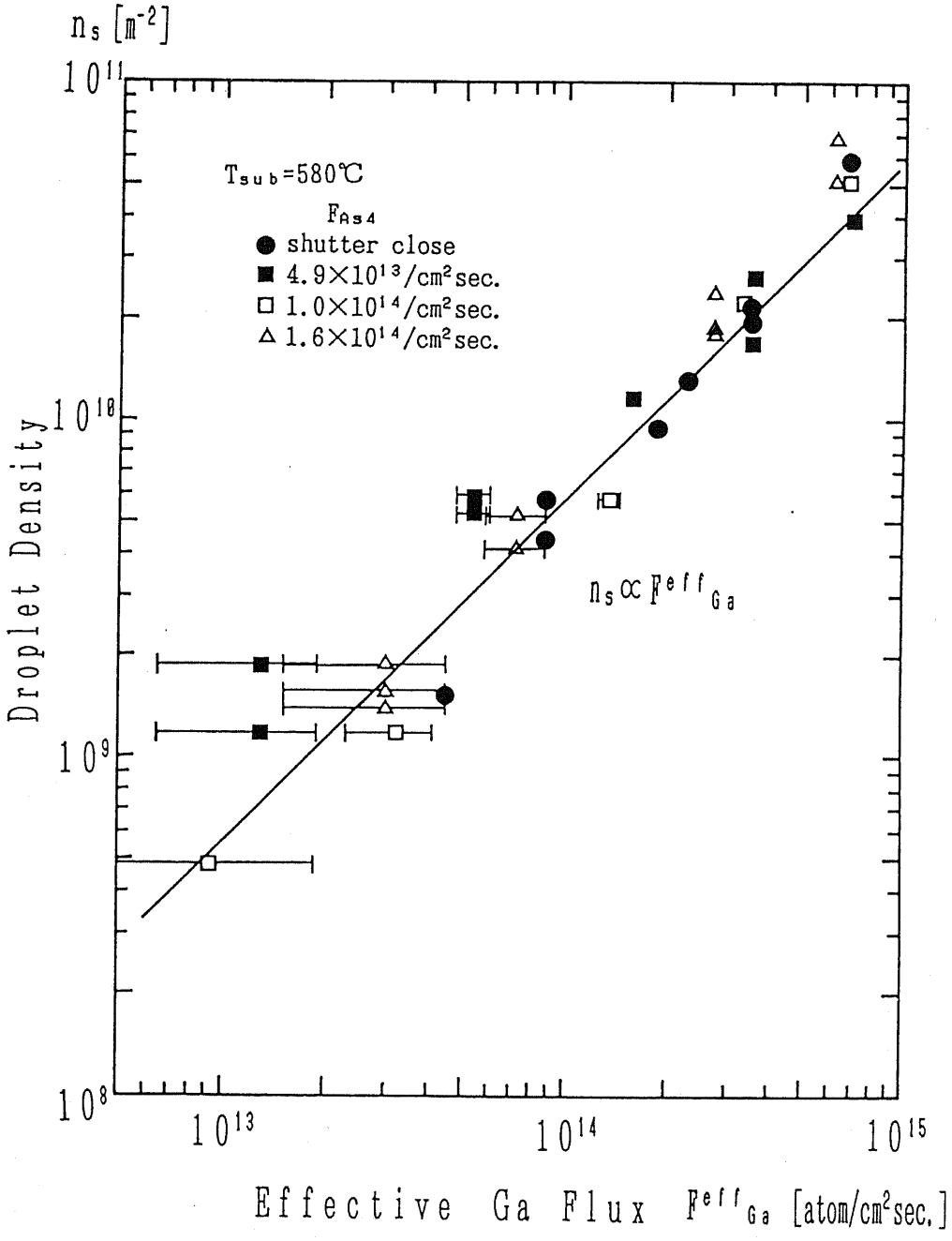

Fig.4-11. Replotted droplet density as a function of effective Ga flux, F^{eff}_{Ga}. The definition of the effective Ga flux is described in the text.

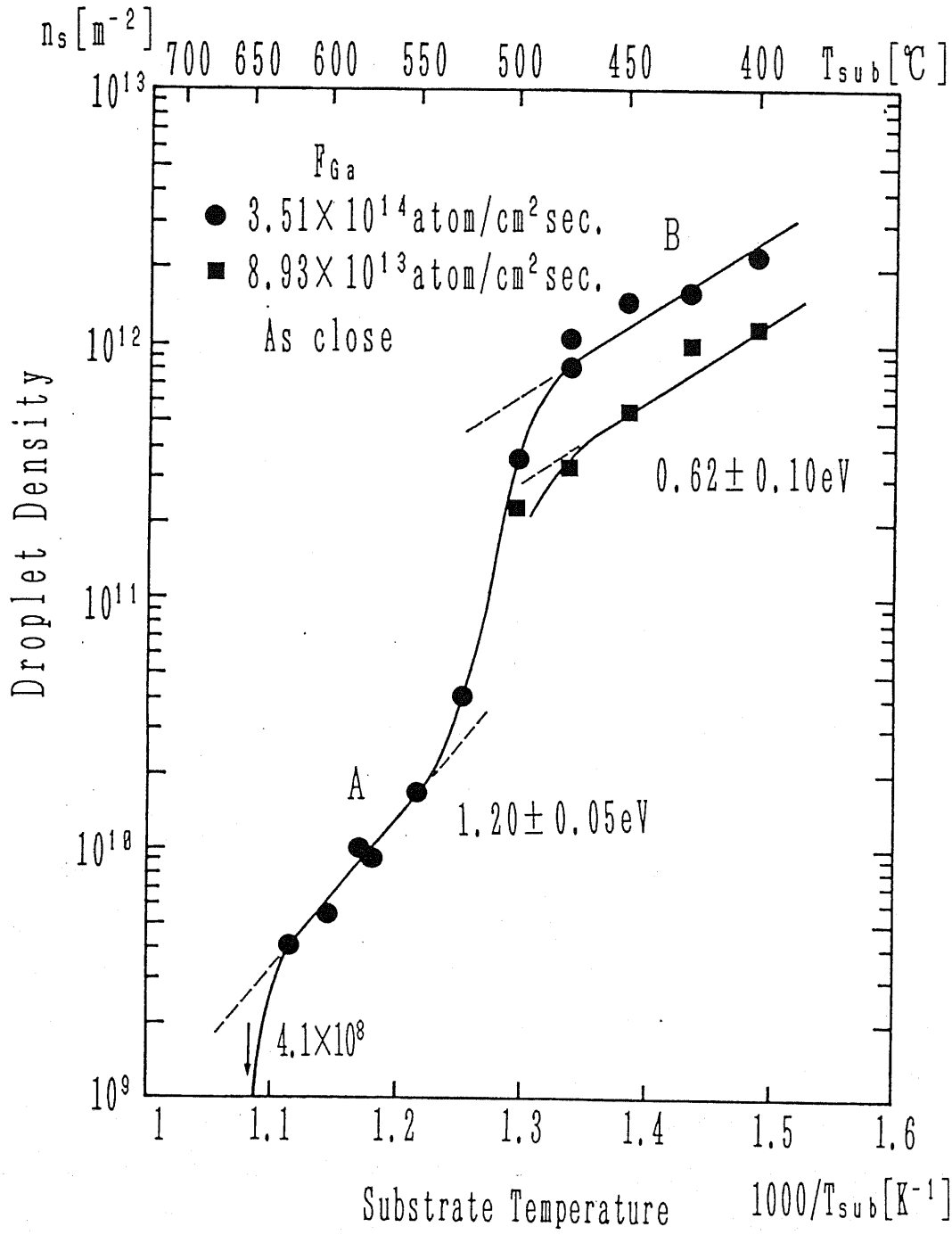

Fig.4-12. Substrate temperature dependence of Ga droplet density. The measurement was carried out with the shutter of As_4 closed.

As the temperature is further decreased, a steep increase of the droplet density to the order of $10^{12}/m^2$ is observed at around 500°C. The activation energy in the region B is nearly a half of that in the region A and takes the value of 0.62±0.10eV. At the temperature of 350°C, the surface with Ga deposition shows continuous wavy morphology of the dark band, and no droplets were observed. There is a possibility that the density and the shape of droplets are under the resolution of our SEM. However, it is a very interesting problem to see whether the Ga deposited on GaAs takes a form of continuous film or droplets at very low temperature. Because in the former case, the same growth condition as liquid phase epitaxy (LPE) might be established by MBE. The further study is to be done in the future.

There is another interesting point to discuss in the region B. Figure 4-13 shows the Ga flux dependence of the density at 475°C with the shutter of As_4 closed. Although the density in region A is proportional to the effective Ga flux as shown in Fig.4-11, the dependence is much weaker in the region B and proportional to $F_{Ga}^{0.85\pm0.07}$. This point is discussed in the next section.

4.4.4 Analyses of Formation Mechanism of Ga Droplets

We have mentioned that the experimental behavior of Ga droplets formed upon the (4×2) reconstructed surface agrees with the observation in the previous report (Inoue 1991). This (4×2) reconstruction is well accepted as the most As deficient structure among the all GaAs(001) reconstructions, and there have been many reports about the degree of As coverage of this reconstruction. In recent papers (Deparis and Massies 1991, Biegelsen *et al.* 1990), the (4×2) reconstructed surface is shown to have almost no As coverage, which means the GaAs(4×2) surface is terminated with only Ga atoms. So that the excess Ga atoms deposited on the GaAs surface grow at first in a continuous monolayer film. The further supplied Ga atoms can not form the second continuous film because of the surface tension, and they aggregate to form droplets. Thus it can be said that the excess Ga atoms grow on GaAs surface in the Stranski-Krastanov (SK) growth mode.

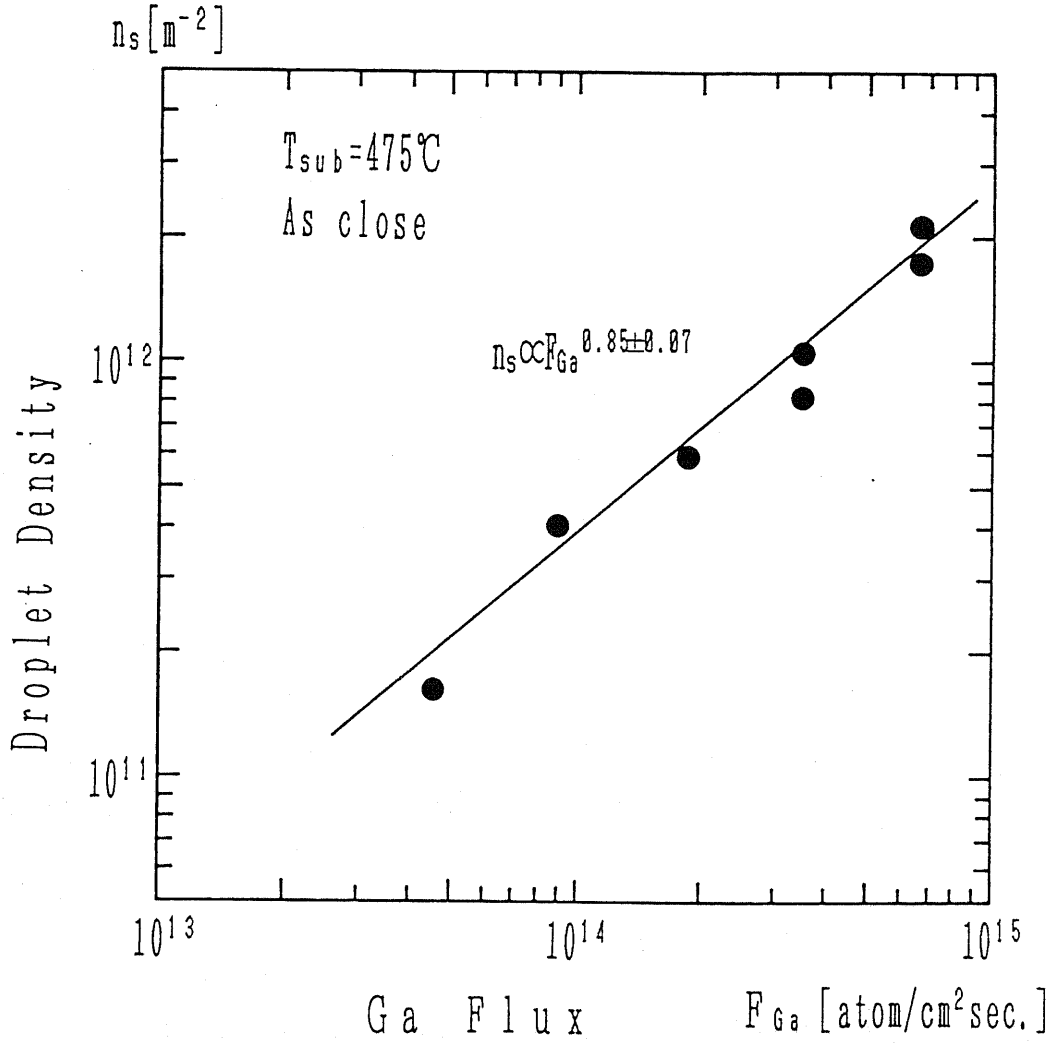

Fig.4-13. Droplet density as a function of the incident Ga flux at 475°C. The droplet was observed with the shutter of As_4 closed.

It has been known from nucleation theory that there are a few typical characteristics in SK growth mode (Venables *et al.* 1984, Reichelt 1989); (a) the nucleation density, which is the Ga droplet density n_s in the present case, changes very weakly with the deposition time, but strongly depends on the substrate temperature compared with the island growth, (b) growth in SK mode is typically observed in metal-semiconductor system, (c) the number of atoms in the critical nucleation, i is as large as ten atoms order.

The present results agree with the first and the second characteristics very well. About the third, we will analyze the results in the same manner as reported by Venables *et al.* (1980) and Spiller *et al.* (1983) who applied the nucleation theory to the Ag on Si(111) and W(110) systems respectively. For the complete condensation where re-evaporation is not significant, the nucleation density is given by (Stowell and Hutchinson 1971);

$$n_s/n_0 = C_i\left(F_{Ga}/n_0\nu\right)^{i/i+2} \cdot \exp\left(\left(E_i + iE_d\right)/(i+2)\cdot kT\right) \qquad (4\text{-}2)$$

where n_0, ν, k, E_i, E_d and T are the surface atom density ($6.3\times10^{14}/cm^2$ for GaAs(001)), an effective surface vibration frequency (10^{12}-$10^{13}s^{-1}$), Boltzmann's constant, the binding energy of the critical cluster relative to i isolated adsorbed adatoms, the adatom surface diffusion energy over the Ga-stabilized surface and the substrate temperature respectively. C_i is a geometric constant which has a value of around unity and has no strong material dependency. From the eq.(4-2), flux dependence of the nucleation density is deduced as;

$$n_s \propto F^{i/(i+2)}. \qquad (4\text{-}3)$$

However, as commented by Venables *et al.* (1984), the more sensitive and reliable method is to compare the extrapolated value of the nucleation density in the limit of $T^{-1}=0$ with the theoretical expression of eq.(4-2);

$$n_s\left(T^{-1}=0\right) = n_0 C_i\left(F_{Ga}/n_0\nu\right)^{i/(i+2)}. \qquad (4\text{-}4)$$

Analysis of the experimental results gives $i=\infty$ for the region A from both of the flux and the temperature dependences. For the region B, the flux dependence gives $7<i<23$, and the temperature dependence does $11<i<48$ to $7<i<16$ by choosing ν from 10^{12} to $10^{13}s^{-1}$. It should be noted that in the region A, $i=\infty$ is given from both of the flux dependence of $n_s \propto F^{eff}_{Ga}$ and the experimental value of $n_s(T^{-1}=0)=7.4\times10^2/m^2$ which is less than the minimum value of $n_s(T^{-1}=0)=8.8\times10^4/m^2$ with $i=\infty$ and $\nu=10^{13}s^{-1}$. This indicates that the number of i is too large to measure in exact number. The large number of i in the both temperature regions agrees with the feature of SK growth mode. Moreover the decrease in i as decreasing the growth temperature has been generally found.

Before arriving the conclusion that the excess Ga atoms grow on GaAs in SK mode, we will discuss about the difference in the present SK mode and the usual SK mode in metal-semiconductor system. Because it is not sure whether the Ga top layer of the GaAs has a property of a metal or a semiconductor. SK mode is generally expressed as layer-plus-island growth, and the underlying layer on which the island is formed has been assumed to be the same material as the island. In our case, the underlying Ga layer forms the (4×2) reconstruction of GaAs(001) surface. Thus the present situation is slightly different from the previous picture of SK mode, whereas the present experimental results agree with the behavior of the SK growth mode. In this respect we can say that the present system is classified into the "extended" SK mode.

Next, we discuss about meanings of the activation energy in Fig.4-12. In the limit of $i=\infty$, eq.(4-2) is well approximated to

$$n_s = C_\infty\left(F_{Ga}/\nu\right)\cdot\exp\left(\left(E-E_a+E_d\right)/kT\right) \qquad (4\text{-}5)$$

where E is the Ga desorption energy from the droplets and E_a is the adsorption energy which is the binding energy between the adatom and the Ga-stabilized surface. E-E_a+E_d have been determined from Fig.4-12. We use E=2.82eV, which is the vaporization energy of the metallic Ga (Honig and Kramer 1969). Although the values of E_a and E_d have not been determined independently, the energy difference, E_a-E_d , is obtained as

1.62±0.05eV and 2.20±0.10eV in the region A and B respectively. It is not clear that the increase of the energy difference by decreasing the temperature is due to either the increase of the adsorption energy or the decrease of the surface diffusion energy. From the value of E_a-E_d , we can calculate a surface diffusion length before the desorption, λ_s, of an isolated Ga atom on the (4×2) surface which is of the order $n_0^{-1/2}exp((E_a-E_d)/2kT)$. The calculated diffusion length is shown in Fig.4-14, where the experimental values of the mean distance between the droplets is simultaneously plotted. It is worth mentioning that Inoue (1991) took the distance between Ga droplets as a shortest limit of the Ga migration distance before the incorporation and the definition of this diffusion length is quite different from ours.

Although there are still unknown factors in evaluating the theoretical formulas, the curves look rather reasonable. In the case of complete condensation, the mean distance between Ga droplets must be less than the diffusion length before the desorption; $\lambda_s > n_s^{-1/2}$. But at the temperature above 625°C, this condition is not fulfilled and the nucleation occurs under incomplete condensation condition. This also indicates that our assumption that there is a high rate of re-evaporation at 650°C is right. In this temperature region, low droplet density is attributed to the decrease of the surface diffusion flux into droplets.

4.4.5 Summary

The direct measurements of Ga droplet formation under the condition of deficient As_4 flux have been carried out. The density of Ga droplets has been investigated under various growth conditions. It has been found that the existence of As_4 flux does not influence the formation process of Ga droplets but reduces the excess Ga flux effectively. In the temperature dependence of the droplet density, there are two characteristic temperature regions, high and low temperature regions. Each covers the region from 525°C to 625°C and from 400°C to 475°C respectively.

The experimental results were analyzed by employing nucleation theory, and the number of Ga atoms in a critical nuclei has been calculated. The surface diffusion

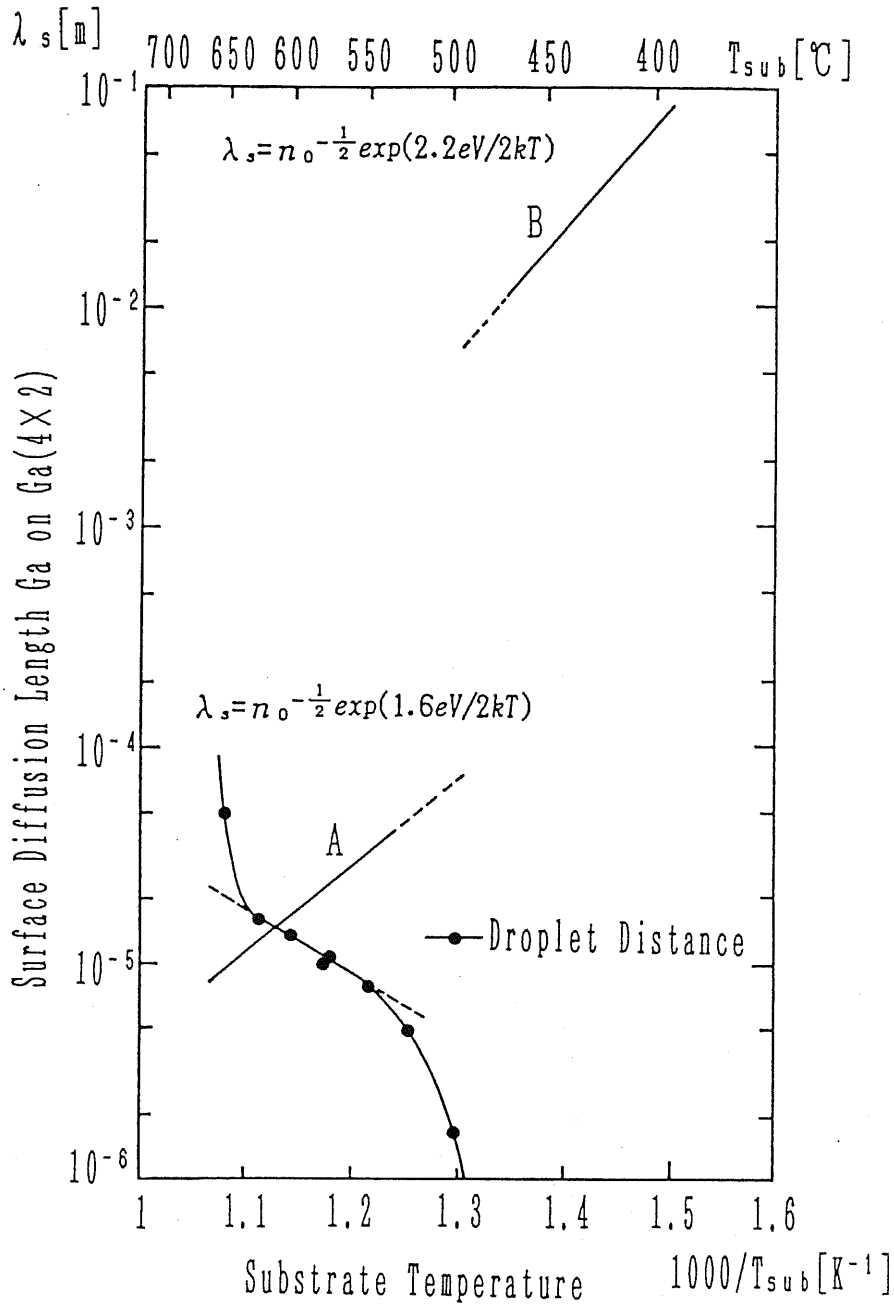

Fig.4-14. Calculated surface diffusion length λ_s of Ga atoms on the Ga-stabilized (4×2) surface before the desorption. The mean distance between Ga droplets which corresponds to $n_s^{-1/2}$ is also shown.

length of a Ga atom on the (4×2) reconstructed surface has been also estimated. This diffusion length is consistent with the steep decrease in the droplet density at 650°C. It is shown that the Ga droplet formation upon the Ga-stabilized surface can be explained by the SK mode growth.

4.5 As_4 Incorporation Growth Studied by RHEED Oscillation

In MBE growth of III-V compounds, flux of group III elements incident to a substrate is usually determined by measuring a thickness of an epitaxial layer or a period of RHEED oscillation in-situ. This method is quite reliable and gives enough accuracy for the most purposes. On the other hand, one does not have to determine flux of group V elements exactly as compared with group III elements.

However, even under sufficient As flux, the surface reconstruction depends very much upon the flux ratio and the growth temperature. Moreover, it has been suggested that the growth is influenced by the amount of As flux. Especially, in the low temperature growth in MEE mode, the exact control of As flux is necessary to avoid the excess As adsorption (Horikoshi and Kawashima 1989b).

In order to determine As flux, an ionization gauge which can be placed at the substrate position, has been used conventionally. The reading of the ionization gauge is calibrated by using the empirical relationship between the sensitivity and the atomic species (Flaim and Ownby 1971). But there are some uncertainties in this measurements. The indication of a gauge is unstable and greatly influenced by the pumping ability of the LN_2 shroud around a gauge. In the MBE system of the present experiment, the stainless case covering the ionization gauge disturbs the measurement. The metallic As deposited inside the case produces the As atmosphere being heated by the filament. The most surprising fact is that there is a big pressure difference in the pressure gauge between our two MBE systems even we employ the same amount of As_4 flux. Therefore, this conventional method is not reliable and does not have much consistency among many systems.

In 1983, Neave *et al.* reported that after the pre-deposition of Ga without As_2 supply, the intensity of RHEED specular beam oscillates upon opening the As shutter as shown in Fig.4-15, where the reconstruction shows (3×1) or (1×1). This RHEED oscillation has been explained as As incorporation process into excess Ga on the GaAs surface. The growth rate obtained by the period of oscillation has been found to be proportional to the incident As flux. Therefore, it is possible to determine the As flux accurately by this method. Recently, RHEED oscillation of Sb incorporation into

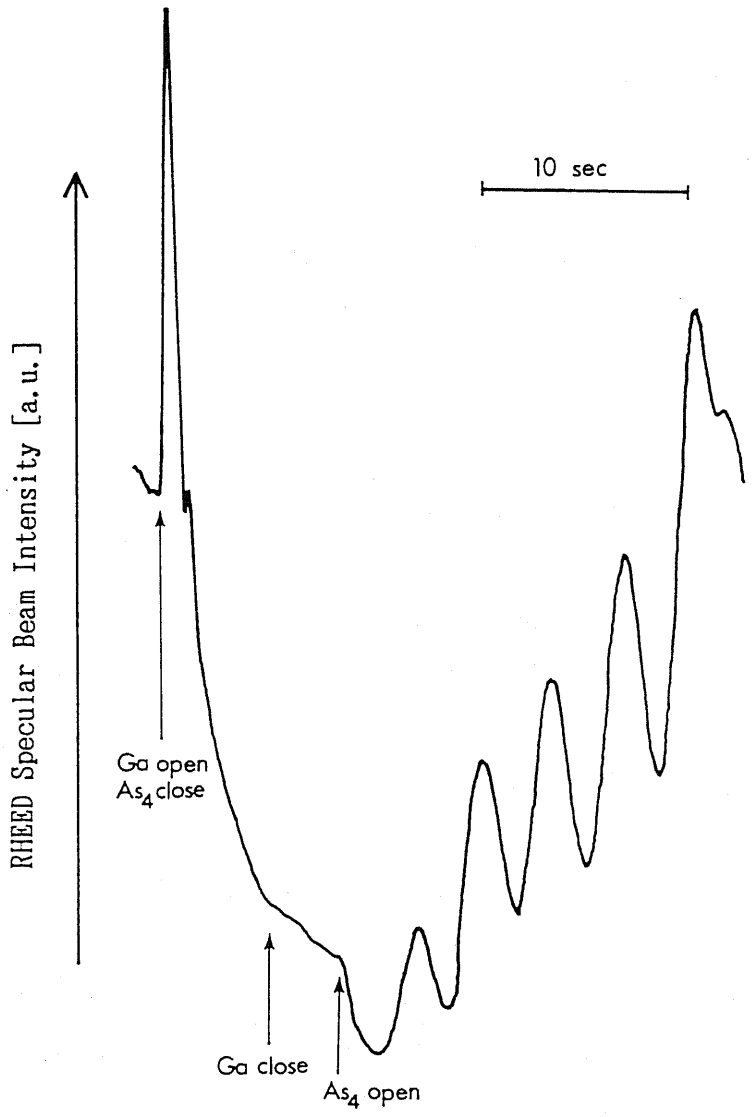

Fig.4-15. Typical RHEED intensity oscillation at 450°C during As_4 incorporation upon excess Ga surface.

excess In on InSb is reported (Ferguson *et al.* 1992).

However, in the As incorporation growth, there are complicated factors as follows.

(a)The incorporation rate depends on the substrate temperature (Lewis *et al.* 1986, Fernandez 1988, Garcia *et al.* 1989, Sugiyama and Kajikawa 1992). At the temperature higher than 500°C, the incorporation rate decreases significantly. At the temperature lower than 500°C, the rate shows very weak temperature dependency.

(b)The incorporation rate at the temperature higher than 500°C depends on the kind of As molecules such as As_2 and As_4. Garcia *et al.* (1989) and Kojima *et al.* (1990) have reported that the As_2 incorporation rate is faster than that of As_4.

(c)The substrate misorientation have an effect on the incorporation rate. Kojima *et al.* (1991) have found that the incorporation rate on GaAs(001) 2° misoriented substrate to [110] is faster than that on GaAs(001) and GaAs(001) 2° misoriented substrate to $[1\bar{1}0]$.

As described in the previous section, there are two modes in Ga droplet disappearance. The different mode appears depending on the droplet density. In this section, As_4 incorporation rate on the surface with various Ga droplet density is measured. Then a relationship between the As_4 incorporation rate and the droplets disappearance process is investigated.

4.5.1 Experimental Procedure

The experiment in this section was carried out by ULVAC-MBC300. Experimental procedure was similar to that of the droplet observation as shown in Fig.4-16. The total amount of the deposited Ga was kept 5ML in this experiment. The electron beam of RHEED was incident along the $[1\bar{1}0]$ azimuth.

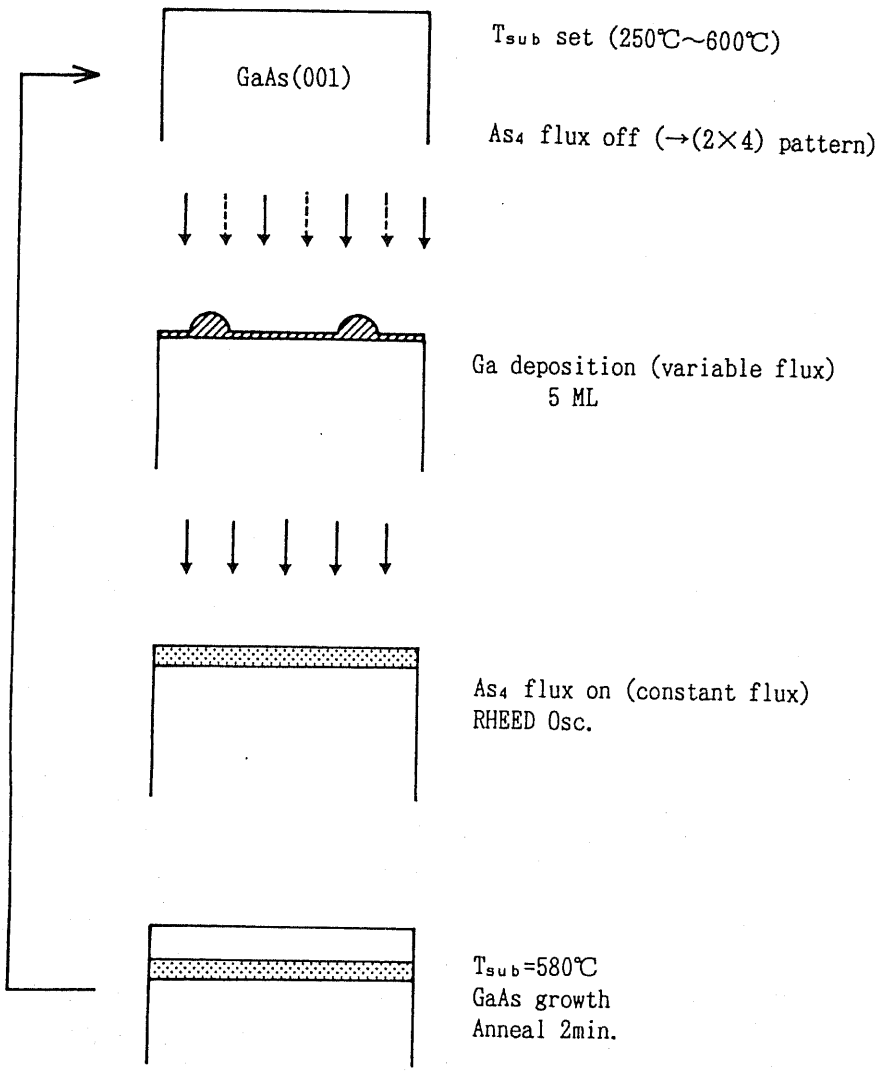

Fig.4-16. Experimental procedure in the experiment.

4.5.2 Experimental Results

(a)Ga flux dependence of As_4 incorporation rate

Figure 4-17 shows typical RHEED oscillations at 550°C after opening the As_4 shutter. When the Ga flux is less than 1.5×10^{14}atom/cm^{2}s, the periods of oscillations are the same. However, this period decreases significantly as increasing the Ga flux to 1.8×10^{14}atom/cm^{2}s. Figures 4-18 and 4-19 show the As_4 incorporation rate as a function of Ga flux at 550°C and 580°C respectively. There is clearly the critical flux, F_c, at which the incorporation rate changes abruptly, whereas the rate at 400°C is independent of Ga flux. It is also found that the critical flux of 580°C is bigger than that of 550°C. In these experiments, the rate is measured many times across the critical flux to reduce the error which comes from the instability of As_4 flux.

(b)Substrate temperature dependence of As_4 incorporation rate

Next, substrate temperature dependence of As_4 incorporation rate was investigated. Figure 4-20 shows typical RHEED oscillations at the growth temperature of 550°C and 450°C with the constant As_4 flux. At 450°C, the growth rate is independent of Ga flux in contrast to the case of 550°C where the rate depends on the Ga flux. Figure 4-21 shows the substrate temperature dependence of As_4 incorporation rate with the Ga flux of 1.2×10^{14} and 6.3×10^{13}atom/cm^{2}s. At the temperature higher than 500°C, the growth rate clearly depends on the pre-deposited Ga flux. It should be noted that at the temperature lower than 500°C, the growth rate weakly depends on the growth temperature. The activation energy in this region is 0.04eV, which is very close to the reported values of 0.04eV (Garcia *et al.* 1989) and 0.07eV (Lewis *et al.* 1986).

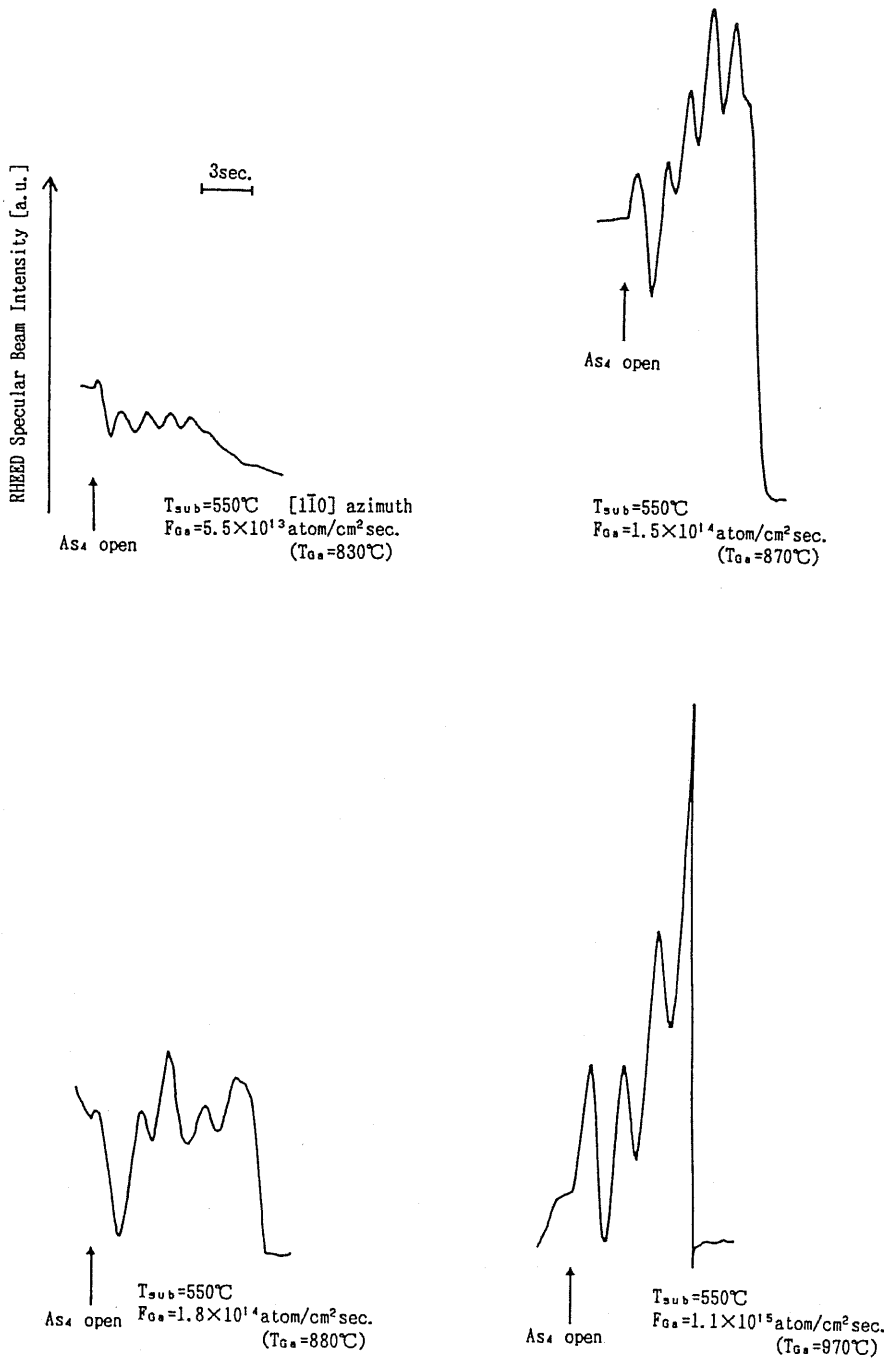

Fig.4-17. Typical RHEED oscillations at 550°C during As_4 incorporation with the constant As_4 flux. Before opening the As_4 shutter, Ga was deposited with each incident flux. The temperature of Ga Knudsen cell is also shown.

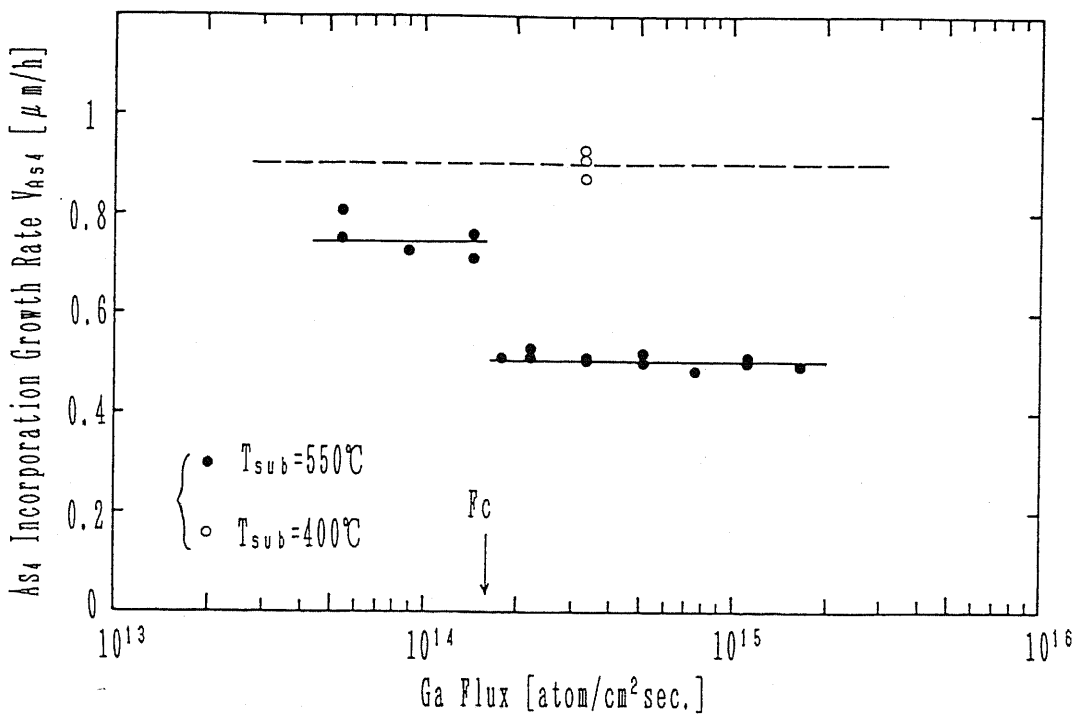

Fig.4-18. As_4 incorporation growth rate as a function of pre-deposited Ga flux at 550°C and 400°C.

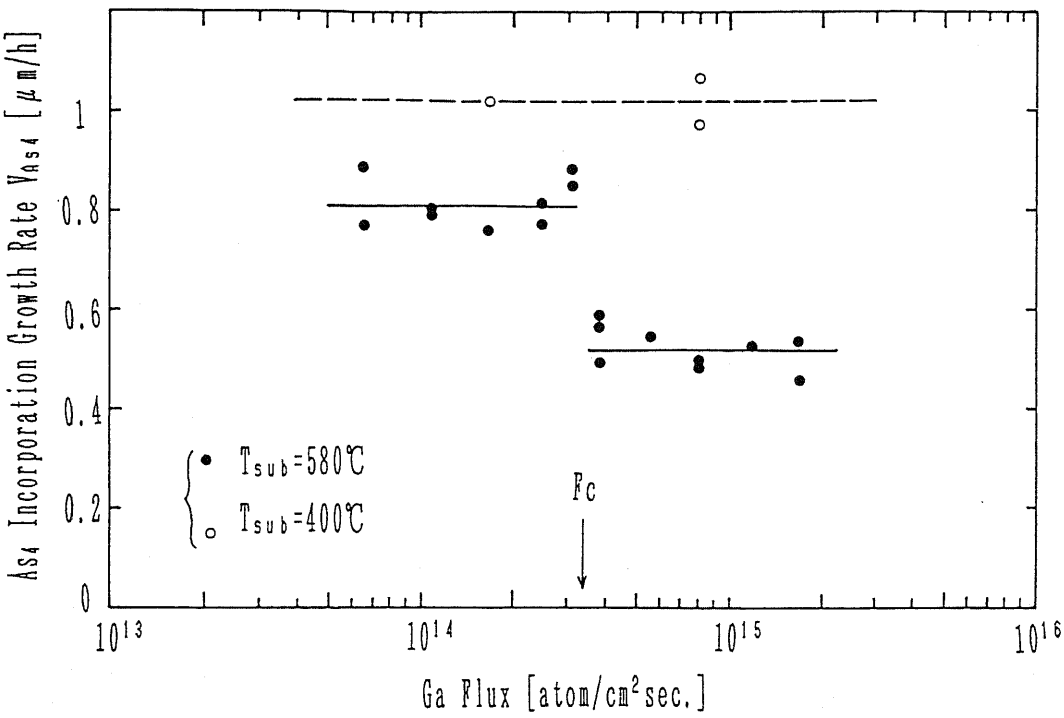

Fig.4-19. As_4 incorporation growth rate as a function of pre-deposited Ga flux at 580°C and 400°C.

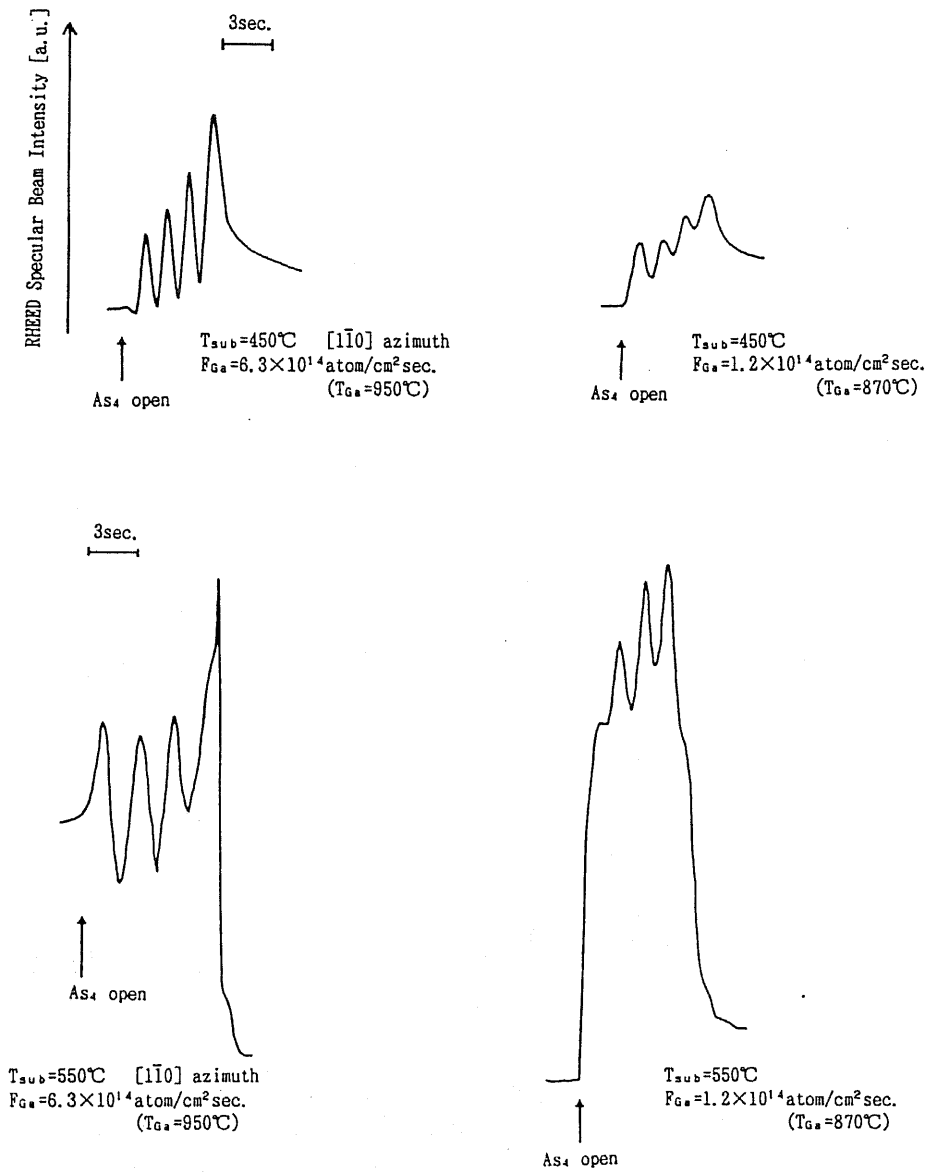

Fig.4-20. Typical RHEED oscillations at 550°C and 450°C during As_4 incorporation with the constant As_4 flux. Before opening the As_4 shutter, Ga was deposited with each incident flux. The temperature of Ga Knudsen cell is also shown.

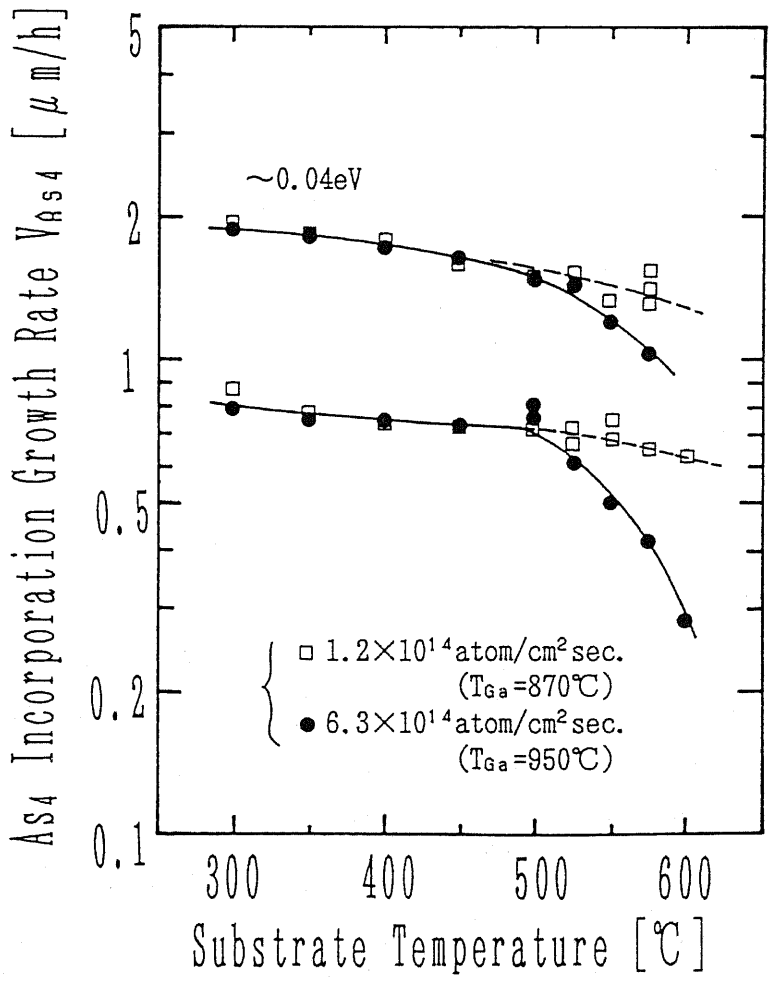

Fig.4-21. Substrate temperature dependence of As_4 incorporation growth rate.

4.5.3 Discussion

Both the temperature and the flux dependence of the incorporation rate show that there are two modes in the As_4 incorporation growth at the temperature above 500°C. When the incident Ga flux before the As_4 supply is bigger than the critical flux, F_c, the incorporation growth rate decreases significantly as increasing the temperature. This decrease of incorporation rate in this mode agrees with what was reported previously. On the other hand, when the incident Ga flux is smaller than the critical value, the incorporation rate shows weak dependence on the substrate temperature. As far as we know, this dependence has not been reported before.

In the section 4.3, it has been shown that there are two disappearance modes of Ga droplets depending on the droplet density. The critical value of the density between these two modes was about $10^{10}/m^2$ at 580°C. In the present experiment, the shutter of As_4 is closed during the Ga supply. Thus the Ga droplet density before the As_4 incorporation given by F_c can be estimated from Fig.4-11 to be $2\times10^{10}/m^2$, which is very close the critical value in droplet disappearance. Therefore, it is suggested that the high density mode of Ga droplet disappearance corresponds to the growth with slow incorporation rate, and the low droplet density mode does to the growth with fast incorporation rate.

In the high density mode, SEM images showed that the whole surface is covered by Ga-stabilized reconstruction and Ga droplets become getting smaller during the As_4 supply, and the surface changes to As rich surface when the droplets disappear. This implies that the As_4 incorporation takes place on Ga-stabilized surface entirely. If the directly impinging flux on Ga droplets is neglected, the As_4 incorporation rate is the condensation rate of As_4 upon Ga-stabilized surface. Therefore, the temperature dependence of incorporation rate is explained by the increase of the desorption rate of As on Ga-stabilized surface as increasing the substrate temperature. After the incorporation of As atoms into the solid phase, Ga is supplied from the droplets by surface diffusion and this continues until the exhaustion of Ga atoms. So that, the As_4 incorporation rate in this mode is independent of the droplet density.

On the other hand, in the low density mode, the surface was covered by As rich

reconstruction except the region surrounding each droplet as soon as the Ga supply was stopped. In the present experiment, droplet disappearance starts by the As_4 supply. The droplet density depends on the incident Ga flux before the start of the As_4 incorporation. But it has been found that the incorporation rate does not depend on the incident Ga flux. Therefore, this result suggests that the As_4 incorporation rate is equal to the local growth rate at the region around each Ga droplet, and thus does not depend on the number of droplets. The region surrounding each droplet is covered by Ga-stabilized reconstruction. Unlike the high density mode, in which the incident As_4 flux uniquely determine the incorporation rate, the fast incorporation rate in the low density mode is explained by an additional supply of As migrating from the outside of the Ga-stabilized region. An increase of the difference in the incorporation rates between the two modes as increasing the growth temperature is due to the increase of As desorption rate in the high density mode. Since the surface outside of the Ga-stabilized region exhibits As rich reconstruction, the surface diffusion flux consists of As atoms migrating on the As rich surface. At the temperature of 600°C, the incorporation rate in the low density mode is about twice as fast as that in the high density mode. This indicates that the lateral flux makes a significant contribution to the incorporation growth rate in the low density mode, and is as large as the flux directly incident to the Ga-stabilized region. Therefore, it can be point out that the migration length of adsorpted As on As rich surface is as long as the size of the each Ga-stabilized region. This length is much longer than that reported previously (Mochizuki and Nishinaga 1989). However, the present model explains the shrinking behavior of each Ga-stabilized region in SEM images. If there is no consideration about the lateral flux, each region should disappear abruptly like the high density mode.

4.5.4 Summary

As_4 incorporation rate on Ga-stabilized surface has been obtained from RHEED intensity oscillations. It has been shown that at the temperature above 500°C, this rate takes two different values depending on the pre-deposited Ga flux. These two

incorporation rates correspond to the two modes in the droplet disappearance which was independently observed in SEM-MBE. In the high droplet density mode, the temperature dependence of the incorporation rate is explained by a desorption of As on Ga-stabilized surface. In the case of low droplet density, As atoms laterally migrating on As rich surface contribute to the increase of the incorporation rate. This model well explains the present results and previous SEM observations.

4.6 Direct Observation of In Deposition on GaAs Substrate

In this section, a real time observation of In deposition on GaAs(001) surface is described. Since the growth of InAs on GaAs(001) is a typical example of the strained heteroepitaxial growth, a lot of works have been devoted on the growth process from the viewpoint of studying both the growth mechanism and device fabrication. Because of the large lattice mismatch, much attention has been paid to the initial stage of InAs growth with the thickness less than about 100nm. So far RHEED have been widely used for the study of such a thin layer during the growth. From the observations of RHEED pattern, it have been found that the initial stage of growth is governed by SK growth mode and the critical thickness is a few ML of InAs (Nakao and Yao 1989). These measurements of RHEED give us much information, hence MBE has great advantages over MOCVD to study of the strained heteroepitaxial growth. But RHEED have no ability to clarify the growth process spatially as explained before.

In the chapter 2, it is found that the In composition of InGaAs has the dependence upon the step density at the high growth temperature. This has been explained in terms of the In adatom diffusion. In this chapter, we employ the SEM-MBE or μ-RHEED to study the initial stage of In growth on GaAs(001) at relatively high temperature. By using the same technique as Ga growth on GaAs(001), the growth mechanism is studied. Futhermore, the growth on a vicinal surface is studied.

4.6.1 Experimental Procedure

The experimental procedure is illustrated in Fig.4-22. A series of observations was performed by opening the In shutter with or without As_4 flux. In this study, the growth temperature was kept at 580°C. In the case without As_4 flux, the shutter of As_4 was closed about 1 min before the In supply to reduce the As_4 atmosphere around the substrate. In order to keep the surface identical for every experimental cycle, the substrate was heated up to the temperature of 640°C after the observation, and In or InAs on the surface was evaporated. As described in chapter 2, 580°C is high enough

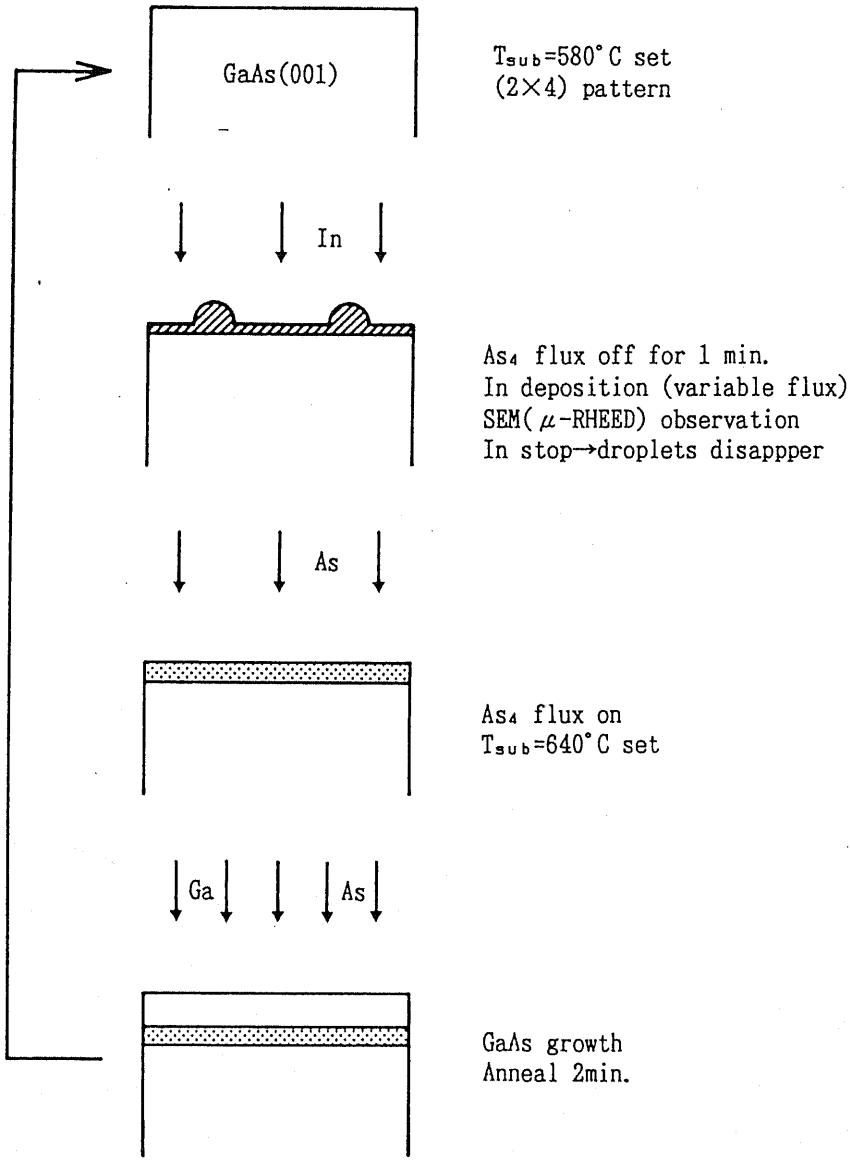

Fig.4-22. Experimental procedure in the experiment.

for the In re-evaporation. But, for the perfect removal of In or InAs, we employed the temperature of 640°C safely. After this process, a GaAs buffer layer was grown under sufficient As_4 flux. Then the substrate was cooled down at the growth temperature of 580°C to start the observation cycle. It was confirmed that the RHEED pattern shows well-defined (2×4) reconstruction at this point.

The samples were prepared in the same manner as described in the section 4.3.1. GaAs(001)<0.5° oriented substrates were usually used. In the investigation of the step density dependence of the growth behavior, GaAs(001) precisely orientated substrate within 0.05° and 4° misorientated substrate towards [110] were used. They were mounted on the same Mo block side by side to reduce the error in the growth rate, which comes from non-uniformity of both incident flux and substrate temperature. The growth condition of GaAs was chosen so as to establish the growth in the step flow mode on the 4° misorientated substrate.

All following observations were made by SEM. The acceleration voltage was 25KeV and the typical glancing angle was about 6° with the azimuth along [1$\bar{1}$0]. The electron beam was scanned at the typical rate of one frame per 1.5 s and SEM images were recorded by the video tape recorder.

4.6.2 Experimental Results

Figure 4-23 shows the SEM image of the growing surface under the In incident flux of F_{In}=1.3×10^{14}atoms/cm^{2}s with the As_4 shutter closed. As soon as the In shutter is opened, the black points appear on the whole surface. Since the melting point of In is much lower than the growth temperature of 580°C, these black points stand for In droplets. The number of these In droplets does not change but the size of each droplet increases during the In supply. These behaviors are very similar to that of Ga droplets on GaAs(001). This growth behavior can be also observed by μ-RHEED. In Fig.4-23, the droplet density dependence upon the step density can be clearly seen. The density on the GaAs(001)<0.05° which is shown in the upper side, is less than that on the 4° misorientated substrate.

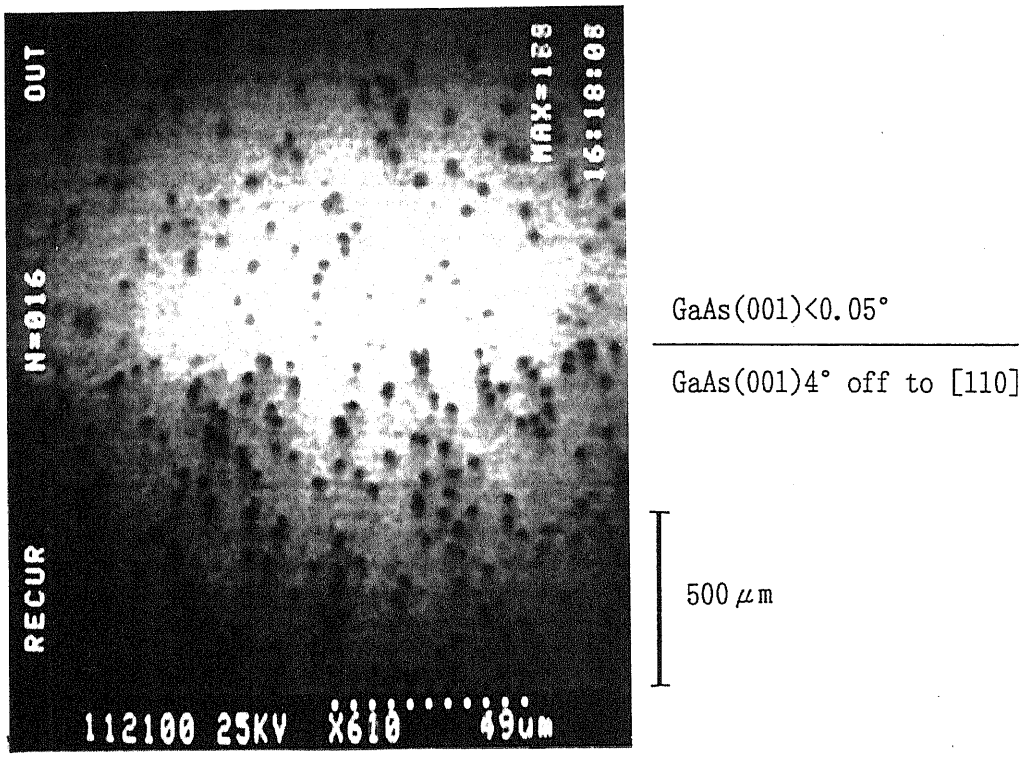

Fig.4-23. Typical SEM image of In droplets at 580°C. The upper side of the picture shows the substrate of GaAs(001) precisely orientated within 0.05°, whereas the lower side corresponds to the (001) 4° misorientated substrate to [110]. The image is foreshortened in vertical direction.

In this experiment, we are not sure about the state of initial growth because the unsteady shutter operation disturbs the observation. Therefore, the amount of In atoms necessary for the droplet formation was not possible to find.

The droplet density is shown in Fig.4-24, where the Ga droplet density obtained in section 4.4 is also shown. Since the growth was repeated several times to complete this figure, the data are scattered. But it is clearly seen that the droplet density decreases as decreasing the incident In flux. The density of In droplets is smaller than that of Ga droplets, but the order is almost the same, namely around 10^9-$10^{10}/m^2$. When As_4 flux of $2.6\times10^{14}/cm^2s$ is supplied, the density decreases as indicated by the open circle. This means that excess In flux for the droplet formation is reduced by the presence of As_4 flux.

Figure 4-25 shows successive SEM images after closing the In shutter with the As_4 shutter closed. These black points gradually shrink and finally disappear in (c). The nominal amount of In deposited is about 31ML and the total time from the opening of the In shutter to the point of droplet disappearance is about 80 s. Therefore the evaporation rate can be estimated to be about 0.4ML/s.

In Fig.4-25, it is shown that some surface roughness even after the droplet disappearance is introduced. This roughness was made by the previous growth sequence, and hardly disappear by both of the high temperature treatment and a GaAs growth. However, the RHEED pattern from the surface shows clear (2×4) reconstruction. It is suggested that an intermixing between the deposited In and the GaAs substrate occurs to produce InGaAs at the heterointerface and this results in the surface roughness (Fewcett *et al.* 1992, Zhang *et al.* 1992).

4.6.3 Discussion

All the growth behaviors indicate that the growth of In on GaAs(001) is governed by SK growth mode as the case of Ga on GaAs(001). Since the droplet density dependence on the growth temperature has not been studied, the number of atoms in the critical nucleation can not be determined. But, it is observed to be much large from

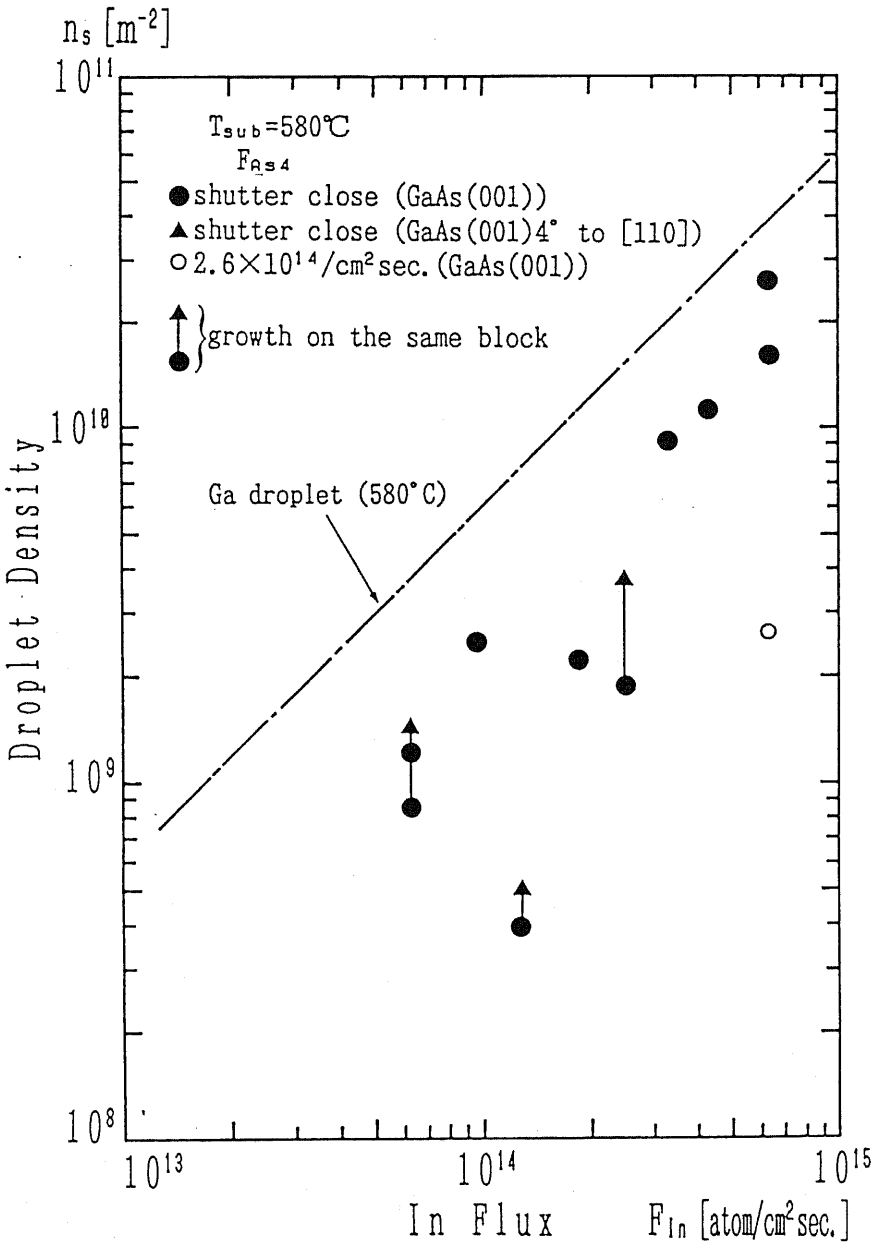

Fig.4-24. Density of In droplet as a function of the incident In flux at 580°C. The value of Ga droplets obtained in section 4.4 is also shown.

(a)

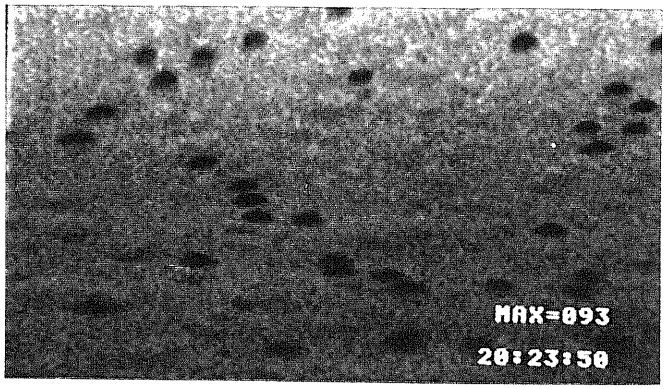

(b)

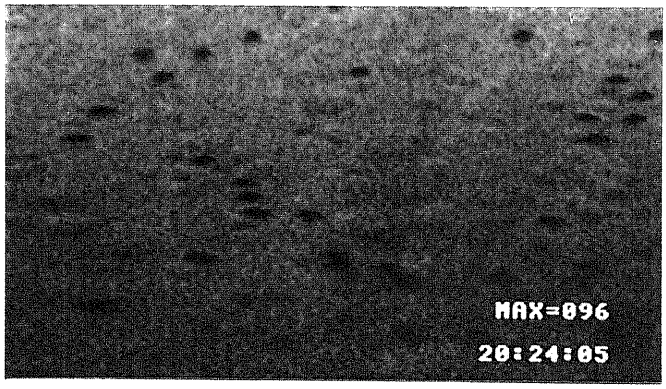

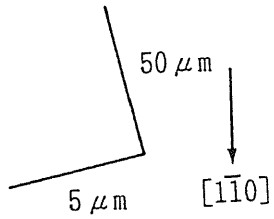

(c)

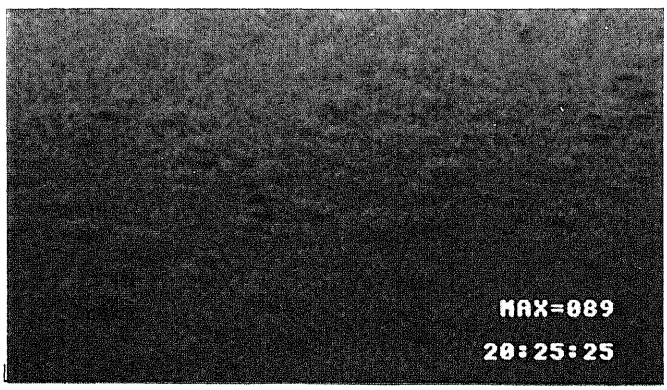

Fig.4-25. Successive SEM images in the disappearance of In droplets after closing the In shutter. From (a) to (b), the size of In droplets gradually decreased. The time interval between (a) and (b) was 15 s. In (c), 80 s after (b), the surface image after the disappearance of these droplets is shown.

Fig.4-24, where the density shows roughly proportional to the incident flux. In addition, it can be concluded that the surface diffusion length of In adatoms at 580°C is longer than the mean distance between In droplets of about 10μm, but not much longer, because there is a significant re-evaporation.

On the other hand, experimental results show that there is a step density dependence of the droplet density. This means that In atoms nucleate preferentially at the step site. Isu *et al.* (1991) have briefly reported that the density of Ga droplets on GaAs(001) within 0.1° orientated surface is nearly the same as that on 2° misorientated substrate to [110]. It is possible to assume that the preferential nucleation at the step is caused by a strain relaxation of In atoms. This behavior is to be understood by the step kinetics discussed in the chapter 2. There is no consideration for the interaction between the adatom and step in the nucleation theory used in the section 4.4. A modification of the theory is necessary for the full understanding of the results.

4.6.4 Summary

Both of In droplet formation and disappearance on GaAs(001) at 580°C were observed in the SEM-MBE. The density of In droplets has been measured under a various incident In flux. It was found that general features of In droplet formation are very much similar to that of Ga droplet formation. It can be concluded that the formation of In droplets is governed by SK growth mode.

Moreover, it was found that there is the step density dependence of the droplet density. This means the nucleation occurs preferentially at the step sites.

Chapter 5

Atomic Model for Facet Formation

5.1 Introduction

In the epitaxial vapor growth, facets such as (113)A, (115)A, *etc.* appear frequently. They appear also in both of MBE and MOCVD on the non-planar substrate as shown in Fig.5-1. In this case, it has been reported that many kinds of facet different from the original surface appear around the boundary between a (111)A and a (001) surfaces (Tsang and Cho 1977, Kapon *et al.* 1987, Hoenk *et al.* 1989a, 1989b). Here, the most typical facets are presented. Recently, many efforts have been paid to try to fabricate the quantum wire or quantum box structures by using such facets.

Although the study of the facet is quite important to understand the crystal growth mechanism and to fabricate quantum structures, there have been almost no researches about the mechanisms of the facet formation. This is partly due to the fact that a complex phenomenon is involved in the facet formation. In the field of crystal growth, an appearance of many kinds of facet has been known empirically, but the orientations of these facets depend on the growth condition and/or the growth method.

The purpose of this chapter is to find out a primitive and simple rule for the facet formation. Real process might be so complicated that this study could be only the first step for understanding the facet formation. Nevertheless, understanding will enable us to control the facet formation.

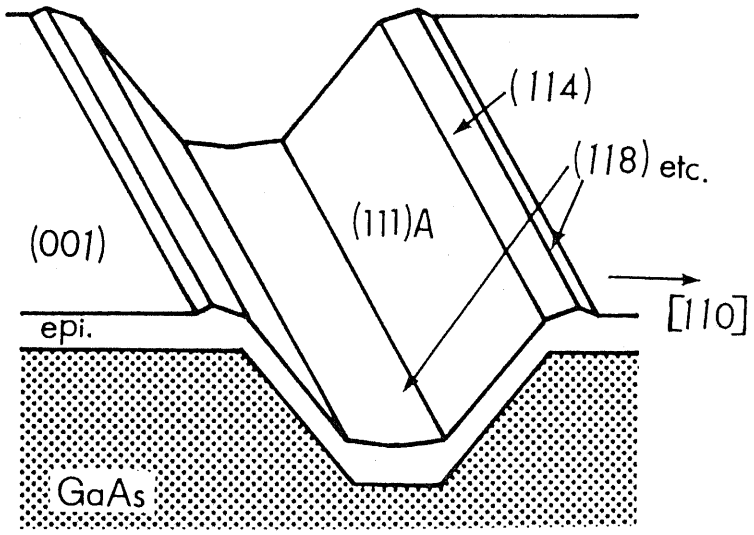

Fig.5-1. Schematic illustration of an example of MBE growth on a non-planar substrate. Typical facets of (114)A and (118)A are shown.

5.2 Basic Model for Facet Formation

An idea of this study comes from the STM image of GaAs(001) vicinal surface reported by Pashley *et al.* (1988, 1991). From the STM images, it has been found that the steps running along the [1$\bar{1}$0] direction which are sometimes called A-type step are relatively straight. In contrast, those running along [110] which are called B-type step are very ragged. These results agree with the RHEED measurements reported by Pukite *et al.* (1989). But the most noteworthy fact in the STM images is that the atomic structures of steps and kinks are determined by the (2×4) unit cell structure of which size is 8×16Å^2. Since measurements of STM were made at the room temperature after the growth of the epitaxial layer, the STM images show the surface after the growth. However, this result suggests that such a surface which is constructed of the (2×4) unit cell should be energetically most stable. Previously, we have studied the nucleation process on a GaAs(001) surface by breaking-bond model, and concluded that the nuclei constructed of reconstruction unit cell becomes the critical one (Suzuki and Nishinaga 1990). This is one of the evidences to show that energetically the most favorable surface consists of unit reconstruction cells.

On the other hand, a facet is well recognized as the surface to have the lowest energy. The formation of the facet is explained by the anisotropy of a growth rate. In the case of the growth upon a non-planar substrate as shown in Fig.5-1, the growth rate of facets is relatively lower than the neighboring planes of (001) and (111)A. Since the flux of growth unit is locally very uniform in MBE, the difference of the growth rate is attributed to nucleation rate and the velocity of surface diffusion. Hence, it is possible to assume that the local growth condition plays an important role in the formation of the facet. In other growth method such as MOCVD which uses the gas sources such as TMG, TEG, there is an additional factor to influence the facet appearance, namely, chemical reactions between adsorpted molecules and the surface.

In the strained heteroepitaxial growth of InAs on GaAs(001), the growth occurs in SK mode as discussed before. After the layer growth of InAs, the following island growth gives a facet. Since the island growth is caused by the strain relaxation process of the epitaxial layer, this transition in growth mode means that the growing form

changes from (001) surface to more stable facet.

So that an appearance of a facet indicates that the surface is more stable than other faces at this particular growth condition. In the present model, it is assumed that a formation of a stable facet is governed by a surface reconstruction. That is to say, a facet itself is (001) vicinal surface with a large misorientation angle. Here, the terrace of the step is constructed of one kind of reconstruction unit cells the kinds of which are determined by the growth conditions.

First of all, we would discuss about the basic idea of an atomic structure of a facet by taking the unreconstructed stepped surface as an example as shown in Fig.5-2. Hereafter, GaAs(001) misorientated towards [110] direction is assumed, because a well-defined A-type facet is frequently observed in the MBE growth of GaAs, AlAs and InAs. This may be due to the fact that the A-step is more straight than that of B-step on GaAs(001) surface (Pukite *et al.* 1989). We adopt following three rules for the formation of facet.

(1)Each (001) terrace consists of the particular reconstruction unit cells.

In our model, terrace between the neighboring steps is a part of GaAs(001) surface. About GaAs(001) surface, many kinds of the reconstructions have been reported depending upon the growth conditions. So that the kind of the reconstruction unit determines the kind of facet.

(2)Each terrace structure should have exactly the same structure.

Without this, the facet is not able to be observed.

(3)All steps have double step height with the height of 5.65Å for GaAs(001).

When a single step is allowed to exist and the terrace has the width of m As atom distance, this facet takes the orientation of (1, 1, $2m$-1) illustrated in Fig.5-2(a). This can not explain the existence of facets such as (114)A (Tsang and Cho 1977), (118)A (Hoenk *et al.* 1989b), *etc.*

In the next section, various facets in the MBE growth are discussed on the basis of these three rules.

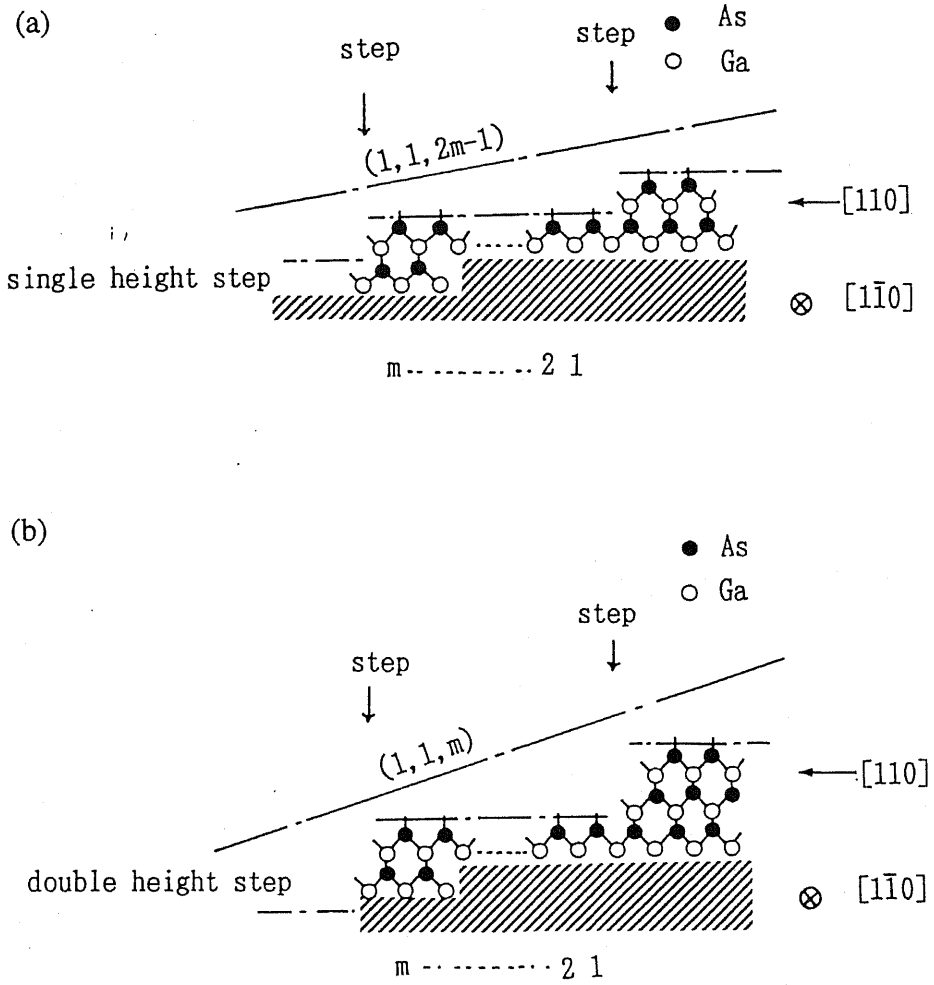

Fig.5-2. Schematic illustrations of unreconstructed GaAs(001) surface misorientated towards [110]. Top layer of the surface is terminated by As atoms. Each terrace consists of *m* As atoms in the [110] direction.

(a)Each step has single step height which is a half of the lattice constant. In this case, (1, 1, 2*m*-1) orientated facet is formed.

(b)Each step has double step height which is the lattice constant. In this case, (1, 1, *m*-1) orientated facet is formed.

5.3 Experimental Results

So far, there is not much reliable knowledge about the atomic structure of GaAs(001) surface reconstructions. Among these reconstructions, the (2×4) reconstructed surface has been studied by STM, and a missing dimer model is well accepted for this reconstruction. But there is still controversy about its As coverage (Farrel *et al.* 1987, Farley *et al.* 1989). While the present model depends to some degree on the atomic structure of the surface reconstructions, we adopt the reconstruction structure model reported by Biegelsen *et al.* (1990). They have observed systematically many kinds of the GaAs(001) surface reconstructions by means of STM.

(a)InAs on GaAs(001)

When InAs with the amount of 2ML is grown on GaAs(001) surface by MBE at 500°C, it can be clearly seen that the RHEED shows arrowhead pattern with the electron beam azimuth of $[1\bar{1}0]$ (Fig.5-3(a)). We have found that the formation of the facet is enhanced most strongly at this growth temperature. From the measurement of the angle of this arrowhead, the fact was determined to be (113)A planes as shown in Fig.5-3(b). This is coincident with the report of Fewcett *et al.* (1992). Before the growth of InAs, the surface of GaAs showed c(4×4) reconstruction, which is well known to have excess As coverage. If (2×4) reconstruction is kept at 500°C by closing the As_4 shutter, opening the shutter of As_4 for the InAs growth changes the surface reconstruction of GaAs(001) from (2×4) to c(4×4). On the assumption that the epitaxial layer has the same reconstruction as that of the substrate (Newstead *et al.* 1987), an atomic structure of the facet in the present case is determined as shown in Fig.5-4. Each terrace of GaAs(001) stepped surface is composed of one unit cell of c(4×4) and each step has double step height. This structure gives a (113)A orientated facet in agreement with the experimental observation. In Fig.5-4, group III element positioned at the step edge is assumed to have free dangling bonds and unreconstructed. This will be discussed later.

On the other hand, Tabuchi *et al.* (1990) have reported another facet with (115)A

(a)

(b)

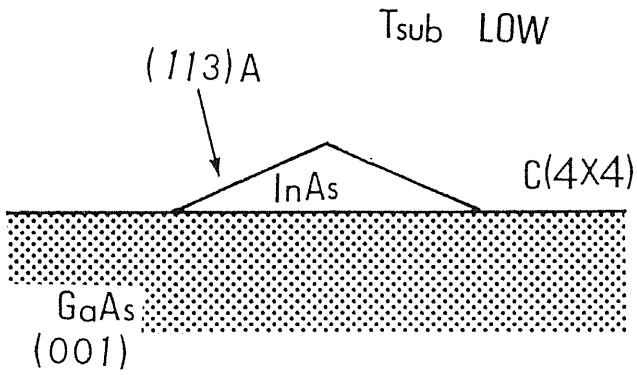

Fig.5-3. (a)RHEED pattern of the growth of InAs on GaAs(001) at 500°C with the azimuth of [1$\bar{1}$0]. The nominal amount of InAs is 2ML.
(b)Schematic model of a facet concluded by the RHEED measurement.

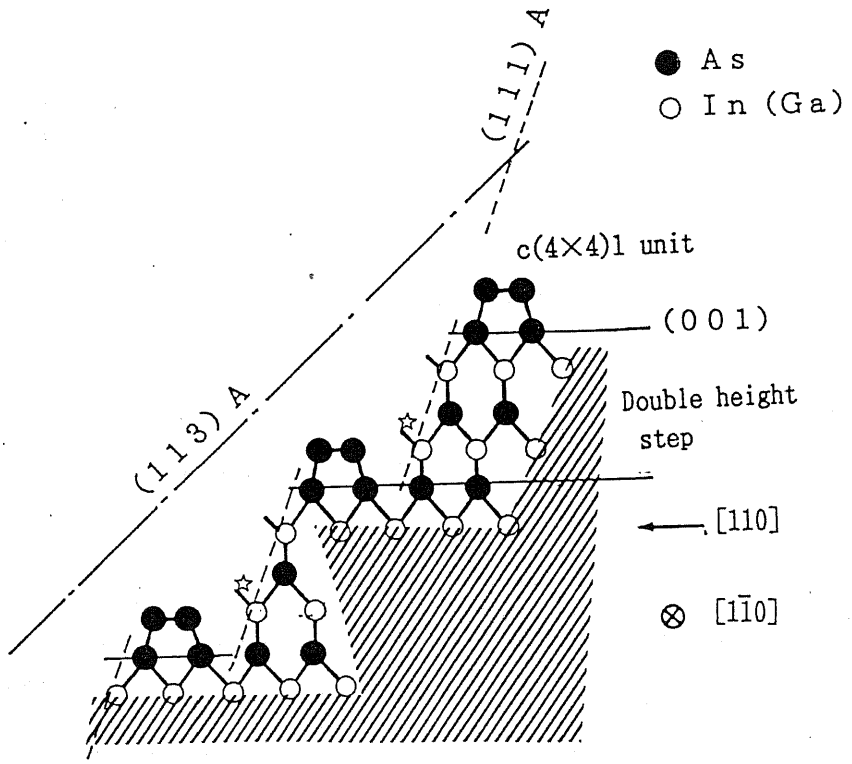

Fig.5-4. Schematic illustration of (113)A facet. c(4×4) unit cells are arranged on each terrace. Half of the Ga atoms marked by stars are missing along the [1$\bar{1}$0] direction as explained in the text.

orientation on the InAs on GaAs(001) by RHEED measurement during MBE growth. In this moment, we do not know about the reason of these different results. However, if a facet is composed of the (2×4) reconstruction unit cells, occurrence of (115)A facet plane can be explained by an atomic model shown in Fig.5-5, in which the missing dimer is positioned at the down layer side of a double height step according to the model of Pasheley *et al.* (1988, 1991). Although it is very likely that the growth temperature higher than 500°C introduces (115)A facet, we could not observe such a plane even at 550°C. About this discrepancy, we will discuss later.

(b)Facets appeared on non-planar substrate

The formation of facets on non-planar substrate shown in Fig.5-1 is attributed to the lateral flux from (111)A to (001) which is much bigger than vertically incident flux. The formation process of facets have been observed directly by means of μ-RHEED (Morishita *et al.* 1991). The lateral Ga flux decreases as the distance from the (111)A plane is increased. So that the effective flux ratio of As_4 to Ga on the (114)A facet is much smaller than that on the (001) surface. On the other hand, (118)A facet is formed under the condition of an intermediate flux ratio. So that it should be noted that both growth condition and growth behavior of these facets are not the same as those of the growth on (114)A and (118)A orientated substrates.

The (4×2) or c(8×2) reconstruction is well known among the surface reconstructions of less As coverage. Biegelsen *et al.* (1990) showed that between the growth conditions for (2×4) As-stabilized and c(8×2) Ga-stabilized reconstructions, there is a condition for the formation of (2×6) reconstructed surface. If the terrace is constructed of the (2×6) reconstruction unit cell, a (118)A facet appears as illustrated in Fig.5-6(a). Moreover, with c(8×2) unit cell, we can get a (114)A facet as shown in Fig.5-6(b). However, in this case one must postulate a jig-zag step, because the c(8×2) reconstruction has a large unit size. Alternate arrangement of one and two unit cells along the step edge is an unique choice for realizing the steps with the equal average distance.

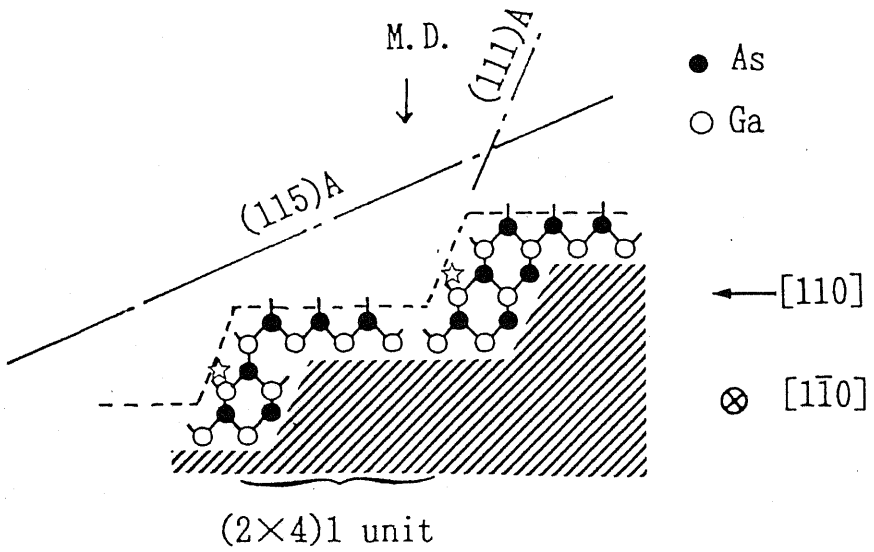

Fig.5-5. Schematic illustration of (115)A facet. (2×4) unit cells are arranged on each terrace. Half of the Ga atoms marked by stars are missing along the [1$\bar{1}$0] direction as explained in the text.

(a)

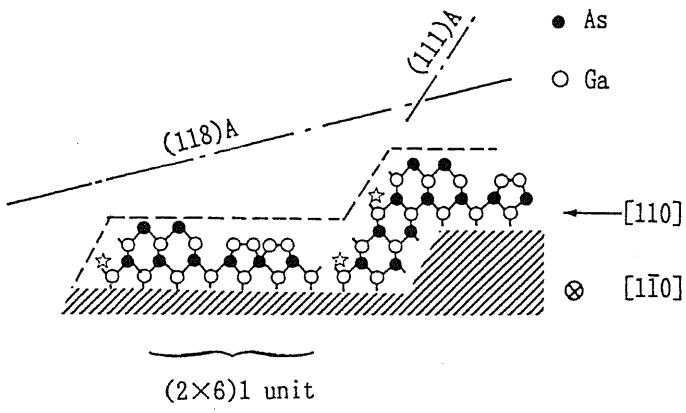

(b)

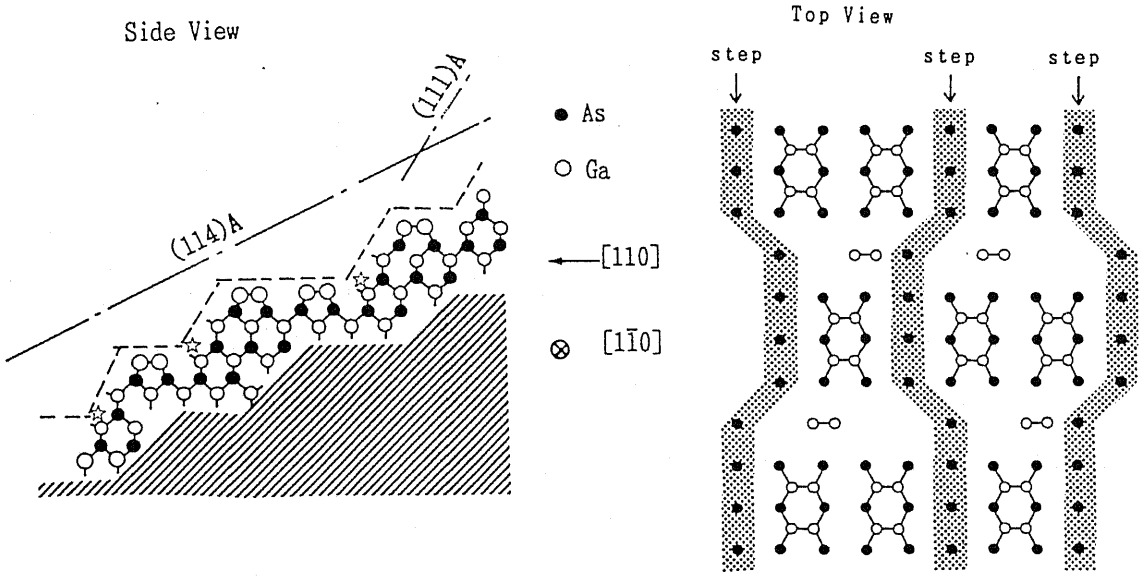

Fig.5-6. (a)Schematic illustration of (118)A facet. (2×6) unit cells are arranged on each terrace.
(b)Schematic illustration of (114)A facet. c(8×2) unit cells are arranged on each terrace.

Half of the Ga atoms marked by stars in the both models are missing along the [1$\bar{1}$0] direction as explained in the text.

5.4 Discussion

In the previous section, a model which is consistent with the experimental results is proposed to explain the formation of facet. However, this model can not always explain the experiments.

First of all, there are some reports which describe the appearance of the facets with different orientations even the material is the same as explained in section 5.3(a). This is probably due to the fact that a slight difference in the growth condition could result in the formation of different reconstruction and hence different facet. In addition, it is rather difficult to measure the exact orientation of a facet. This is especially true for the measurement of the facet with a high index. For example, the angle difference between (117)A and (118)A orientation is only 1.4°. Moreover in the RHEED method, the RHEED pattern is distorted by the refraction of the crystal (Joyce *et al.* 1986, Larsen *et al.* 1986). This distortion is large enough to identify the facet of low index such as (113)A facet.

Secondly, it can be mentioned that not all structures of reconstructions are known except several special reconstructions. As for the GaAs(001) surface, reconstructions have not been extensively studied except (2×4) and c(4×4) because of the instability of the surface. In the growth of MOCVD, the surface is usually kept under the atmosphere of H_2 or AsH_3. It is quite possible that the surface in the gas phase takes a different structure compared with that in the vacuum. However, because of the limitation of the tool, there are few reports and models about the surface structure in MOCVD (Kamiya *et al.* 1992). Much more knowledge should be accumulated in order to understand a facet grown in MOCVD by applying the above rules.

In the above discussion, the double step height was assumed to explain the experimentally observed facets. From the STM experiments on GaAs(001) 1-3° vicinal surface, it has been found that the step height of GaAs(001) is the half of the lattice constant (2.83Å) which is the minimum interplaner distance between each As or Ga lattice planes. However, this is not always true for a vicinal surface with a large misorientation. Because the area of the step edge occupies a considerable part of the whole surface area, a step structure has an important role in determining the surface free

energy. In the present model, the step edge is composed of GaAs(111)A surface as shown in Figs.5-4, 5-5 and 5-6. As for the reconstruction on a GaAs(111)A surface, it is well known that only (2×2) reconstructed surface can be observed under any growth condition (Cho and Hayashi 1971). There are a few theoretical and experimental studies about this reconstruction and a Ga-vacancy model has been widely accepted (Tong *et al.* 1984, Chadi 1984). This model has one quarter of Ga atoms in each (2×2) unit cell missing. These Ga vacancies are located along the direction of <110>, for example $[1\bar{1}0]$, $[\bar{1}01]$, *etc.* When this (2×2) reconstruction model is compared with the steps of the present model, it is found that the assumption of double step height agrees well with the (2×2) reconstruction surface. Namely, if the half of the Ga atoms marked by the stars in each model are missing along the $[1\bar{1}0]$ direction, the side of the double step forms one unit of the (2×2) reconstruction.

As far as we know, there have been almost no STM studies on the facet except Ge on Si(001). Mo *et al.* (1990) have reported that deposition beyond 3ML Ge leads to Ge cluster formation on Si(001) surface. From the STM observations, it has been found that the clusters have a {105} facet and they proposed a model to explain the formation of this facet. In the field of III-V compounds, 2 dimensional structure such as the surface reconstruction and the form of the steps is gradually clarified by STM. However, the structure of steps and kinks have not been clarified. Not only from the viewpoint of the facet formation, but from that of the crystal growth mechanism at steps or kinks, further experimental and theoretical studies for the facet should be carried out.

5.5 Summary

An atomic model to understand the structure of a facet which is observed in the strained heteroepitaxial growth or in the growth on the non-planar substrate, has been proposed. In this model, the facet consists of (001) terraces which have the width of one or two unit cells of surface reconstructions and are separated by double steps. By choosing the proper kind of reconstructions for a growth condition, orientation of the facet which agrees with the experimental results has been obtained.

Chapter 6

Conclusions

In this thesis, elemental growth process in MBE has been studied and a new growth method based on this understanding has been proposed.

Firstly, in chapter 2, III-III-V alloy semiconductors and GaAs were grown on various vicinal surfaces at high temperature. A theory has been developed to understand the growth of III-V semiconductors taking account of the degree of equilibrium at growth steps. By comparing the present theory with the experimental results, the following conclusions were obtained. In InGaAs growth, the supersaturation ratio at the step edge has been found of the order of 1.5. In the alloys of AlGaAs and InAlAs, high density nuclei makes the incorporation process close to equilibrium. In the case of GaAs, it has been shown that the equilibrium or near-equilibrium at the step edge with the supersaturation ratio of less than 1.2 is established. Consequently, it can be concluded that near-equilibrium is established in MBE at the step edges at least under relatively high growth temperature.

In chapter 3, modulation molecular beam epitaxy (M-MBE) has been proposed. In this technique, the growth is carried out on a group III stabilized or group III rich surfaces by intermittent supply of group III element under constant and relatively low pressure of As. The growth mechanism in this method has been studied in detail for homo- and heteroepitaxy by using RHEED and PL. It has been shown by RHEED that the present method can be expressed as a growth with both of growth interruptions and As incorporation at every monolayer. SQWs grown at 300°C show good characteristics almost comparable to those grown at high temperature by conventional MBE method. On the other hand, SQWs grown at 580°C have poor characteristics because of the

intermixing at the interfaces. Hence, it has been concluded that this method can give an excellent crystal quality at the low growth temperature.

In chapter 4, real time observations of growing surface by SEM-MBE or μ-RHEED have been described. It has been found that surface reconstruction transition under excess Ga condition occurs not uniformly but by the expansion of domains. It has been shown that the Ga droplet formation upon the Ga-stabilized surface is explained by the growth in SK mode. In the disappearance of Ga droplets, there are two modes depending on the droplet density and these modes give different As_4 incorporation rates. This novel feature has been explained by a model taking account of a migration of As atom on As-rich surface. From the observations of In droplets on GaAs(001) at 580°C, it has been found that the general features of In droplet formation are very much similar to that of Ga droplet formation and that the formation is governed again by the SK growth mode.

In chapter 5, an atomic model for a facet formation has been proposed. The experimental orientations of the facet show a good agreement with the prediction made by this model.

Although this work is only one step towards the final goal of the full understanding of the MBE growth mechanism, the author truly hopes this work may throw some light on this problem.

References

Aseev, A. L., A. V. Latyshev and A. B. Krasilnikov, 1991 : J. Cryst. Growth **115**, 393.

Arthur, J. R., 1968 : J. Appl. Phys. **39**, 4032.

Bennema, P., and G. H. Gilmer, 1973 : Crystal Growth An Introduction, ed. P. Hartman (North-Holland, Amsterdam) Chap. 10.

Biegelsen, D. K., R. Bringans, J. E. Northrup and L. -E. Swartz, 1990 : Phys. Rev. **B41**, 5701.

Briones, F., D. Golmayo, L. Gonzalez and A. Ruiz, 1987a : J. Cryst. Growth **81**, 19.

Briones, F., L. Gonzalez, M. Recio and M. Vazquez, 1987b : Jpn. J. Appl. Phys. **26**, L1125.

Briones, F., L. Gonzalez and A. Ruiz, 1989 : Appl. Phys. **A49**, 729.

Briones, F. and A. Ruiz, 1991 : J. Cryst. Growth **111**, 194.

Burton, W. K., N. Cabrera and F. C. Frank, 1951 : Philos. Trans. R. Soc. London **A243**, 299.

Chadi, D. J., 1984 : Phys. Rev. Lett. **52**, 1912.

Chika, S., H. Kato, M. Nakayama and N. Sano, 1986 : Jpn. J. Appl. Phys. **25**, 1441.

Cho, A. Y., 1970 : J. Appl. Phys. **41**, 2780.

Cho, A. Y., 1971 : J. Appl. Phys. **42**, 2074.

Cho, A. Y. and I. Hayashi, 1971 : Solid State Electron. **14**, 125.

Clarke, S., D. D. Vvedensky and M. W. Ricketts, 1989 : J. Cryst. Growth **95**, 28.

Deparis, C. and J. Massies, 1991 : J. Cryst. Growth **108**, 157.

Farley, C. W., G. J. Sullivan, M. J. Mondry and D. L. Miller, 1989 : J. Cryst. Growth **96**, 19.

Farrel, H. H. and C. J. Palmstrøm, 1990 : J. Vac. Sci. & Technol. **B8**, 903.

Ferguson, I. T., A. G. de Oliveira and B. A. Joyce, 1992 : J. Cryst. Growth **121**, 267.

Fawcett, P. N., B. A. Joyce, X. Zhang and D. W. Pashley, 1992 : J. Cryst. Growth **116**, 81.

Fernandez, R., 1988 : J. Vac. Sci. & Technol. **B6**, 745.

Flaim, T. A. and P. E. Ownby, 1971 : J. Vac. Sci. & Technol. **8**, 661.

Foxon, C. T. and B. A. Joyce, 1975 : Surf. Sci. **50**, 434.

Foxon, C. T. and B. A. Joyce, 1977 : Surf. Sci. **64**, 293.

Foxon, C. T., D. Hilton, P. Dawson, K. J. Moore, P. Fewster, N. L. Andrew and J. W. Orton, 1990 : Semicond. Sci. & Technol. **5**, 721.

Gaines, J. M., P. M. Petroff, H. Kroemer, R. J. Simes, R. S. Geels and J. H. English, 1988 : J. Vac. Sci. & Technol. **B6**, 1378.

Garcia, J. C., C. Neri and J. Massies, 1989 : J. Cryst. Growth **98**, 511.

Guille, C., F. Houzay, J. M. Moison and F. Barthe, 1987 : Surf. Sci. **189/190**, 1041.

Harris, J. J., B. A. Joyce and P. J. Dobson, 1981 : Surf. Sci. **103**, L90.

Hata, H., T. Isu, A. Watanabe and Y. Katayama, 1990 : Appl. Phys. Lett. **56**, 2542.

Heckingbottom, R., 1985 : J. Vac. Sci. & Technol. **B3**, 572.

Hoenk, M. E., H. Z. Chen, A. Yariv, H. Morkoç and K. J. Vahara, 1989a : Appl. Phys. Lett. **54**, 1347.

Hoenk, M. E., C. W. Hieh, H. Z. Chen and K. J. Vahara, 1989b : Appl. Phys. Lett. **55**, 53.

Honig, R. E. and D. A. Kramer, 1969 : RCA Review **30**, 285.

Horikoshi, Y., M. Kawashima and H. Yamaguchi, 1986 : Jpn. J. Appl. Phys. **25**, L868.

Horikoshi, Y., M. Kawashima and H. Yamaguchi, 1988 : Jpn. J. Appl. Phys. **27**, 169.

Horikoshi, Y. and M. Kawashima, 1989a : Jpn. J. Appl. Phys. **28**, 200.

Horikoshi, Y. and M. Kawashima, 1989b : J. Cryst. Growth **95**, 17.

Horikoshi, Y., H. Yamaguchi and M. Kawashima, 1989 : Jpn. J. Appl. Phys. **28**, 1307.

Ichikawa, M., T. Doi, M. Ichihashi and K. Hayakawa, 1984 : Jpn. J. Appl. Phys. **23**, 913.

Inoue, N., 1991 : J. Cryst. Growth **111**, 75.

Irisawa, T., Y. Arima and T. Kuroda, 1990 : J. Cryst. Growth **99**, 491.

Isu, T., A. Watanabe, M. Hata and Y. Katayama, 1988a : 5th Int. Conf. on Molecular Beam Epitaxy (MBE-V), Sapporo, LN-9.

Isu, T., A. Watanabe, M. Hata and Y. Katayama, 1988b : Jpn. J. Appl. Phys. **27**, L2259.

Isu, T., M. Hata and A. Watanabe, 1991 : J. Cryst. Growth **111**, 210.

Joyce, B. A., P. J. Dobson, J. H. Neave, K. Woodbridge, J. Zhang, P. K. Larsen and B. Bôlger, 1986 : Surf. Sci. **168**, 423.

Kamiya, I., D. E. Aspnes, H. Tanaka, L. T. Florez, E. Colas, J. P. Harbison, and R. Bhat, 1992 : Appl. Surf. Sci. **60/61**, 534.

Kanisawa, K., J. Osaka, S. Hirono and N. Inoue, 1991 : J. Cryst. Growth **115**, 348.

Kapon, E., M. C. Tamargo and D. M. Hwang, 1987 : Appl. Phys. Lett. **50**, 347.

Kojima, T., N. J. Kawai, T. Nakagawa, K. Ohta, T. Sakamoto and M. Kawashima, 1985 : Appl. Phys. Lett. **47**, 286.

Kojima, T., K. Ohta and T. Nakagawa, 1990 : National Conf. Cryst. Growth-21, (in Japanese).

Kojima, T., K. Ohta and T. Nakagawa, 1991 : National Conf. Cryst. Growth-22, (in Japanese).

Larsen, P. K., P. J. Dobson, J. H. Neave, B. A. Joyce, B. Bölger and J. Zhang, 1986 : Surf. Sci. **169**, 176.

Lewis, B. F., R. Fernandez, A. Madukar and F. J. Grunthaner, 1986 : J. Vac. Sci. & Technol. **B4**, 560.

Longenbach, K. F., S. Xin, C. Schwartz, Y. Jiang and W. I. Wang, 1991 : Appl. Phys. Lett. **59**, 820.

Mo, Y. -W., D. E. Savage, B. S. Swartzentruber and M. G. Lagally, 1990 : Phys. Rev. Lett. **65**, 1020.

Mochizuki, K. and T. Nishinaga, 1989 : Jpn. J. Appl. Phys. **27**, 1585.

Morishita, Y., Y. Nomura, S. Goto, Y. Katayama and T. Isu, 1991 : Workbook of 5th Int. Conf. of Modulated Semiconductor Structures, p132.

Morishita, Y., Y. Nomura, S. Goto, T. Isu and Y. Katayama, 1992 : Proc. of the 7th Int. Conf. of Molecular Beam Epitaxy.

Nakao, H. and T. Yao, 1989 : Jpn. J. Appl. Phys. **28**, L352.

Neave, J. H., B. A. Joyce, P. J. Dobson and N. Norton, 1983 : Appl. Phys. **A31**, 1.

Neave, J. H., B. A. Joyce and P. J. Dobson, 1984 : Appl. Phys. **A34**, 179.

Neave, J. H., P. J. Dobson and B. A. Joyce, 1985 : Appl. Phys. Lett. **47**, 100.

Newstead, S. M., R. A. A. Kubiak and E. H. C. Parker, 1987 : J. Cryst. Growth **81**, 49.

Nishinaga, T. and K. I. Cho, 1988 : Jpn. J. Appl. Phys. **27**, L12.

Nishinaga, T. and T. Suzuki 1991 : to be published in Proc. 7th Int. Conf. Vapour Growth and Epitaxy, Nagoya, J. Cryst. Growth.

Ohta, K., T. Kojima and T. Nakagawa, 1988 : J. Cryst. Growth **95**, 71.

Ohta, K., T. Kojima and T. Nakagawa, 1991 : J. Cryst. Growth **110**, 509.

Osaka, J., N. Inoue, Y. Mada, K. Yamada and K. Wada, 1990a : J. Cryst. Growth **99**, 120.

Osaka, J. and N. Inoue, 1990b : Mater. Res. Soc. Sym. Proc. **159**, 33.

Osaka, J., K. Kanisawa, S. Hirono and N. Inoue, 1990c : 9th Symposium Record of Alloy Semicondoctor Physics and Electronics, p123.

Osakabe, N., K. Yagi and G. Honjo, 1980 : Jpn. J. Appl. Phys. **19**, L309.

Osakabe, N., Y. Tanishiro, K. Yagi and G. Honjo, 1981 : Surf. Sci. **102**, 424.

Pashley, M. D., K. W. Haberern, W. Friday, J. M. Woodall and P. D. Kirchner, 1988 : Phys. Rev. Lett. **60**, 2176.

Pashley, M. D., K. W. Haberern and J. M. Gaines, 1991 : Appl. Phys. Lett. **58**, 406.

Pukite, P. R., G. S. Petrich, S. Batra and P. I. Cohen, 1989 : J. Cryst. Growth **95**, 269.

Reichelt, K., 1989 : Vacuum **38**, 1083.

Sakaki, H., M. Tanaka and J. Yoshino, 1985 : Jpn. J. Appl. Phys. **24**, L417.

Seki, H. and A. Koukitu, 1986 : J. Cryst. Growth **78**, 342.

Sekiguchi, Y., S. Miyazawa and N. Mizutani, 1991 : Jpn. J. Appl. Phys. **30**, L1726.

Shitara, T. and T. Nishinaga, 1989 : Jpn. J. Appl. Phys. **28**, 1212.

Spiller, G. D., P. Akhter and J. A. Venables, 1983 : Surf. Sci. **131**, 517.

Stowell, M. J. and T. E. Hutchinson, 1971 : Thin Solid Films **8**, 41.

Sugiyama, N. and Y. Kajikawa, 1992 : J. Cryst. Growth **123**, 393.

Suzuki, T. and T. Nishinaga, 1990 : Proc. of The Third Topical Meeting on Crystal Growth Mechanism, p41.

Tabuchi, M., S. Noda and A. Sasaki, 1990 : 9th Symposium Record of Alloy Semicondoctor Physics and Electronics, p349.

Tanaka, M. and H. Sakaki, 1987 : J. Cryst. Growth **81**, 153.

Tanaka, M. and H. Sakaki, 1988 : Superlattice and Microstructures **4**, 237.

Tanaka, M., T. Suzuki and T. Nishinaga, 1990 : Jpn. J. Appl. Phys. **29**, L706.

Tong, S. Y., G. Xu and W. N. Mei, 1984 : Phys. Rev. Lett. **52**, 1693.

Tsang, W. T. and A. Y. Cho, 1977 : Appl. Phys. Lett. **30**, 293.

Van Hove, J. M. and P. I. Cohen, 1985 : Appl. Phys. Lett. **47**, 726.

Venables, J. A., J. Derrien and A. P. Janssen, 1980 : Surf. Sci. **95**, 411.

Venables, J. A., G. D. T. Spiller and M. Hanbucken, 1984 : Rept. Progr. Phys. **47**, 399.

Wood, C. E. C., 1981 : Surf. Sci. **108**, L441.

Yamada, K., N. Inoue, J. Osaka and K. Wada, 1988 : 5th Int. Conf. on Molecular Beam Epitaxy (MBE-V), Sapporo, LN-8.

Yamada, K., N. Inoue: J. Osaka and K. Wada, 1989 : Appl. Phys. Lett. **55**, 622.

Zhang, J., J. H. Neave, P. J. Dobson, and B. A. Joyce, 1987 : Appl. Phys. **A42**, 317.

Zhang, X., D. W. Pashley, J. H. Neave, J. Zhang and B. A. Joyce, 1992 : J. Cryst. Growth **121**, 381.

Publication List

[1] Papers related to this thesis

1)T.Suzuki and T.Nishinaga: "Role of Step Kinetics in the Growth Mechanism of MBE": 9th Symposium Record on Alloy Semiconductor Physics and Electronics, 1990, p187-194.

2)T.Suzuki and T.Nishinaga: "Surface Diffusion and Atom Incorporation Kinetics in MBE of InGaAs and AlGaAs": J. Cryst. Growth **111**(1991)173-177.

3)T.Suzuki, I.Ichimura and T.Nishinaga: "Dependence of Ga Desorption Rate upon the Step Density in Molecular Beam Epitaxy of GaAs": Jpn. J. Appl. Phys. **30**(1991)L1612-L1615.

4)T.Nishinaga and T.Suzuki: "The Role of Step Kinetics in MBE of Compound Semiconductors": J. Cryst. Growth **115**(1991)398-405.

5)T.Suzuki, I.Ichimura and T.Nishinaga: "Equilibrium at the Step of GaAs in Molecular Beam Epitaxy": 10th Symposium Record on Alloy Semiconductor Physics and Electronics, 1991, p57-64.

6)T.Nishinaga and T.Suzuki: "Degree of Equilibrium at Step Edge during MBE Growth of III-V Compounds": Proceedings of The Fifth Topical Meeting on Crystal Growth Mechanism, 1992, p61-68.

7)T.Nishinaga and T.Suzuki: "Towards Understanding the Growth Mechanism of III-V Semiconductors on an Atomic Scale": to be published in J. Cryst. Growth.

Others

8)M.Tanaka, T.Suzuki and T.Nishinaga: "Surface Diffusion of Al Atoms on GaAs Vicinal Surfaces": Proceedings of The Third Topical Meeting on Crystal Growth Mechanism, 1990, p45-48.

9)M.Tanaka, T.Suzuki and T.Nishinaga: "Surface Diffusion of Al Atoms on GaAs Vicinal Surfaces in Molecular Beam Epitaxy": Jpn. J. Appl. Phys. **29**(1990)L706-L708.

10)T.Nishinaga and T.Suzuki: "Surface Diffusion Coefficient in MBE by Collision Time Approximation": Proceedings of The Fourth Topical Meeting on Crystal Growth Mechanism, 1991, p37-40.

11)M.Tanaka, T.Suzuki and T.Nishinaga: "Surface Diffusion of Al and Ga Atoms on GaAs(001) and (111)B Vicinal Surfaces in Molecular Beam Epitaxy": J. Cryst. Growth **111**(1991)168-172.

12)T.Shitara, T.Suzuki, D.D.Vvedensky and T.Nishinaga: "Concentration Profiles of Surface Atoms during Epitaxial Growth on Vicinal Surfaces": to be published in Appl. Phys. Lett.

13)T.Shitara, T.Suzuki, D.D.Vvedensky and T.Nishinaga: "Adatom Concentration Profiles on Simulated Vicinal Surfaces During Epitaxial Growth": to be published in Mater. Res. Soc. Symp. Proc.

[2] International Conference

Presentation related to this thesis

1)T.Suzuki and T.Nishinaga: "Surface Diffusion and Atom Incorporation Kinetics in MBE of InGaAs and AlGaAs": 6th International Conference on Molecular Beam Epitaxy, San Diego, America, August, 1990.

Other

2)M.Tanaka, T.Suzuki and T.Nishinaga: "Surface Diffusion of Al and Ga Atoms on GaAs(001) and (111)B Vicinal Surfaces in Molecular Beam Epitaxy": 6th International Conference on Molecular Beam Epitaxy, San Diego, America, August, 1990.